Evaluation of phosphate and ammonium removal and alorization from urban waste waters by impregnated metal hydrated oxides inorganic natural zeolites

Diana Elizabeth Guaya Caraguay

UNIVERSITAT POLITÈCNICA DE CATALUNYA

Escola Tècnica Superior d'Enginyeria Industrial de Barcelona

Department of Chemical Engineering

Ph. D. Program: Chemical processes engineering

EVALUATION OF PHOSPHATE AND AMMONIUM REMOVAL AND VALORIZATION FROM URBAN WASTE WATERS BY IMPREGNATED METAL HYDRATED OXIDES INORGANIC NATURAL ZEOLITES

Author: Diana Elizabeth Guaya Caraguay

Supervisors: José Luis Cortina Pallás / Adriana Farran Marsà

Barcelona, February 2017

Abstract

Phosphate and ammonium removal from waste water by adsorption using inorganic natural sorbents has been identified as a promising technology. The advantages of this methodology are associated with its availability and effective low cost.

Some natural and synthetic zeolite materials have been used for the individual phosphate and ammonium removal from aqueous solutions. The zeolites revealed high affinity for ammonium removal. However, some modifications stages are indispensable to enhance their oxyanionic sorption capacity to achieve high phosphate removal ratios. So, it is highly desirable to obtain a single sorbent for both cation and anion removal capacity from aqueous solutions. For this purpose, a natural zeolite with clinoptilolite as major mineral phase, was impregnated with metallic oxyhydroxides after conversion to the sodium form. As a result, hydrated metal oxides (HMO) of Al, Fe and Mn were immobilized on the zeolite surface structure.

The efficiency of aluminium, iron and manganese hydrated metal oxides was individually evaluated for the simultaneous phosphate and ammonium removal from aqueous solutions through batch and continuous mode assays using a granular natural zeolite sample. High selectivity was developed by modified zeolites towards these species in the presence of competing ions commonly present in urban and industrial waste waters. The regeneration assays demonstrated the limited use of modified zeolites in operational cycles as losses of the hydrated metal oxide along within the operation cycles will require re-impregnation stages. Then, an alternative option for final valorization of ammonium and phosphate is the use of the loaded zeolites as soil amendment for agricultural and forestry purposes or for environmental rehabilitation of degraded soils.

Therefore, a second approach could be to use the impregnated zeolites as nutrients carriers, improving their fertilizing properties by including potassium. For this purpose, powder samples of the natural zeolite in the potassium form were impregnated with the metallic oxyhydroxides and were enriched on nutrients (N,P,K) by using treated waters from the secondary effluent from “El Prat” Waste Water Treatment Plant using batch mode assays. The N-P-K release rates of the enriched zeolite samples were determined by column test using mixtures with three different types of agricultural soils.

Keywords: Phosphate, ammonium, removal, waste water treatment, natural zeolites, granular and powder, impregnation, hydrated metal oxides modified zeolites, potassium zeolites, N-P-K enriched zeolites, soil amendment, slow release fertilizer.

Ph.D. thesis organization

This thesis addressed to the evaluation of phosphate and ammonium removal and valorization by using a natural inorganic ion-exchanger (zeolite) from urban waste waters was performed according to the structure depicted in Figure 1. The study was focused in the approach of:

a) Modification of a natural zeolite, rich in clinoptilolite as major mineral phase, by impregnation of hydrated metal oxides, for promoting the simultaneous removal of phosphate and ammonium. In this case granular samples are applied in sorption and regeneration cycles to recover concentrated brines of ammonium and phosphate

b) Using a powder form of a potassium natural zeolite impregnated with metal hydrated oxides, as N-P-K carriers to improve soil quality in agriculture, forestry and environmental rehabilitation of degraded soils applications.

Chapter 1 comprises a brief introduction to the serious environmental problem of eutrophication and the available technologies for ammonium and phosphate removal from waste water in order to contribute with the fulfilment of legislation and the environment protection.

Chapter 2 describes the objectives and the experimental methodology used in this PhD thesis.

The results obtained have been grouped in chapters which correspond to specific objectives of the project that were:

Chapter 3 Simultaneous phosphate and ammonium removal from aqueous solution by a hydrated aluminum oxide modified natural zeolite.

Chapter 4 Modification of a natural zeolite with Fe(III) for simultaneous phosphate and ammonium removal from aqueous solutions.

Chapter 5 Simultaneous nutrients removal by using a hybrid inorganic sorbent impregnated with hydrated manganese oxide.

Chapter 6 Recovery of ammonium and phosphate from treated urban waste water by using potassium clinoptilolite impregnated hydrated metal oxides as N-P-K fertilizer.

Chapter 7 Valorisation of N and P from waste water by k-zeolites as fertilizers: evaluation of nutrients release in amended soils by dynamic experiments.

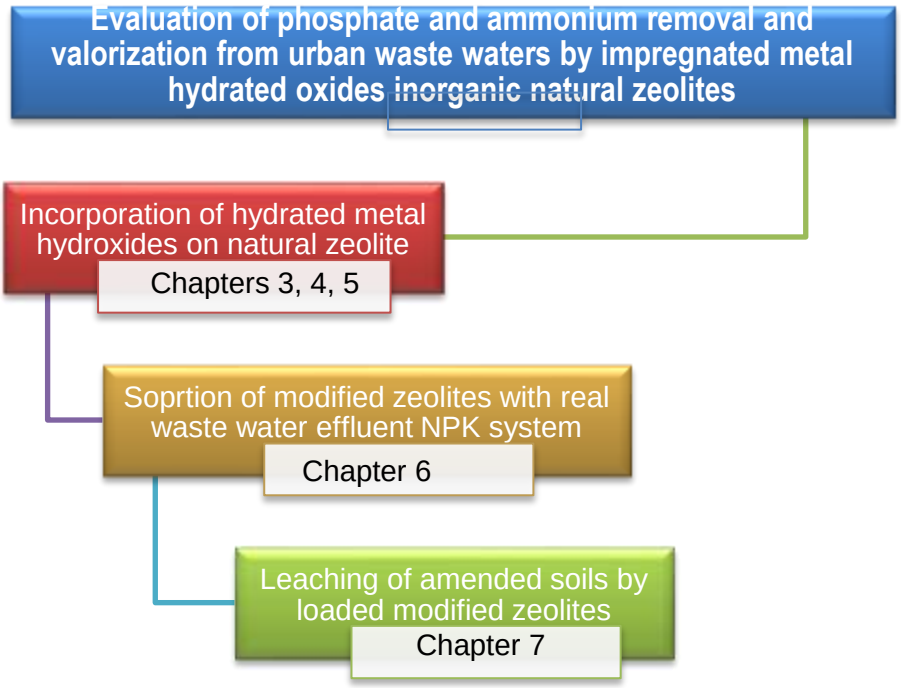

Figure 1 Structure of development of PhD thesis entitled: “Evaluation of phosphate and ammonium removal and valorization from urban waste waters by impregnated metal hydrated oxides inorganic natural zeolites “

Summary

List of Acronyms

HMO: hydrated metal oxides

WWTP: waste water treatment plant

EBPR: enhanced biological phosphorus removal

BPR: biological phosphorus removal

PLE: polymeric ligand exchangers

HAIX: hybrid anion exchanger

CEC: cation exchange capacity

SAC: strong acid cation

WAC: weak acid cation

CFA: coal fly ash

$N\text{-}NH_4^+$: nitrogen - ammonium ion

$P\text{-}PO_4^{3-}$: phosphorous – phosphate ion

Z-N: natural zeolite

HAIO: hydrated aluminum oxide

Z-Na: sodium zeolite

Z-Al: aluminum zeolite

EBHRT: empty bed hydraulic retention times

LB-P: loosely bound phosphorus fraction

(Fe,Al,Mn)-P: iron, aluminum and manganese phosphorus fraction

(Ca^+Mg)-P: phosphorus linked to the calcium and magnesium compounds

R-P: residual phosphorus ()

$NH_4MnPO_4 \cdot H_2O$: ammonium manganese phosphate hydrate oxide compound

HPDM: homogenous particle diffusion model (

N-P-K zeolite: zeolite containing nitrogen – phosphorus and potassium elements

KAlC: aluminium/potassium zeolite

KFeC: iron/potassium zeolite

KMnC: manganese/potassium zeolite

NPOC: non-purgeable organic carbon

TC: total carbon

TOC: total organic carbon

IC: inorganic carbon

NT: total nitrogen

Chapter 1 Introduction

The removal of pollutants from waste water must be performed by treatment facilities. However, the conventional methods used for waste water treatment are not able to remove some pollutants at limits that do not represent risk for human health and natural ecosystems. In fact, the domestic waste water effluents discharged into receiving waters bodies represent a serious and well identified environmental problem associated with the phosphorus and nitrogen overloading in surface waters. Both species, incorporated mainly from treated municipal waste water discharges and agricultural runoffs, are responsible for the eutrophication of water bodies.

1.1. Phosphorus and nitrogen cycle in waste water treatment plants

Typical municipal waste water consists of 99% of water and 1% of pollution load, mainly of organic nature, where; phosphorous and nitrogen are included as the main ones [1]. In municipal waste water phosphorus and nitrogen comes mainly from human activities. Phosphorus occurs in three main forms: orthophosphates ($H_2PO_4^-$, HPO_4^{2-}, PO_4^{3-}), condensed (pyro-, meta-, and poly-) phosphates, and organic phosphates [2]. The orthophosphate form is around 50-70% of total phosphorus and the rest are polyphosphates and phosphorus bound to organic compounds. In aqueous environments the phosphate solubility and ionic orthophosphate forms are controlled by the pH, as it is represented by **Eq. 1** [3]. The average concentration of total phosphorus in the influent waste waters is in the range of 10 – 20 mg P/L [4]. In a normal waste water treatment plant the organic phosphate is converted to inorganic orthophosphate. Under normal conditions the 60 - 65% of the total phosphorus load is removed providing an effluent of 2-2.5 mg P/L [5].

Eq. 1

$$H_3PO_4 \xrightarrow{pKa\ 2.15} H_2PO_4^- + H^+ \xrightarrow{pKa\ 7.2} HPO_4^{2-} + H^+ \xrightarrow{pKa\ 12.3} PO_4^{3-} + H^+$$

On the other hand, nitrogen is a major component of waste water and appears in various oxidation states depending on the physical and biochemical conditions. The total nitrogen concentration in a typical waste water treatment plant comprises about 15 – 50 mg N/L. Inorganic ammonia/ ammonium forms represent around the 60-65% of the total nitrogen and the remainder is in the organic form [6]. Also nitrite (NO_2^-) and nitrate (NO_3^-) forms are the result of a biological oxidation reaction from ammonia [3]. Ammonia (NH_3) is usually found as ammonium ion (NH_4^+) in aqueous environments [7]. The proportion of these forms depends on the pH, the toxic ammonia form predominates when pH is high while relatively non-toxic ammonium

ion dominates at low pH, as **Eq. 2** represent [8]. During the treatment processes organic nitrogen is almost quantitatively converted to ammonium. Usually, the total nitrogen concentration in the effluent is around 5 – 10 mg N/L; therefore removal efficiencies over 90% could be reached [9].

Eq. 2

$$NH_4^+ \xrightarrow{pKa\ 9.24} NH_3 + H^+$$

Conventionally a waste water treatment facility is divided into a sequence of preliminary, primary, secondary and tertiary processes. Nitrogen and phosphorus are removed from waste water by means of physical and biological units. However specialized tertiary systems are needed in order to reduce the concentrations of nitrogen and phosphorus to reach low levels.

1.2. Eutrophication of water receptors

Waste water treatment lines include a final effluent disposal which includes discharge to oceans, rivers, lakes, infiltration to groundwater, reuse for irrigation or recycling for other purposes [1].

The increase and accumulation of nutrients in water and the resultant fast-grown of algal productivity is called eutrophication [10]. Phosphorus is an essential nutrient for the growth of photosynthetic algae and other biological organisms in water bodies [11], as well as nitrogen is a limiting biological component [12].

Although, eutrophication is a natural process it is greatly accelerated by the supply of nutrients through human activities like the discharge of domestic sewage, industrial wastes, agricultural and urban run-off [13, 14]. Then eutrophication has become a serious environmental problem worldwide that is associated with the reduction of water quality due to decrease in the availability of the dissolved oxygen [15], the development of odors and the unsightly scenes [16].

1.3. Regulations for waste water treatment discharges

The population growth leads the increment of the volume of waste water produced as well as it adverse impact on water resources. Consequently, water reuse and recycling have become essential for closing the water cycle. Therefore, nowadays the concern is focused on developing effective and affordable treatment technologies in accordance with the emission limits required for water resource management [17].

At worldwide the European and North American legislations for water management are the basic reference guides for the protection of groundwater and surface water.

The Directorate-General for the Environment of the European Commission as an executive body of the European Union (EU) is the responsible for the policy area. The Urban Waste Water Treatment Directive (91/271/EEC) concerns the discharges of municipal and some industrial waste waters. The Directive 98/15/EC amended Directive 91/271/EEC to clarify the requirements in relation to urban waste water treatment plants discharges to sensitive areas which are subject to eutrophication.

Spain legislation for the protection of water sources is based in the "Real Decreto 2116/1998" which amends the "Real Decreto 509/1996" for municipal waste water treatment. There are established total nitrogen and phosphorus concentrations for effluents in waste water facilities in sensitive zones of eutrophication as shown in **Table 1.1**.

Parameter		*Concentration (mg/L)*
Total phosphorus	2	(10000 – 100000 equivalent inhabitants)
	1	(>100000 equivalent inhabitants)
Total nitrogen	15	(10000 – 100000 equivalent inhabitants)
	10	(>100000 equivalent inhabitants)

Table 1.1. Permissible concentrations for total phosphorus and nitrogen in waste water effluents (RD 2116/1998).

On the other hand, the United States Environmental Protection Agency (EPA), through the Clean Water Act (CWA) establishes the basic structure for regulating discharges of pollutants into the waters of the United States and regulates quality standards for surface waters. In order to reduce the problems associated with excess nutrients in water bodies, the EPA criteria for phosphates establishes surface waters are maintained at 0.01 to 0.03 mg P/L of total phosphorus [18]. As well as through the National Pollutant Discharge Elimination System (NPDES), it has been established in 2008 the discharge of ammonia nitrogen to a monthly average of 1.5-1.9 mg N/L.

1.4. Phosphorous and nitrogen sources

Phosphorus is the eleventh most common element on Earth [19]. Nowadays, it is considered as non-renewal resource, with a predicted stock to dwindle in next fifty years [20]. The most important deposits of phosphate rocks are located in America, China, Morocco, Western Africa, the Middle East, Russia and South Africa. The

industry uses phosphate rocks as the main source for the production of mineral fertilizers in average of 80%, for detergents about 12%, for foodstuffs for animal around 5% and other special applications approximately 3% [21].

Phosphates enter surface water and groundwater from two basic sources: agriculture and liquid urban wastes as well as sewage disposal [22]. The end-products of the phosphate industry are also introduced in the environment via sewage discharges; if they have not been reduced appropriately [23]. As a result this current practice has led to face an environmental problem of phosphorus.

Nitrogen in gas state (N_2) represents the 7% of the earth´s atmosphere. Around the world rarely nitrogen has been accumulated in large mineral deposits, as in Chile where is a huge sodium nitrate deposit. Meanwhile in natural environment nitrogen is cycled through food chain continuously. Nitrogen changes its form via the nitrogen cycle in ecological systems [24]. So, atmospheric nitrogen has to be converted into others forms to be used by plants and animals. The fixation process as well as electrical discharges transforms the atmospheric nitrogen. So through rainwater nitrogen reaches the earth´s surface where plant roots absorbed it from soil and water. Finally, nitrogen is returned to soil through animal urine and feces in high content [3]. Also the runoff of fertilized farmlands allows ammonium and nitrates to reach rivers and lakes. This is known that fertilizer contribute with 82 Tg/year of reactive nitrogen [12].

Based on the population and economic growth, urbanization, development of sewage systems, and waste water treatment installations, there have been projected a rapid increase in global sewage emissions. Then the tendencies for nitrogen and phosphorus discharges are predicting for a rising from 6.4 Tg of N and 1.3 Tg of P per year in 2000 to 12.0–15.5 Tg of N and 2.4–3.1 Tg of P per year in 2050 [25].

Waste water is nowadays a sustainable and economical source of water for cities that can be used further applications [26]. In addition, the avoiding of the environmental problem of eutrophication and the possible depletion of phosphorus makes necessary to recycle these valuable elements. Besides, it should be considered the nitrogen and phosphorus deficiency in soil that implicate the widely use and application of synthetic inorganic fertilizers [12].

Therefore, the simultaneous removal and recovery of these nutrients is an opportunity to obtain materials with soil amendment purposes to satisfy the food demand caused by the increasing global population [27].

1.5. Conventional technologies for phosphorus and nitrogen removal

The secondary treatments in waste water treatment plants removes some nitrogen and phosphorus; however further specific processes are need to reduce them. Nitrification and denitrification is used for nitrogen removal, while biological processes and chemical precipitation are applied for phosphorus removal [1]. Usually the waste water treatment effluent contains 5-10 mg N/L of total nitrogen and 2 to 7 mg/L of total phosphorus [9].

1.5.1. Nitrogen removal processes

1.5.1.1. Nitrification

Nitrification is a biological process where mainly two bacteria genera are the responsible. This occurs in two-step process; in a first step ammonia is converted to nitrite by *Nitrosomonas*; in the second step nitrite is converted to nitrate by *Nitrobacter*. The nitrifying bacteria are sensitive to the culture temperature, dissolved oxygen, pH and the presence of toxic substances. The ammonium and nitrite oxidizers can develop biochemical activity in an environment containing dissolved oxygen [9].

1.5.1.2. Denitrification

Denitrification is a biological reduction from nitrate to nitrite and then to nitrogen gas. In this process nitrite and nitrate act as electron acceptors due to denitrification occurs only in anaerobic conditions. Depending on the bacteria specie either nitrous oxide or nitrogen gas can be the end products. Nutrients as phosphate, sulfate, chloride, sodium, potassium, magnesium and calcium are required by the denitrifying bacteria growth [9].

1.5.1.3. Nitrification and Denitrification

Biological nitrogen removal can be performed into one single-stage sludge and two-stage sludge systems. Nitrification can be accomplished by suspended-growth or attached-growth systems. In two-stage sludge nitrification is performed in aerobic reactor for carbon oxidation and then nitrification is achieved in a separate anoxic reactor. The two-stage sludge has the great advantage of protection against most of toxicants and low ammonia flow can be expected [16].

1.5.1.4. Emerging biological processes

The conventional biological nitrogen removal processes implies time and space for the separation of two phases. However, there have been developed new processes for sustainable, space-saving, less organic requirements and energy consumption

[16]: a) nitrite route allows a direct nitrification from nitrite; b) aerobic denitrification by using specific bacteria species; c) denitrification by autotrophic nitrifies; d)heterotrophic nitrification and e) anaerobic ammonia oxidation.

1.5.2. Phosphorus removal processes

1.5.2.1. Chemical processes

The classical chemical treatment method for phosphorus removal is based in the addition of iron or aluminum salts and lime. Then iron/aluminum phosphorus complexes are formed and precipitate as result of the combination with the free orthophosphate forms (e.g. $H_2PO_4^-$ and HPO_4^{-2} at the typical pH values of waste waters). Conventionally salts such as ferric chloride and aluminum chloride are used for this process to ferric and aluminium phosphates. When lime is used the main mechanism involves the formation of hydroxyapatites ($Ca_5(OH)(PO_4)_3$). However, there are two significant disadvantages associated to this strategy: a certain overdosing of metal salts is necessary to obtain the required low effluent phosphorus values, resulting in a high cost of chemicals; and the accumulation of ions (increased salinity) may seriously restrict the reuse possibilities of the effluent [9].

1.5.2.2. Biological processes

The phosphorus content in waste water is partially removed in the conventional activated sludge system for nitrogen removal. However enhanced biological phosphorus removal (EBPR) has been used when phosphorus needs to be removed from waste water containing high nutrient levels. Several biological suspended growth process configurations have been used to accomplish biological phosphorus removal, and they all include the basic steps of an anaerobic zone followed by an aerobic zone [16]. The biological phosphorus removal (BPR) configurations that are more commonly used are *Phoredox*, A/O^{TM}, A^{2}O^{TM}, SBR with biological phosphorus removal and pHoStrip processes [9].

1.5.3. Technologies for phosphorus and nitrogen recovery

Nowadays, the development of systems for the reduction of nutrients concentrations to trace levels is the main concern of waste water treatment facilities. However they have not been implemented at real scale yet, but some experimental works and pilot plants have been developed about. So, adsorption is recognized as an efficient and selectively technique for target compounds recovery from aqueous solutions. It is based on the accumulation of a solute at the interface between the adsorbent and adsorbate phases. It could be associated to weak Van der Waals forces as physical

adsorption. Also, chemisorption could occurr by interaction between adsorbent and adsorbate molecule. Ion exchange process is also used for pollutants removal purposes where the ionic species are exchanged between an electrolyte solution and a complex.

1.5.3.1. Selective phosphorus recovery

The use of weak-base and strong-base anion exchangers resins has been reported for phosphate removal from waste water. The flow rate, concentration, water hardness, competitive ions and suspended solids conditioned their efficiency [28]. The main advantages over other kind of adsorbents are the chemical stability and a durable physical structure, so they could be regenerated and reused [29].

Also, polymeric ligand exchangers (PLE) or hybrid anion exchangers (HAIX) have been developed for the phosphate removal due to their selectivity over competing sulfate and chloride ions [30]. They are composed by a polymeric supporting matrix and a transition metal which are immobilized and act as the functional group.

Other approaches for phosphorous recovery have been developed by means of precipitation and crystallization of struvite ($MgNH_4PO_4(s)$). The struvite is a profitable by-product with low chemicals reagents cost and slow release properties to be used for fertilizing applications. However, the formation of struvite deposits in pipes, pumps and screens in waste water treatment plants are associated problems.

Therefore, considerable attention has been paid to developing effective and low-cost adsorbents from natural and synthetic minerals for phosphate adsorption with agricultural reuse potential.

1.5.3.2. Selective nitrogen recovery

The use of ion exchangers is an important method for nitrogen recovery in the ammonium form. This is associated with short contact time, low operational costs and the further use as nitrogen source in fertilizers. Zeolites in natural and synthetic forms are associated with high cation exchange capacity (CEC). They are hydrated aluminosilicates with three-dimensional framework [31]. The substitution of an aluminum (Al^{3+}) ion for silicon (Si^{4+}) generates one negative charge which is balanced by the exchangeable cations like sodium, potassium, calcium, etc. The main types of zeolites are: mordenite, clinoptilolite, erionite, chabazite and phillipsite [32]. Conventionally, natural zeolites need to be purified and modified in order to improve its ion-exchange and adsorption properties for ammonium remove. Also, other synthetic cation exchange materials as the strong acid cation (SAC) and the

weak acid cation (WAC) polymeric exchange resins have been developed for this purpose [33].

1.5.3.3. Selective simultaneous phosphorus and nitrogen recovery

In the last years many materials have been evaluated for the individually phosphate and ammonium removal. However, the simultaneous removal of ammonium and phosphate is not often reported although both nutrients need to be removed from waste water. In the common practice it implies the combination of a cation and anion exchanger, or a cation exchanger and an inorganic precipitant species. However, natural and synthetic zeolites could be used as bifunctional adsorbents for this purpose that include or not regeneration stages. A loaded ammonium natural zeolite was used as seed for the precipitation of calcium phosphate [34]. Also, the synthetic zeolites from coal fly ash (CFA) have been used for the simultaneous ammonium and phosphate removal for waste water treatment [35]. Some modification procedures have been performed in order to improve the sorption capacity of both natural and synthetic forms of zeolite. Particularly, the incorporation of metal species that promote the formation of hydrated oxides composites at zeolite surfaces has been identified as a suitable alternative [36].

1.6. References

1. Libhaber, M. and Á. Orozco-Jaramillo, *Sustainable treatment and reuse of municipal wastewater*2012, United Kingdom: IWA Publishing.
2. Sincero, A. and G. Sincero, *Physical-Chemical Treatment of Water and Wastewater*2003, United States of America: IWA Publishing.
3. Girard, J., *Principles of Environmental Chemistry*2010, United States of América: Jones and Bartlett Publishers.
4. Bitton, G., *Wastewater Microbiology*. Fourth ed2011, United States of America: Wiley-Blackwell.
5. Russell, D., *Practical wastewater treatment*2006, Canada: John Wiley & Sons.
6. Crites, R., J. Middlebrooks, and S. Reed, *Natural wastewater treatment systems*2006, United States of america: Taylor & Francis.
7. Alshameri, A., et al., *An investigation into the adsorption removal of ammonium by salt activated Chinese (Hulaodu) natural zeolite: Kinetics, isotherms, and thermodynamics.* Journal of the Taiwan Institute of Chemical Engineers, 2014. **45**(2): p. 554-564.

8. Rahmani, A.R., M.T. Samadi, and H.R. Ehsani, *Investigation of clinoptilolite natural zeolite regeneration by air stripping followed by ion exchange for removal of ammonium from aqueous solutions.* Iranian Journal of Environmental Health Science & Engineering, 2009. **6**(3): p. 167-172.
9. Van Haandel, A. and J.G.M. Van der Lubbe, *Handbook of Biological Wastewater Treatment: Design and optimisation of activated sludge systems*2012, United Kingdom: IWA Publishing.
10. Raicevic, V., et al., *Eutrophication: Status, Trends and Restoration Strategies for Palic Lake*. Water Treatment2013.
11. Zhao, Y., et al., *Removal of phosphate from aqueous solution by red mud using a factorial design.* Journal of Hazardous Materials, 2009. **165**(1-3): p. 1193-1199.
12. Mosier, A., K. Syers, and J. Freney, *Agriculture and the Nitrogen cycle*2004, United States of America: SCOPE.
13. Goel, P.K., *Water pollution Causes, Effects and Control*2006, India: New Age International Publishers.
14. Sen, B., et al., *Relationship of Algae to Water Pollution and Waste Water Treatment*. Water Treatment2013.
15. Jellali, S., et al., *Phosphate mine wastes reuse for phosphorus removal from aqueous solutions under dynamic conditions.* Journal of Hazardous Materials, 2010. **184**(1-3): p. 226-233.
16. Liu, Y., L. Qin, and S.-F. Yang, *Microbial Granulation Technology for Nutrient Removal from Wastewater*2007, United States of America: Nova Science Publishers.
17. Segneanu, A.E., et al., *Waste Water Treatment Methods*. Water Treatment2013.
18. Peleka, E.N. and E.A. Deliyanni, *Adsorptive removal of phosphates from aqueous solutions.* Desalination, 2009. **245**(1–3): p. 357-371.
19. Valsami-Jones, E., *Phosphorus in Environmental Tehnology Principles and Applications*2004, United Kingdom: IWA Publishing.
20. Bradford-Hartke, Z., P. Lant, and G. Leslie, *Phosphorus recovery from centralised municipal water recycling plants.* Chemical Engineering Research and Design, 2012. **90**(1): p. 78-85.

21. Notholt, A.J.G., R.P. Sheldon, and D.F. Davidson, *Phosphate deposits of the world*. Vol. 2. 2005, United States of America: Cambridge University Press
22. Deliyanni, E.A., E.N. Peleka, and N.K. Lazaridis, *Comparative study of phosphates removal from aqueous solutions by nanocrystalline akaganéite and hybrid surfactant-akaganéite.* Separation and Purification Technology, 2007. **52**(3): p. 478-486.
23. Cooper, J., et al., *The future distribution and production of global phosphate rock reserves.* Resources, Conservation and Recycling, 2011. **57**: p. 78-86.
24. Kuzawa, K., et al., *Phosphate removal and recovery with a synthetic hydrotalcite as an adsorbent.* Chemosphere, 2006. **62**(1): p. 45-52.
25. Van Drecht, G., et al., *Global nitrogen and phosphate in urban wastewater for the period 1970 to 2050.* Global Biogeochemical Cycles, 2009. **23**(4): p. GB0A03.
26. Sharma, S. and R. Sanghi, *Wastewater reuso and managment*2013, London: Springer.
27. Cordell, D., et al., *Towards global phosphorus security: A systems framework for phosphorus recovery and reuse options.* Chemosphere, 2011. **84**(6): p. 747-758.
28. Awual, M.R., et al., *A weak-base fibrous anion exchanger effective for rapid phosphate removal from water.* Journal of Hazardous Materials, 2011. **188**(1–3): p. 164-171.
29. Sarkar, S., et al., *Hybrid ion exchanger supported nanocomposites: Sorption and sensing for environmental applications.* Chemical Engineering Journal, 2011. **166**(3): p. 923-931.
30. Sengupta, S. and A. Pandit, *Selective removal of phosphorus from wastewater combined with its recovery as a solid-phase fertilizer.* Water Research, 2011. **45**(11): p. 3318-3330.
31. Huang, H., et al., *Ammonium removal from aqueous solutions by using natural Chinese (Chende) zeolite as adsorbent.* Journal of Hazardous Materials, 2010. **175**(1–3): p. 247-252.
32. Widiastuti, N., et al., *Removal of ammonium from greywater using natural zeolite.* Desalination, 2011. **277**(1–3): p. 15-23.
33. Malovanyy, A., et al., *Concentration of ammonium from municipal wastewater using ion exchange process.* Desalination, 2013. **329**: p. 93-102.

34. Karapınar, N., *Application of natural zeolite for phosphorus and ammonium removal from aqueous solutions.* Journal of Hazardous Materials, 2009. **170**(2–3): p. 1186-1191.
35. Xie, J., et al., *Synthesis of Zeolite/Aluminum Oxide Hydrate from Coal Fly Ash: A New Type of Adsorbent for Simultaneous Removal of Cationic and Anionic Pollutants.* Industrial & Engineering Chemistry Research, 2013. **52**(42): p. 14890-14897.
36. Xie, J., et al., *Synthesis and properties of zeolite/hydrated iron oxide composite from coal fly ash as efficient adsorbent to simultaneously retain cationic and anionic pollutants from water.* Fuel, 2014. **116**(0): p. 71-76.

Chapter 2 Objective and methodology

2.1. Objective

The general objective of this Ph.D. thesis is the evaluation of phosphate and ammonium valorization by using impregnated inorganic ion – exchangers from waste waters. The reactive sorbents were prepared by using a natural zeolite, having clinoptilolite as main mineral phase, as ammonium sorbent, and then properly modified by impregnation with hydrated metal oxides to extract phosphate ions.

Two different technological scenarios were defined for the implementation of the developed materials:

a) Use of granular forms of the impregnated zeolite material to work on sorption-desorption cycles to produce concentrated effluents of ammonium and phosphate ions that could be used to produce struvite or other ammonium and phosphate sources for fertilizers production
b) Use of powder forms of impregnated zeolite material in the potassium form, to be used as carriers of N,P,K for applications on agriculture, forestry or rehabilitation of degraded soils (e. mining areas). In this second alternative the zeolitic material will not be reused

The evaluation of the materials efficiency was carried out using municipal secondary waste water streams from Municipal Waste water Treatment Plants of the Barcelona Metropolitan Area. The reduction of the presence of both inorganic pollutants is focused on close their loop on nature minimizing wastes generation. As well as, the challenges of reusing waste water is comply with local legislation and contribute with environmental protection. The thesis scheme is detailed in Figure 2.1, where the valorization of these wastes is considered through the use of loaded sorbents as slow release fertilizer products in agricultural applications.

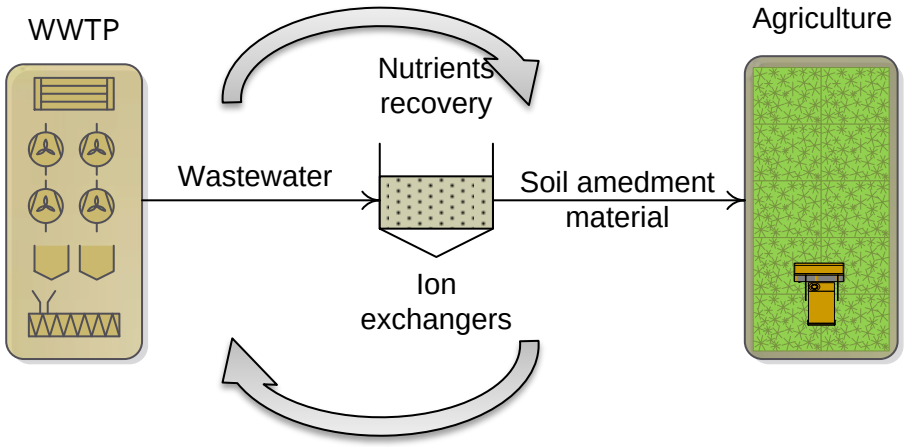

Figure 2.1. Thesis diagram scheme: phosphate and ammonium removal and valorization by ion exchangers

The aim this work is to develop synthetic routes for modification of natural zeolites by using hydrated metal oxides to provide them sorption properties for the simultaneous removal of phosphate and ammonium ions. This study is devoted to evaluate the developed materials through batch and column laboratory assays, and their feasibility of removal of both pollutants by sorption and desorption cycles.

2.2. Specific objectives

The specific objectives of this thesis are:

1. To synthesize supported hydrated metal hydroxides on natural zeolites in granular and powder forms.
2. To determine chemical, physical and mineralogical characterization of the natural and modified zeolites.
3. To study the influence of pH and competing ions on the removal capacity of modified zeolites.
4. To determine the equilibrium sorption and desorption parameters of the impregnated zeolites in batch experiments.
5. To evaluate the kinetic sorption parameters of the impregnated zeolites in batch experiments.
6. To determine the zeolites performance on sorption and desorption cycles by column experiments using impregnated granular zeolites in the sodium form.
7. To evaluate the sorption capacity of impregnated powder zeolites in the potassium form using secondary domestic waste water effluent.

8. To characterize the speciation of phosphorus in the loaded zeolites and evaluate the soil bioavailability of loaded zeolites.
9. To study of the release rate of loaded N-P-K powder zeolites using column experiments with soils/zeolites amendment mixtures
10. To evaluate the release of toxic elements from loaded zeolite samples.

2.3. Case study as ammonium and phosphate source

The El Prat de Llobregat waste water treatment plant at Barcelona, Spain was designed for a population of 2'275.000 equivalent inhabitants and 420.000 m^3 / day of average flow. In this waterwork the processes described on Figure 2.2. treat domestic and industrial waste water. The use of stages of nitrification – denitrification and the sludge anaerobic digestion stage contribute to the conservation of water resources of Llobregat River and the coast.

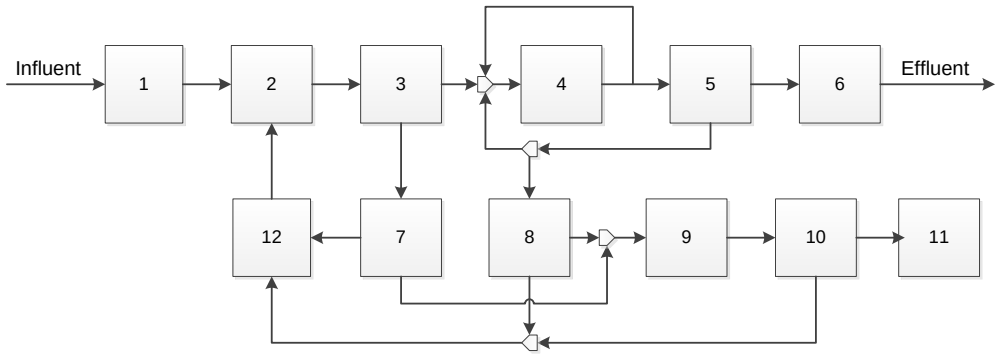

1. Pretreatment
2. Grit and grease removal
3. Primary clarifier
4. Bioreactor
5. Secondary clarifier
6. Effluent pumping
7. Primary sludge thickener
8. Secondary sludge thickener
9. Anaerobic digester
10. Dewatering of digested sludge
11. Sludge dryer
12. Return to the head of plant

Figure 2.2. Flow sheet of El Prat de Llobregat WWTP at Barcelona, Spain.

The effluent stream as well as the dewatering digested sludge side stream has been identified as potential streams for phosphate and ammonium recovery. However in this study samples used were sampled at the outlet of the secondary treatment in the main water treatment line.

Chapter 3 Simultaneous phosphate and ammonium removal from aqueous solution by a hydrated aluminum oxide modified natural zeolite

Abstract

A natural zeolite (Z-N), rich in clinoptilolite, was modified (Z-Al) by incorporation of hydrated aluminum oxide (HAlO) for the simultaneous phosphate and ammonium removal. The incorporation of surface hydroxyl groups (≅Al-OH) into the zeolite structure, as active groups for phosphate removal, was characterized by acid-base titrations (pH_{PZC}=4.5±0.2). The phosphate sorption increases from 0.6 mg-P/g for Z-N up to 7.0 mg-P/g while only a slight decrease on the ammonium sorption capacity from 33 mg-N/g of Z-N to 30 mg-N/g for Z-Al was observed. The HAlO modified zeolite sorption capacity for both phosphate and ammonium was slightly reduced by common ions typically present in secondary waste water effluents. Column experiments revealed higher enrichment factor for ammonium (120) than for phosphate (50) using 1 M NaOH as elution solution. A reduction of zeolite phosphate capacity with regeneration cycles was observed.

Keywords: clinoptilolite; natural zeolite; modification; hydrated aluminum oxide; adsorption; kinetic

3.1. Introduction

Nitrogen and phosphorus are essential nutrients for all living forms. However, an excessive growth of algae and the consequently depletion of the dissolved oxygen is an effect of the nutrient overloading (phosphate and ammonium) in natural water bodies [1, 2]. Therefore, it has become a great challenge addressed to the simultaneous removal of both species (phosphate and ammonium) to avoid the consequences of eutrophication processes. Natural and synthetic zeolites have been widely studied for ammonium removal due to its high cationic exchange property [1, 3, 4] and they have been postulated as promissory materials for its removal from waste waters [5-8]. Zeolites and their modified forms have been widely used as effective adsorbents for waste water treatment according to their mechanical and thermal properties, capability of cation-exchange and significant worldwide occurrence. Additionally, the safety, easy operation and maintenance, low treatment costs, high selectivity and the release of non-toxic exchangeable cations (K^+, Na^+, Ca^{2+} and Mg^{2+}) make zeolites an attractive alternative [3, 9, 10]. Zeolite are hydrated crystalline aluminum-silicate materials with a framework structure where micro- and mesopores located by water and typically alkaline cations [11]. However, they have been rarely used for phosphate sorption due to the constant negative charge on their surface [12]. In order to improve the ion exchange capacity of natural zeolites for anionic species the incorporation or impregnation of iron and aluminum oxides, are the most widespread and excellent candidates for phosphate removal [13-18]. Zeolites exhibit different properties which depend on the geological location and they deserve a detailed characterization [19, 20]. This study describes the modification of a Slovakian natural zeolite (clinoptilolite) with Al (III) to enhance the formation of hydrated aluminum oxide (HAIO) onto the zeolite structure. Utilization of hydrated aluminum oxide in treatment processes cause difficulties in separation due to their small sizes that could be overcome by its impregnation into zeolite porous particles. No previous studies have been found about the hydrated aluminum oxide modification of a natural clinoptilolite for the simultaneous removal of both nutrients. Therefore, the findings of the present work provide insight into the simultaneous phosphate and ammonium sorption potential of hydrated aluminium oxide supported on a clinoptilolite and its regeneration for re-use in sorption and desorption cycles as low cost materials for industrial and domestic waste water treatment applications. The objectives of this study are: (i) synthesize supported hydrated aluminum

hydroxide zeolites, (ii) characterize the modified zeolite, (iii) study the influence of pH and ions concentration on zeolites removal capacity, (iv) determine the equilibrium and kinetic sorption parameters, (v) determine the sorption selectivity in front of common ions in waste waters effluents and, (vi) evaluate their performance (sorption and desorption) on column experiments.

3.2. Materials and methods

3.2.1. Impregnation of hydrated aluminum oxide onto a natural zeolite

A natural zeolite (Z-N) obtained from Zeocem Company, Slovak Republic was used. Samples were washed with deionized water and dried in an oven at 80 °C for 24 hours. Particles below 200 μm mesh were used for batch experiments and particles between 800 – 1200 μm mesh were used for column experiments. Z-N was modified to the aluminum form by using an adaptation of the method reported by Jiménez-Cedillo [14]. Thirty grams of natural zeolite were treated with 250 mL of NaCl (0.1 M) two consecutive times under reflux conditions for 4 hours. Then, the zeolite in the sodium form (Z-Na) was washed with ~1500 mL of deionized water until no chloride was detected by the $AgNO_3$ test. Thirty grams of sodium zeolite (Z-Na) were treated two consecutive times with 250 mL of $AlCl_3$ (0.1 M) under reflux for 4 hours. The aluminum zeolite (Z-Al) was washed using ~1500 mL of deionized water until no chloride was detected by the $AgNO_3$ test. Finally, it was dried in an oven at 80 °C for 24 hours.

3.2.2. Physicochemical characterization of the zeolites

Z-N, Z-Na and Z-Al were characterized by X-ray diffraction (XRD) using a powder X-ray Diffractometer (D8 Advance A25 Bruker). Samples morphology and chemical composition were analyzed by a Field Emission Scanning Electron Microscope (FSEM) (JEOL JSM-7001F) coupled to an Energy Dispersive Spectroscopy system (Oxford Instruments X-Max). Samples composition reported are the average of at least four analyses for each sample. Infrared absorption spectra were recorded with a Fourier Transform FTIR 4100 Jasco spectrometer in the range of 4000 – 550 cm^{-1} range. The specific surface area of Z-N and Z-Al was determined by the nitrogen gas sorption method on an automatic sorption analyzer (Micrometrics). The essays were replicated four times for each sample and the average data are reported. The point of cero charge (PZC) of Z-N and Z-Al was determined by the pH drift method [21, 22]. An amount 0.1 g of zeolite was equilibrated in 25 mL of deionized water and 0.01 and 0.05 M NaCl solutions (pH from 2 to 11) for 24 hours at 200 rpm and 21±1 °C. The

final pH was measured in a Crison GLP21 potentiometer, and the PZC was determined as the pH at which the addition of the sample did not induce a shift in the pH ($DpH=pH_f-pH_i=0$). The CIP method, common intersection point of potentiometric titration curves obtained at three ionic strengths was also used [23-25]. An amount of 0.1 g of zeolite was equilibrated with 25 mL of solution at three different ionic strengths (0.01, 0.05 and 0.1 M NaCl) during 24 h at 200 rpm and 21±1°C. After the equilibration the suspension was basified to pH 11 using 0.1 M NaOH. The suspension was titrated until pH ≈ 3, with 0.01 M HCl using an automatic titrator (Mettler Toledo). The net surface charge is correlated with PZC from the titration data for the adsorbed amounts of $[H^+]$ and $[OH^-]$ ions. Therefore, titration curves of different ionic strength would intersect at pH = pH_{PZC}. The surface charge was calculated from the Eq. 1 [26].

$$\boldsymbol{b = C_b - C_a + [H^+] - [OH^-]} \qquad (1)$$

where: b (mol/g) is the net hydroxide ions consumed, C_b and C_a (mol/L) are the base and acid concentrations, respectively and $[H^+]$ and $[OH^-]$ denote the protons and hydroxide concentration calculated from the measured solution pH for a given mass of zeolite (g) and a given volume of volume of solution (L). All measurements were performed in triplicate and the average value was reported.

3.2.3. Equilibrium and kinetic batch sorption studies

Batch equilibrium sorption experiments were carried out using standard batch methodology described elsewhere [8]. Given volumes (25 mL) of phosphate (P) and ammonium (N) aqueous solutions were shaken overnight with weighed amounts of dry samples (particle size < 200 μm) in polyethylene tubes using a continuous rotary mixer. Three different types of experiments were conducted:

i) Sorption capacity as function of phosphate and ammonium concentration: 0.25 g of Z-N and Z-Al samples were added to solutions in the concentration range: 1 - 2000 mg-P/L and 10 – 5000 mg-N/L, without pH adjustment.

ii) Sorption capacity as function of equilibrium pH: 0.1 g of Z-Al sample was equilibrated in solutions containing 25 mg-P/L and 25 mg-N/L. The pH was adjusted from 2 to 11 (using 0.1 M HCl/NaOH).

iii) Sorption capacity as function of phosphate and ammonium concentration in the presence of individual and mixtures of common competing ions present on waste water effluents: 0.1 g of Z-Al sample is added to 25 mg-P/L, 25 mg-N/L and individual competing ion (25 mg/L) solutions without pH adjustment. Also, the interference ions

concentrations were fixed taking as reference the average annual composition of the stream from a tertiary treatment including a reverse osmosis step at the El Prat waste water treatment plant (Barcelona – Spain). The anions solution composition was: chloride (625 mg/L), bicarbonate (325 mg/L), sulphate (200 mg/L) and nitrate (30 mg/L) (prepared from the corresponding sodium salts). The cations solution composition was: sodium (260 mg/L), calcium (160 mg/L), magnesium (50 mg/L) and potassium (40 mg/L) (prepared from corresponding chloride salts).Then, 0.25 g of Z-Al sample was equilibrated in solutions ranging 1 - 2000 mg-P/L and 10 – 5000 mg-N/L and the mixture of competing ions.

iv) Batch kinetic sorption experiments were performed by addition of 0.1 g of Z-Al in solution containing 20 mg-N/L and 10 mg-P/L. Tubes were withdrawn sequentially at given times. All tests were performed by triplicate at 200 rpm and room temperature (21±1 °C) and the average data are reported. Before to be analyzed samples were centrifuged for 10 min and filtered using cellulose nitrate membrane filters (45 µm). The total concentrations of phosphate and ammonium ions in the initial and remaining aqueous solution were determined.

3.2.4. Phosphate speciation in loaded Z-Al samples by fractionation assays

The phosphorus speciation was performed based on an adaptation of the sequential extraction protocol [27] with three extraction steps. Z-Al samples (0.25 g) were equilibrated in 25 mL of solution containing 25 mg-P/L at 200 rpm for 24 h. Loaded samples were filtered, washed with deionized water and dried. The fraction of loosely bound phosphorus was extracted in two consecutive extractions by 0.25 g of loaded Z-Al sample in 20 mL of 1 M NH_4Cl at pH 7. Then, the phosphorous bound to iron and aluminum components was determined by means of two consecutive extractions in 20 mL of 0.1 M NaOH followed by extraction in 1 M NaCl. In the third step, the potential content of phosphorus immobilized in the form of calcium and magnesium was extracted in two consecutive times in 20 mL of 0.5 M HCl. Finally, residual content is determined by the mass balance between the phosphorus adsorbed and the extracted fractions. Tests were performed in triplicate at 21±1 °C and the average values are reported.

3.2.5. Phosphate and ammonium batch desorption studies

Samples of Z-Al (0.5 g < 200 µm) were saturated in 25 mL of solution containing 25 mg-P /L and 25 mg-N/L at 200 rpm for 24 h. Z-Al samples were separated by filtration and rinsed several times with deionized water for the desorption trials. The

desorption studies were performed by adding 0.5 g of the saturated zeolite into 25 mL of elution solution at 200 rpm for 24 h. Solutions of NaOH (1 M), $NaHCO_3$ (0.1 M), Na_2CO_3 (0.1 M) and $NaHCO_3$/Na_2CO_3 (0.1 M) were evaluated. Tests were performed in two sorption – desorption cycles by triplicate at 21±1 °C and average values are reported.

3.2.6. Phosphate and ammonium sorption and desorption column studies

Samples of Z-Al (<800 µm particles) were packed in a glass column (15mm inner diameter and 100mm length). Initially, the column was equilibrated with ~20 BV of deionized water. The feed composition was established taking as reference the expected values of effluents streams after secondary treatment from the El Prat waste water treatment plant (Barcelona – Spain). The feed solution composition was: phosphate (12.5 mg/L), ammonium (25 mg/L), chloride (312.5 mg/L), bicarbonate (162.5 mg/L), sulphate (10 mg/L), nitrate (15 mg/L), sodium (130 mg/L), calcium (80 mg/L), magnesium (25 mg/L) and potassium (20 mg/L). The solution with and without competing ions was supplied in countercurrent through the column at EBHRT of 4 minutes. After saturation the Z-Al was regenerated with 1 M NaOH solution at EBHRT of 13 minutes.

3.2.7. Analytical methods

Phosphate (P) and ammonium (N) concentration were determined based on the Standard Methods [28]. P-PO_4^{3-} was determined by the vanadomolybdophosphoric acid colorimetric method (4500-P C) in a Shimadzu UVmini-1240 UVvis spectrophotometer. N-NH_4^+ was determined by the ammonia-selective electrode method (4500-NH3 D). A Hach 51927-00 ammonia gas sensing gas combination electrode was used for this purpose. Ions were determined using a Thermo Scientific Ionic Chromatograph (Dionex ICS-1100 and ICS-1000). On the completion of the batch experiments, samples of the loaded zeolites were examined by field scanning electron microscope (FSEM-EDX) and mineral phases were identified by X-Ray Diffractometry (XRD).

3.3. Results and discussion

3.3.1. Materials characterization of hydrated aluminum oxide zeolites

Clinoptilolite was found to be the major component of Z-N, but also small amounts of other crystalline phases as quartz and albite were detected. In this study Z-Na is considered as an intermediary step of the zeolite modification process, due to the easily sodium removal in ion exchange applications [29]. The presence of crystalline

aluminum phases (e.g. hydrated aluminum oxide) was not identified in Z-Al samples as it was described by Jimenez-Cedillo about the formation of amorphous oxide species on a modified zeolite surface [14, 15, 30]. For Z-Al only differences on the reflexions intensity but not on their positions were observed. This fact is attributed to the occupation of aluminum ions in the cation exchange sites of the zeolitic structure after the $AlCl_3$ treatment. However, some characteristic reflexions (2θ at 9.9°, 11.2°, 17.3°, 22.5° and 32.0°) for clinoptilolite were not affected through modification of Z-Na and Z-Al. The specific surface area of Z-N is slightly reduced from 19.8±0.3 m^2/g to 17.8±0.1 m^2/g of Z-Al as consequence of the impregnation of hydrated aluminum oxide and the interaction between compensating cations (e.g. Al(III)) and water molecues which are coordinated in the zeolite framework [31].

The FSEM – EDX analyses revealed the presence of O, Na, Mg, Al, Si, K, Ca and Fe as the main elements on the zeolites composition (Table 3.1). In Z-Na, the sodium content increase from 0.4 % to 1.5 % and a decrease of potassium and calcium content was observed due to the exchange with sodium ions. As well as, in Z-Al the aluminum content increased from 5.3 % to 6.3 % with a reduction of sodium and magnesium content was observed from 1.5 % to 0.9 % and 0.4 % to 0.2 % as consequence of the ion exchange occur between these cationic species and aluminum.

Element	Z-N	Z-Na	Z-Al
O	57.8 ± 2.6	60.3 ± 1.4	58.1 ± 1.5
Na	0.3 ± 0.0	1.5 ± 0.1	0.9 ± 0.3
Mg	0.4 ± 0.1	0.4 ± 0.0	0.2 ± 0.2
Al	5.3 ± 0.2	5.3 ± 0.0	6.3 ± 0.4
Si	29. 7 ± 1.7	29.1 ± 1.5	30.3 ± 0.5
K	2.9 ± 0.5	1.8 ± 0.2	2.2 ± 0.3
Ca	1.9 ± 0.3	1.1 ± 0.1	1.3 ± 0.5
Ti	0.2 ± 0.2	< loq*	< loq*
Fe	1.6 ± 0.4	0.5 ± 0.0	1.1 ± 0.3

*loq: limit of quantification

Table 3.1. Chemical composition (wt. %) of the zeolitic materials: Natural zeolite (Z-N), sodium zeolite form (Z-Na) and hybrid hydrated aluminum oxide zeolite (Z-Al).

FSEM images showed the networks of crystal clusters for the Z-N with homogeneous crystal size distribution. It is observed for clinoptilolite the characteristically plate-like

morphology crystals and large cavities and entries to the channels inside the zeolite framework in accordance to previous reports [32]. The existence of lamellar crystals and small particles covering the surface was observed in Z-Na and Z-Al confirms the surface modification achieved in the clinoptilolite after the sodium and aluminum treatments.

The acid - base characterization provides a pH_{PZC} of 4.5±0.2 for Z-Al (Figure 3.1) by both methods employed in comparison with Z-N with a value of 5.2±0.2. The decrease of the pH_{PZC} suggests that Z-Al become more acid as an effect of formation of hydrated aluminum oxide onto the zeolite after the modification with Al (III) salt. The determined pH_{PZC} is in agreement with reported values for natural zeolite (clinoptilolite) supporting mono Fe(II) (Z-Fe(II)), Al (Z-Al) and bimetallic Fe-Al (Z-Fe/Al)) with pH_{PZC} values of 4.2, 4.6 and 5.2, respectively [13]. It is also in aggrement with pH_{PZC} for α-$Al(OH)_3$(s) (pH_{PZC} 5.0) but far from the values reported for α-Al_2O_3(s) (pH_{PZC}=9.1) and for γ-AlOOH(s) (pH_{PZC}=8.2) [33].

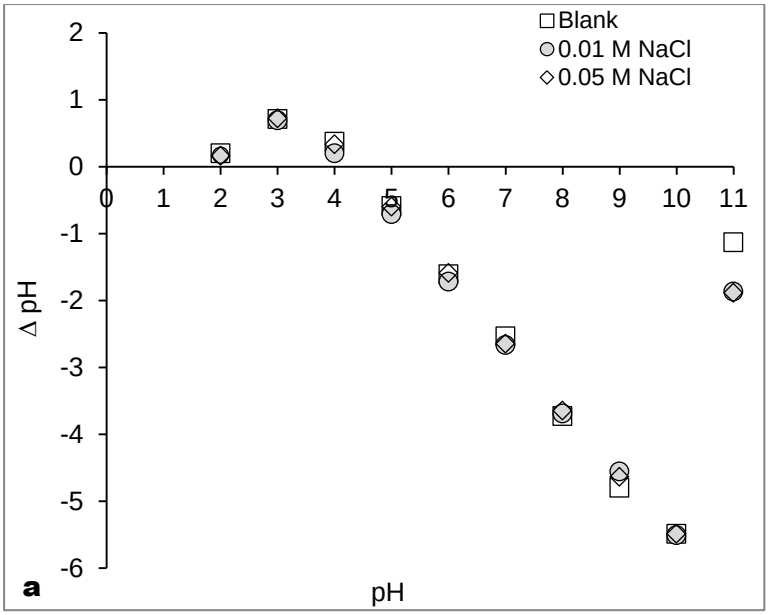

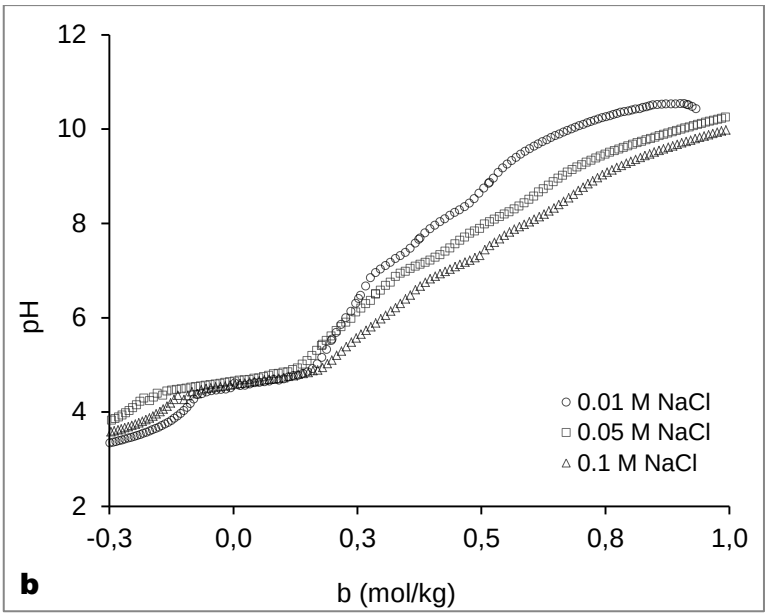

Figure 3.1. a) Plot of pH_{final}− $pH_{initial}$ vs initial pH of Z-Al with and without electrolyte NaCl and b) Potentiometric titration curve for Z – Al, at 0.01, 0.05 and 0.1 M NaCl.

In FTIR spectra for Z-N, Z-Na and Z-Al, peaks between 798 cm^{-1} and 547 cm^{-1} are assigned to deformation vibration of OH, Al-O-Si and Si-O-Si groups. The band at ~1100 cm^{-1} is attributed to the stretching vibration of Si–O groups and the one at ~1630 cm^{-1} represents the deformation vibration of water. The peaks in the range from 3700 cm^{-1} to 3100 cm^{-1} have been associated to the hydroxyl groups of the zeolitic structure [11, 34]. The small differences in the spectra for Z-N and Z-Na are consistent with the ion exchange reactions between cations of the same valence [35]. Contrary, after the modification with a trivalent cation (Al (III)) important changes in the zeolite structure are observed on the Z-Al spectra, with new peaks at 1396 cm^{-1}, 1455 cm^{-1} and 1541 cm^{-1} associated with the presence of the surface hydroxide groups (≅AlOH) [36-38]. The shift of the band at ~3396 cm^{-1} in the Z-N spectra and the new band at 3616 cm^{-1} on Z-Al spectra are attributed to hydroxyl groups associated with tetrahedral framework aluminum and octahedral non-framework aluminum oxide species [39, 40]. It results in the formation of cationic OH groups and bridging OH groups which are situated in the channels of zeolite as well as at the outer surface of particles [41]. All these changes confirm the formation of aluminum hydroxyl groups which promote the acidity increase of natural clinoptilolite as it was identified on surface layers of Z-Al in SEM analysis.

3.3.2. Phosphate and ammonium isotherms

The equilibrium uptake for phosphate and ammonium (q_e) was calculated by Eq. 2.

$$q_e = (C_o - C_e) \times \frac{v}{w} \qquad (2)$$

where C_o (mg/L) and C_e (mg/L) represents the initial and equilibrium concentration, respectively; v (L) is the aqueous solution volume and w (g) is the mass of zeolite. The phosphate and ammonium equilibrium sorption was evaluated according to Langmuir and Freundlich isotherms by Eq. 3 and Eq. 4, respectively.

$$\frac{C_e}{q_e} = \frac{1}{K_L . q_m} + \frac{C_e}{q_m} \qquad (3)$$

$$\log q_e = \log K_F + \frac{1}{n} log\ C_e \qquad (4)$$

where q_m (mg/g) is the maximum sorption capacity and K_L (L/mg) is the Langmuir sorption equilibrium constant. K_F ((mg/g)/(mg/L)$^{1/n}$) is the Freundlich equilibrium sorption constant.

The phosphate and ammonium sorption data are well described by the Langmuir isotherm ($R^2 \geq 0.99$) while Freundlich isotherm ($R^2 \leq 0.97$) (Table 3.2 and Figure 3.2) provides a good description only at the lower concentration ranges. Therefore, monolayer and homogenous sorption or/and ion exchange at specific and equal affinity sites available on the zeolites surface is supposed to occur. A favorable sorption is revealed by the values of K_L (0.02 and 0.011 for phosphate and ammonium, respectively) [42]. For Z-N the maximum sorption capacities for ammonium and phosphate were found to be 33 mg-N/g and 0.6 mg-P/g, respectively; while Z-Al phosphate capacity was enhanced tenfold 7.0 mg-P/g. A small decrease of sorption capacity for ammonium (30 mg-N/g) was reported in Z-Al and consequently the increase of bonding sites for phosphate ions represents a slightly reduction for ammonium ones.

		Langmuir			Freundlich		
		q_m (mg/g)	K_L (L/mg)	R^2	K_F ((mg/g)/(mg/L)$^{1/n}$)	1/n	R^2
Z-N	Phosphate	0.6	0.01	0.99	0.02	0.47	0.97
	Ammonium	33	0.006	0.99	1.84	0.36	0.94
Z-Al	Phosphate	7.0	0.02	0.99	0.85	0.32	0.85
	Ammonium	30	0.011	0.99	2.64	0.32	0.92

Table 3.2. Isotherm parameters for phosphate and ammonium sorption on natural zeolite (Z-N) and hybrid hydrated aluminum oxide zeolite (Z-Al).

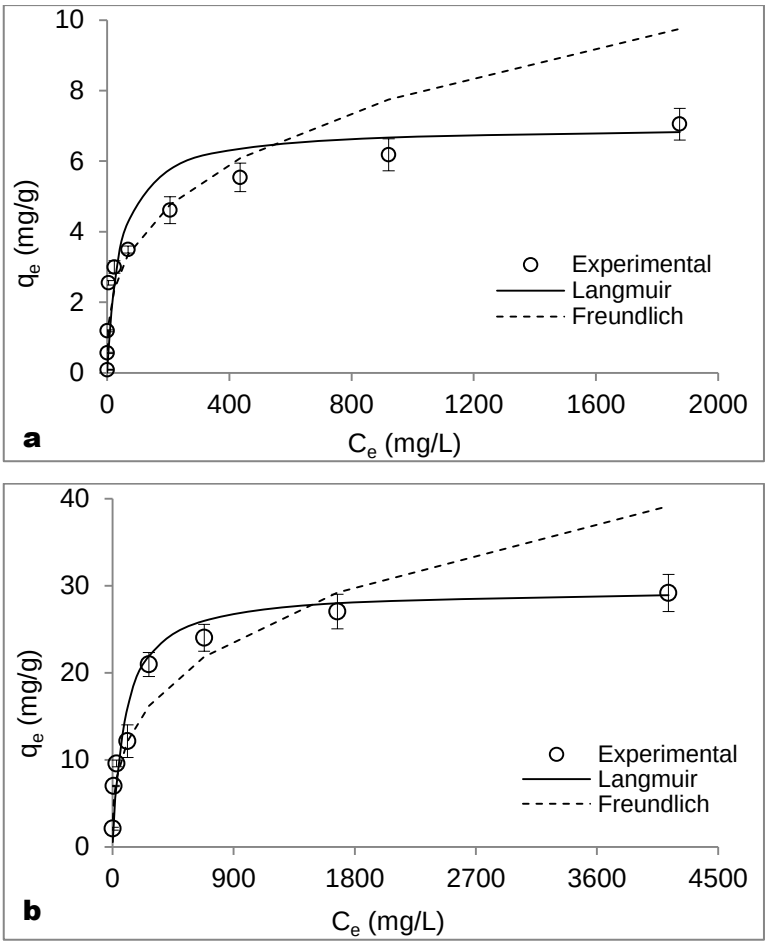

Figure 3.2. Experimental and theoretical equilibrium isotherms for a) phosphate and b) ammonium removal by hybrid hydrated aluminum oxide zeolite (Z-Al) at 21±1°C. Sorption experiments were carried at constant equilibrium pH 4.2±0.2.

Sorption of ions with acid base properties (e.g. phosphate and ammonium) on adsorbent surface sites occurs by specific and/or nonspecific interactions. The specific type of sorption takes place by ligand exchange reactions while nonspecific sorption involves columbic forces generally depends on the aqueous pH and the pH_{PZC} of the adsorbent. The pH dependence on the phosphate removal of Z-Al (Figure 3.3) shows the lowest phosphate removal at pH below than 2; and the highest with a plateau between pH 3 and 6 to decreases then from pH 6 to 11.

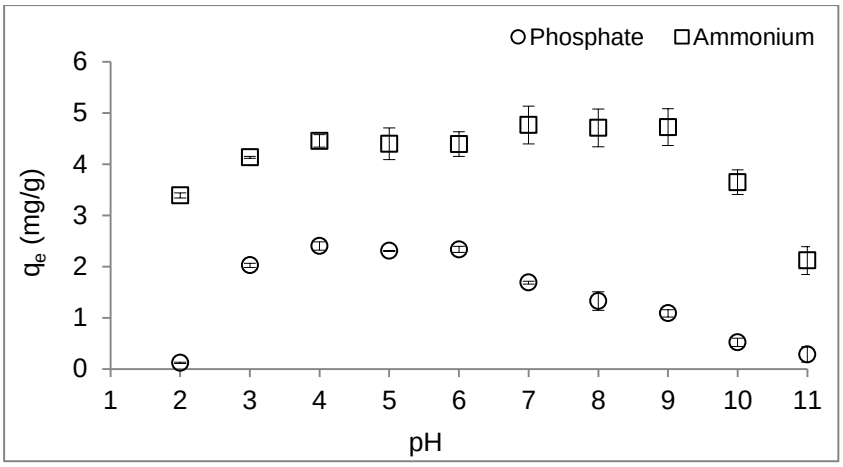

Figure 3.3. Effect of pH on the phosphate and ammonium removal by the hybrid hydrated aluminum oxide zeolite (Z-Al).

The sorption mechanism of phosphate oxyanions ($H_2PO_4^-$ - HPO_4^{2-} – PO_4^{3-}) is associated with the formation of complexes with the hydroxyl surface groups of the hydrated aluminum oxide layer impregnated on the zeolite structure (specific adsorption) [17, 43-45] or by means of columbic forces depending of the pH_{pzc} (non-specific adsorption) [13, 23, 45].

Then, taking into account that pH_{pzc} of the aluminum hydrated oxide in Z- Al was found to be 4.5±0.2, below the pH_{PZC}, the Z-Al surface is positively-charged, which becomes an opportunity for anions sorption as is depicted in Eq. 5. However, the reduction of pH below 2.3 (pK_{a1}) favours the conversion of $H_2PO_4^-$ to H_3PO_4 and therefore the anion exchange mechanism is not favoured as phoshate is a non-charged form. Instead, above the pH_{PZC} the adsorbent surface is negatively-charged (Eq. 7) and anions sorption is not favourable.

$$Z-Al-OH \xrightarrow[pH < pH_{PZC}]{Protonation} Z-Al-OH^{2+} \xrightarrow[H_2PO_4^-/HPO_4^{2-}]{Electrostatic\ attraction} \begin{cases} Z-Al-OH^{2+}\ldots H_2PO_4^- \\ Z-Al-OH^{2+}\ldots HPO_4^{2-} \end{cases} \quad (5)$$

$$H_2PO_4^- \quad Z-Al-O-\underset{\underset{O}{\|}}{\overset{\overset{OH}{|}}{P}}-OH + OH^- \quad Monodentate$$

$$Z-Al-OH + \xrightarrow[pH \geq pH_{PZC}]{Complexation} Z-Al<\begin{matrix}O\\O\end{matrix}>P\leqslant\begin{matrix}OH\\O\end{matrix} + OH^- \quad \begin{matrix}Bidentate\\Mononuclear\end{matrix} \quad (6)$$

$$HPO_4^{2-} \quad \begin{matrix}Z-Al-O\\Z-Al-O\end{matrix}>P\leqslant\begin{matrix}OH\\O\end{matrix} + 2OH^- \quad \begin{matrix}Bidentate\\Binuclear\end{matrix}$$

$$Z-Al-OH \xrightarrow[pH \gg pH_{PZC}]{Hydroxilation} Z-Al-O^{-} + H_2O \quad (7)$$

At pH ≥ pH_{PZC} the Al-OH groups are involved in the formation of inner sphere species by means of monodentate and bidentate complexation (Eq. 6) [17, 46, 47]. Then, an increase of pH above 11 is traduced in the gradual conversion of the HPO_4^{2-} onto PO_4^{3-} and consequently, a reduction of the phosphate removal. The reduction is associated to both, the high charge of the ion (-3) and the fact that the hydrated hydroxide surface in negatively charged (≅AlO^-).

The ammonium sorption by Z-Al (Figure 3.3) increases progressively from pH 2 until 9. Below the pH_{PZC} the existence of positive charges on the Z-Al surface is the responsible for a reduction of the ammonium removal. On other hand, above the pH_{PZC} the increase of ammonium (NH_4^+) sorption is attributed to the electrostatic interaction with the deprotonated surface groups (≅AlO^-). The decrease of ammonium sorption at pH 10 is associated with the decrease of the NH_4^+ concentration as it is converted to the NH_3. So, the ion exchange reaction on a sodium zeolite is described as a chemical process involving valence forces through the sharing or exchange of electrons between zeolite sites with negative charge and ammonium cations as described by Eq. 8 [5, 48]:

$$Z\text{-}Na^+ + NH_4^+ \leftrightarrow Na^+ + Z\text{-}NH_4^+ \quad (8)$$

Analysis of the aqueous phase (data not reported) confirm the release of Na^+ and in minor degree of K^+, Mg^{2+}, Ca^{2+}. SEM data revealed the reduction of these cations in the ammonium loaded Z-Al.

3.3.3. Effect of competing ions on ammonium and phosphate sorption

Sorption capacity of Z-Al for both phosphate and ammonium in the presence of common anions and cations in treated waste water is shown in Figure 3.4. The ammonium sorption capacity was maintained as the variations were below 5 %. A similar effect was confirmed for phosphate uptake in the presence of nitrate, sulfate and chloride as reported for other zeolitic materials [1, 48]. These species are mainly supposed to form outer-sphere complexes and they do not represent any competition for the same binding sites [2, 49]. The presence of HCO_3^- was found to promote the reduction of 32 % on the phosphate uptake as reported for a modified zeolite [50].

The combined effect of anions revealed the decrease of phosphate and ammonium removal of 29 % and 9 %, respectively.

The evaluation of the effect of cations towards ammonium uptake by Z-Al revealed an important decrease for K^+ (17 %) > Ca^{2+} (15 %) > Na^+ (12 %) > Mg^{2+} (6 %) as was previously reported with natural zeolites [48]. Contrary, no significant differences were measured in phosphate sorption with differences below 5 % (e.g. Mg^{2+} (6 %) > Na^+ (3 %) > K^+ (3 %) and Ca^{2+} (1 %)). The combined effect of cations leads the reduction of phosphate and ammonium uptake of 3 % and 33 %, respectively.

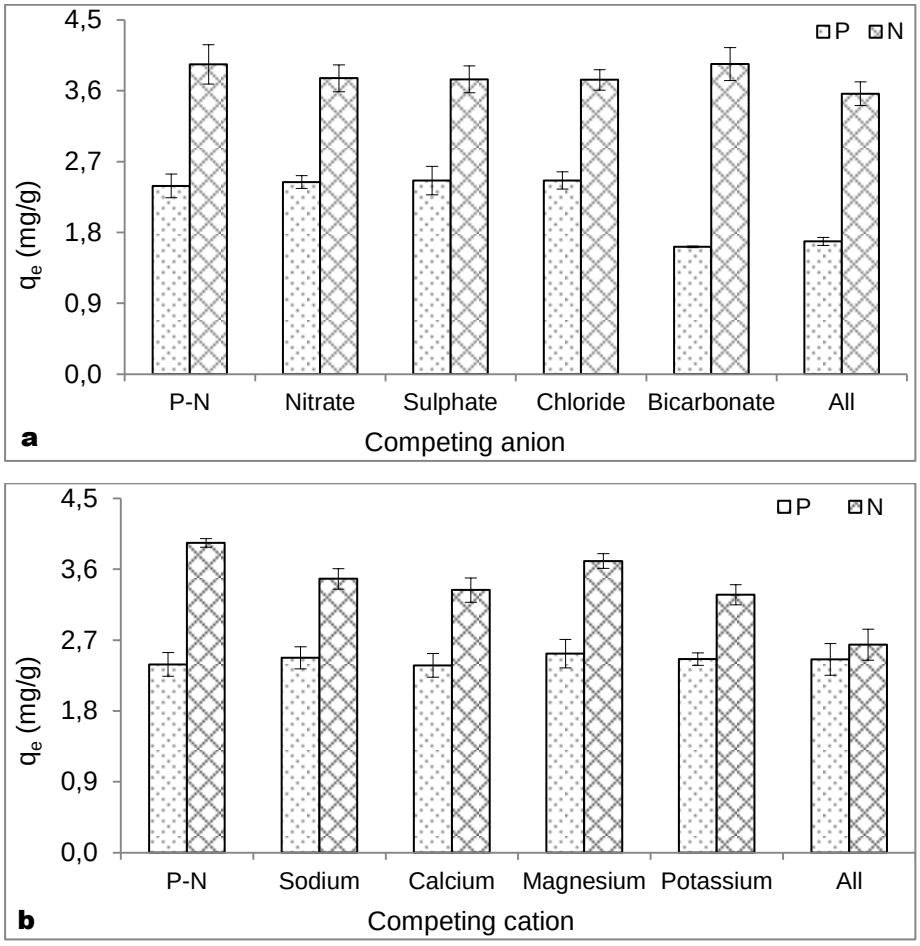

Figure 3.4. Individually effect of a) anions and b) cations for phosphate (P) and ammonium (N) removal onto the hybrid hydrated aluminum oxide zeolite (Z-Al).

The phosphate and ammonium equilibrium sorption by Z-Al in the presence of the anions and cations mixtures (Table 3.3) are better described by the Langmuir isotherm ($R^2 \geq 0.99$) than by the Freundlich isotherm ($R^2 \leq 0.84$). The maximum phosphate uptake capacity without competing ions (7.0 mg-P/g) was slightly reduced by the presence of ions mixtures to 6.3 mg-P/g, in the presence of anions to 6.4 mg-

P/g and in the presence of cations to 6.7 mg-P/g. Similarly, the ammonium uptake capacity (30 mg-N/g) slightly decreased to 26 mg-N/g when all competing ions were present, to 27 mg-N/g in presence of cations and to 28 mg-N/g in presence of anions. Phosphate and ammonium sorption data for Z-Al in the presence of competing ions at different concentrations are shown in Figure 3.5.

	Langmuir			Freundlich		
	q_m (mg/g)	K_L (L/mg)	R^2	K_F ((mg/g)/(mg/L)$^{1/n}$)	1/n	R^2
Phosphate (single)	7.0	0.02	0.99	0.85	0.32	0.85
P (Anions mixture)	6.4	0.01	0.98	0.52	0.36	0.93
P (Cations mixture)	6.7	0.02	0.99	0.78	0.32	0.84
P (Ions mixture)	6.3	0.02	0.99	0.59	0.36	0.86
Ammonium (single)	30	0.011	0.99	2.64	0.32	0.92
N (Anions mixture)	28	0.008	0.99	1.62	0.39	0.91
N (Cations mixture)	27	0.009	0.99	1.25	0.42	0.92
N (Ions mixture)	26	0.007	0.99	0.93	0.47	0.87

Table 3.3. Isotherm parameters for phosphate and ammonium sorption by hybrid hydrated aluminum oxide zeolite Z-Al in the presence of competing ions.

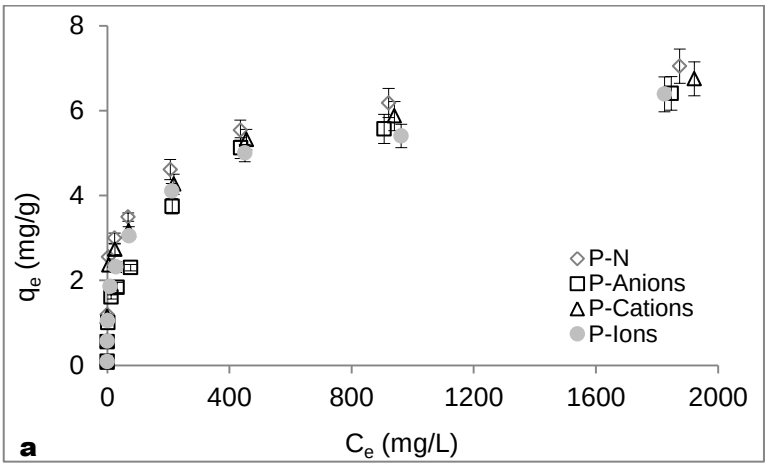

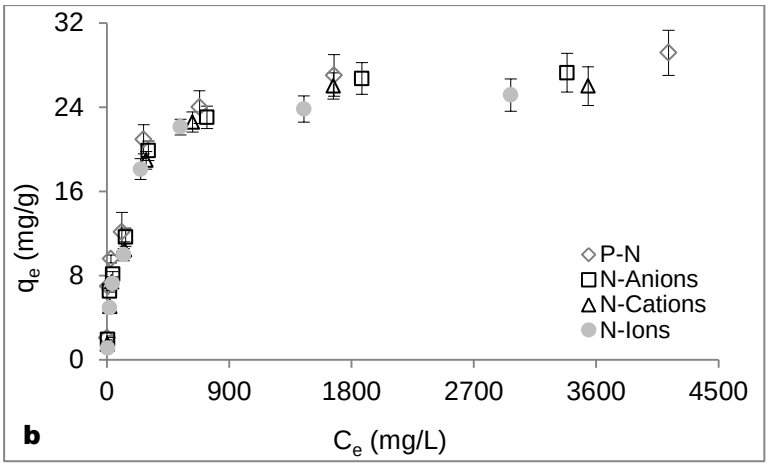

Figure 3.5. Equilibrium capacity for a) phosphate and b) ammonium in presence of competing ions with the hybrid hydrated aluminum oxide zeolite (Z-Al).

3.3.4. Phosphate and ammonium sorption kinetics

Kinetic data of both phosphate and ammonium removal by Z-Al are similar to those typically shown by polymeric ion exchangers as it is shown in Figure 3.6. More than 150 minutes were needed to reach the equilibrium, however; ammonium shows faster sorption rate than phosphate. This observation is attributable to the fact that the exchange of Na^+ by NH_4^+ ions is a faster process than the complexation of phosphate ions with the surfaces groups (≅AlOH).

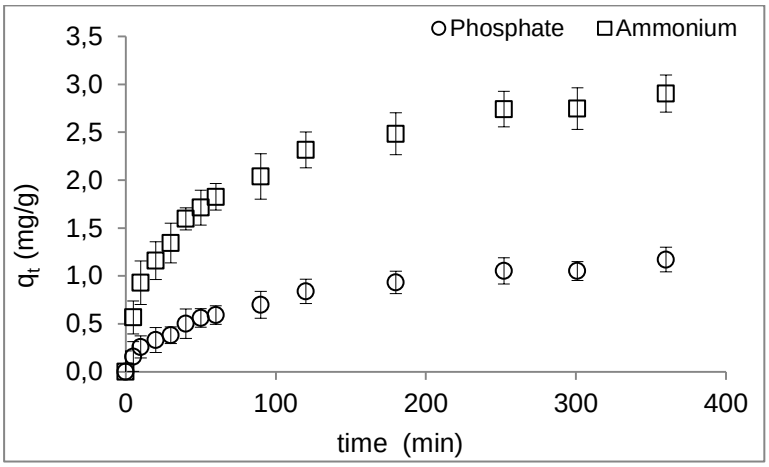

Figure 3.6. Evolution of phosphate and ammonium sorption uptake versus time for Z-Al in batch experiments at 21 ±1 ºC.

The kinetic data of phosphate and ammonium sorption onto modified zeolite were fitted to the pseudo-first order and pseudo-second order kinetic model by Eq. 9 and Eq. 10.

$$\ln(q_e - q_t) = \ln(q_e) - k_1 t \qquad (9)$$

$$\frac{t}{q_t} = \frac{1}{k_2 q_e^2} + \frac{t}{q_e} \qquad (10)$$

where k_1 (h^{-1}) and k_2 ($g.mg^{-1}.h^{-1}$) are the kinetics constants. The pseudo-second order model provided a good description for phosphate and ammonium sorption. However, the intraparticle diffusion model developed by Weber and Morris [51] also was used for describing sorption processes on the zeolite. The mathematical dependence of uptake q_t of adsorbates on $t^{1/2}$ is obtained if the sorption process is considered to be influenced by diffusion in the spherical adsorbent and by convective diffusion in the adsorbate solution. This dependence is described by the Eq. 11:

$$q_t = k_t\, t^{1/2} + A \qquad (11)$$

where k_t ($mg.g^{-1}.h^{-1/2}$) is the intraparticle diffusion rate constant and A (mg/g) is a constant providing an indication of the thickness of the boundary layer, i.e. the higher the value of A, the greater the boundary layer effect. If the sorption uptake q_t is plotted versus $t^{1/2}$ gives a straight line, this means that the sorption process is only controlled by intraparticle diffusion. However, two or more steps influence the sorption process if the data exhibit multi-linear plots.

The intra-particle diffusion model fitted well the experimental data as can be seen in Figure 3.7 indicating that the whole sorption process is divided into two linear regions. Hence, the ammonium and phosphate sorption process might be described by film diffusion followed by particle diffusion process [52].

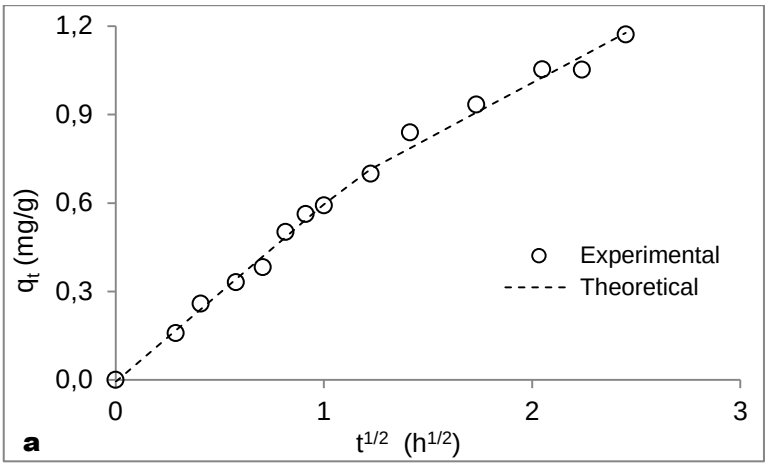

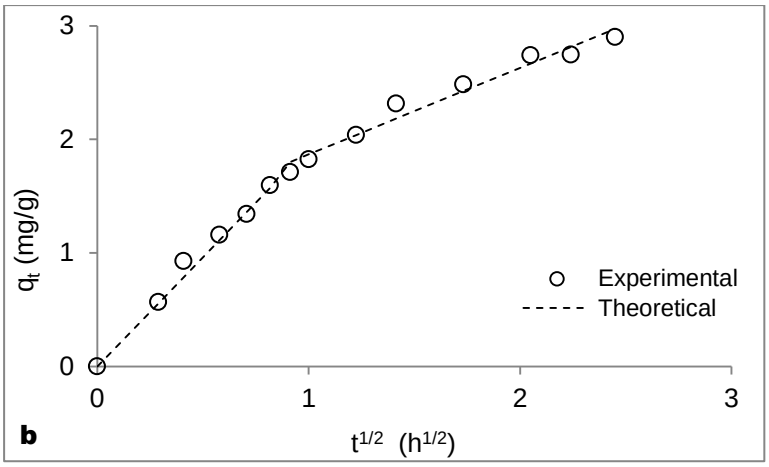

Figure 3.7. Intra-particle diffusion plots for a) phosphate and b) ammonium removal by hybrid hydrated aluminum oxide zeolite (Z-Al).

The contribution of each rate controlling step in the phosphate and ammonium sorption onto Z-Al can be further analyzed through the homogenous particle diffusion model (HPDM) and film diffusion model (HPDF) by calculating the film diffusion (D_f) and particle diffusion (D_p) [53]. In this model the species originally in the solution phase must diffuse across the liquid film surrounding the adsorbent particle, transfer across the solution/ particle interface, diffuse into the bulk of the adsorbent particle and possibly interact with a moiety on the surface of the adsorbent [54]. Sorption on spherical particles under particle diffusion control is described by Eq. 12:

$$-\ln\left(1-\left(\frac{q_t}{q_e}\right)^2\right)=\frac{2\,\pi^2 D_p}{r^2}t \qquad (12)$$

If liquid film diffusion controls the rate of sorption is described by Eq. 13:

$$-\ln\left(1-\left(\frac{q_t}{q_e}\right)^2 t\right)=\frac{D_f C_s}{h\,r\,C_z}t \qquad (13)$$

where q_t and q_e are solute uptake on the adsorbent phase at time t and when equilibrium is attained (mg/g) respectively and C_s and C_z (mg/kg) are the concentrations of solute in solution and in the zeolite, respectively; r is the average radius of zeolite particles ($1x10^{-4}$ m), t is the contact time (min or s); and h is the thickness of film around the zeolite particle ($1x10^{-5}$ m for poorly stirred solution) [55]. Kinetic experimental data were fitted to equations 12 and 13 and D_p and D_f values for ammonia and phosphate sorption onto Z-Al as well as the linear regression analysis are summarized in Table 3.4. The D_p values for both ions were considerably lower than those of D_f, indicating that particle diffusion was the rate-limiting step for both ions and their sorption was mainly occurred at the surface of zeolite with monolayer

molecular adsorption. Similar results were reported for natural zeolites [52, 55, 56] at low initial ammonium concentrations.

Model	Kinetic parameters	Phosphate	Ammonium
Pseudo-first order	q_e (mg·g^{-1})	1.4	2. 6
	k_1 (h^{-1})	0.2	0.3
	R^2	0.93	0.91
Pseudo-second order	q_e (mg·g^{-1})	1.3	3.1
	k_2 (g·mg^{-1}·h^{-1})	0.6	0.1
	R^2	0.99	1.00
Intraparticle diffusion	k_{t1} (mg·g^{-1}·h$^{-1/2}$)	0.6	1.9
	R^2	0.99	0.99
	k_{t2} (mg·g^{-1}·h$^{-1/2}$)	0.4	0.8
	R^2	0.97	0.97
HPDF Film diffusion	D_f (m^2·s^{-1})	4.9x10^{-10}	9.9x10^{-10}
	R^2	0.93	0.91
HPDM Particle diffusion	D_f (m^2·s^{-1})	8.8x10^{-13}	1.5x10^{-12}
	R^2	0.98	0.97

Table 3.4. Kinetic parameters for phosphate and ammonium removal by hybrid hydrated aluminum oxide zeolite (Z-Al).

FSEM analyses of loaded phosphate and ammonium Z-Al revealed that the surface is almost covered by several lamellar particles and EDAX analysis of the loaded adsorbent revealed the presence of phosphorous. Nitrogen was not detected as the content is below the limit of quantification. The size of the cavities in the unload material decreased with the sorption process. Then the surface turned to be a compact crystalline framework. The FTIR analysis performed after the phosphate and ammonium sorption (Figure 3.8) showed changes in bands at 3616 cm^{-1}, 1015 cm^{-1} and the appearance of a new band at 1436 cm^{-1}. These variations are associated with the participation of hydroxyl groups of Al(OH) by means complexation with phosphate and ammonium when sorption has taken place over zeolite surface [57-60]. This fact may explain the phosphate and ammonium ions competition for the same binding sites. It explains the increase of the phosphate removal leading the slight reduction of the ammonium sorption capacity as it occurred in natural as well as modified zeolite.

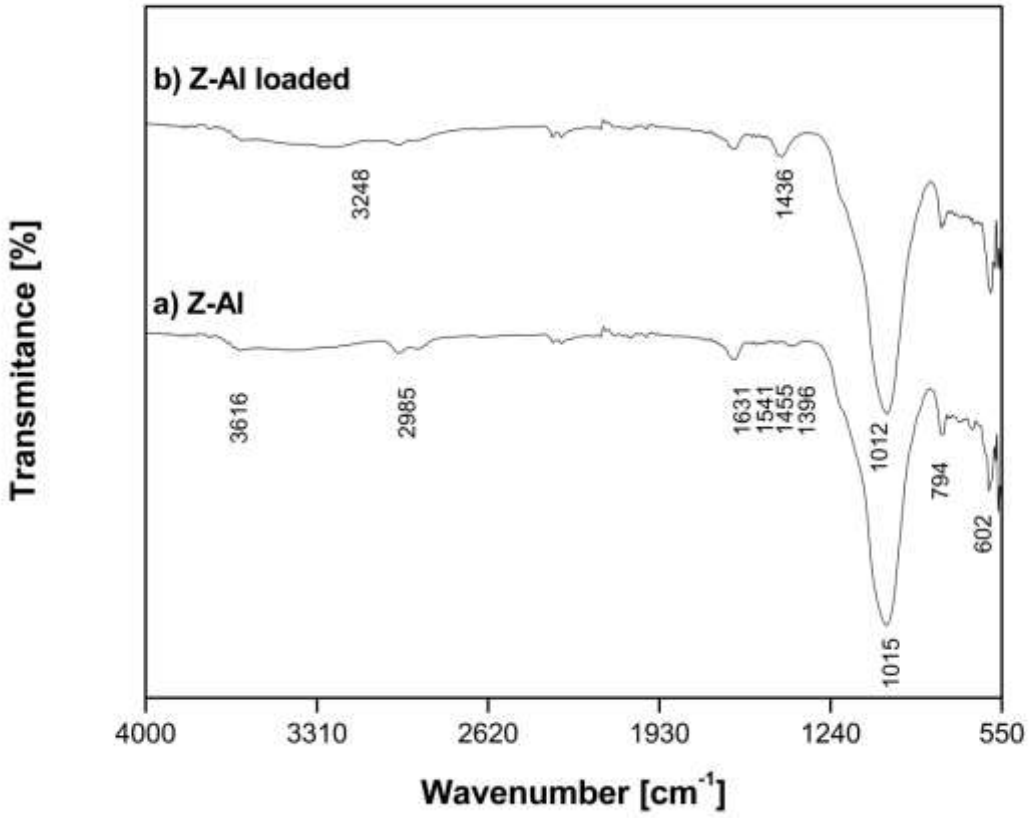

Figure 3.8. FTIR of the zeolitic materials a) unloaded hybrid hydrated aluminum oxide zeolite (Z-Al) and b) P and N loaded Z-Al.

3.3.5. Phosphate speciation in loaded Z-Al samples

Phosphate speciation results are collected in Table 3.5. For Z-Al the content of residual phosphorus (R-P) was found to be 9±3 %. The loosely bound phosphorus fraction (LB-P) was found to be 4±1 % as reported for a synthetic zeolite [6]. The major phosphorus fraction retained by Z-Al was associated to Al and Fe hydroxides (Fe+Al)-P which represent the 53±1 %. Thus, it revealed the Al-OH groups of the hydrated aluminum oxides in the modified zeolite Z-Al to be the main responsible for the phosphate removal. Finally, the 35±3 % of phosphorus immobilized was related to calcium and magnesium (Ca+Mg)-P fraction. Then, phosphate removal is also performed by means of chemical precipitation with these cationic species; although these mineral phases were not identified by XRD analysis.

q_e	LB-P		(Fe+Al)-P		(Ca+Mg)-P		R-P	
(mg/g)	(mg/g)	%	(mg/g)	%	(mg/g)	%	(mg/g)	%
2.04	0.1	4±1	1.0	53±1	0.7	35±3	0.2	9±3

Table 3.5. Fractionation of phosphate immobilized on the hybrid hydrated aluminum oxide zeolite (Z-Al) associated to the different chemical forms: LB-P; (Fe+Al)-P; (Ca+Mg)-P; R-P.

3.3.6. Phosphate and ammonium desorption

Desorption efficiency of phosphate and ammonium from loaded zeolites using NaOH, $NaHCO_3$, Na_2CO_3, and mixtures of $NaHCO_3$/Na_2CO_3 in the first sorption – desorption cycle are summarized in Table 3.6:

Elution solution	Desorption (%)	
	Phosphate	Ammonium
1 M NaOH	20±3	83±4
0.1 M $NaHCO_3$	24±3	50±4
0.1 M Na_2CO_3	79±3	92±4
0.1 M $NaHCO_3$/0.1 M Na_2CO_3	64±3	76±4

Table 3.6. Desorption efficiency of phosphate and ammonium from loaded Z-Al in batch experiments at 21±ºC.

Ammonium is much better desorbed than phosphate with high recoveries from 50 up to 92 % for most of the elution solutions used while phosphate recovery varied from 20 up to 79 % in the first sorption – desorption cycle. The strong phosphate complexation with the hydrated aluminum oxide seems to be the responsible for this irreversible sorption. However, in the second sorption cycle it was found a strong reduction of phosphate capacity (≈96 %) in contrast to the slight variation in ammonium removal of all four regenerated Z-Al samples. Concentrated alkaline solutions promote the dissolution of the hydrated oxide aluminum [61] as well as the partial dissolution of the zeolite structure as it has been postulated [38]. Although, the regeneration using NaOH solutions have been proposed effective for oxyanions from zeolites [61] scarce data could be found in literature as typically these materials were not developed for regeneration purposes. According to these results, and taking into account that ammonium and phosphate are not efficiently desorbed it is necessary to

evaluate the possibility of direct used of the loaded zeolites for soils quality improvement.

3.3.7. Simultaneous removal of ammonium and phosphate in column tests

The breakthrough curves of the simultaneous phosphate and ammonium sorption by Z-Al in absence and presence of competing ions are shown in Figure 3.9. The breakthrough point (C/C_0= 0.05) for phosphate and ammonium sorption was found at 15 BV instead in the presence of competing ions was 7 BV. The phosphate maximum sorption capacity reached at column saturation (C/C_0= 0.95) was 5 mg-P/g at 194 BV, contrary in the presence of competing ions it decreased to 3 mg-P/g at 137 BV. Similarly behaviour was found for ammonium sorption capacity with 28 mg-N/g at 430 BV in absence of competing ions and 16 mg-N/g at 211 BV in presence of interferences.

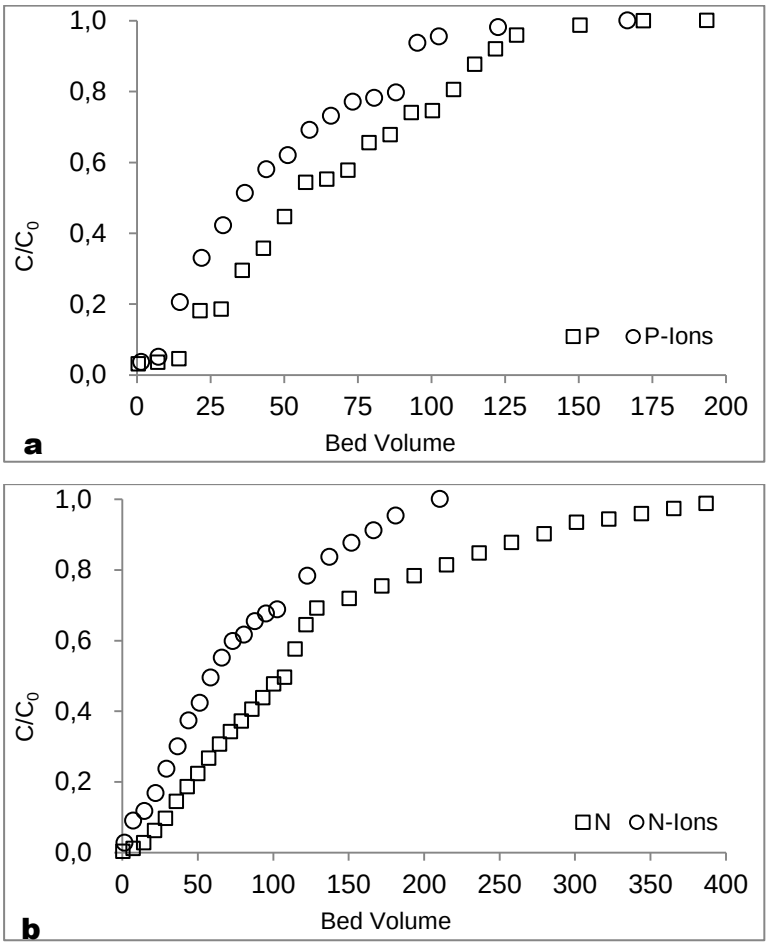

Figure 3.9. Breakthrough curves of a) phosphate and b) ammonium sorption by the hybrid hydrated aluminum oxide zeolite (Z-Al) with and without competing ions at EBHRT of 4 minutes.

The simultaneous phosphate and ammonium desorption from Z-Al was performed using 1 M NaOH solution after column operation in absence of competing ions. The profiles of ammonium and phosphate desorption are shown in Figure 3.10. The highest phosphate concentration was found to be 378 mg-P/L. Almost, the 90 % of the eluted phosphate was recovered within 4 BV. On the other hand the highest ammonium concentration was 3538 mg-N/L. The 95 % of the eluted ammonium was found at 3.5 BV. Under, these conditions enrichment factors of 50 and 120 for phosphate and ammonium respectively were achieved.

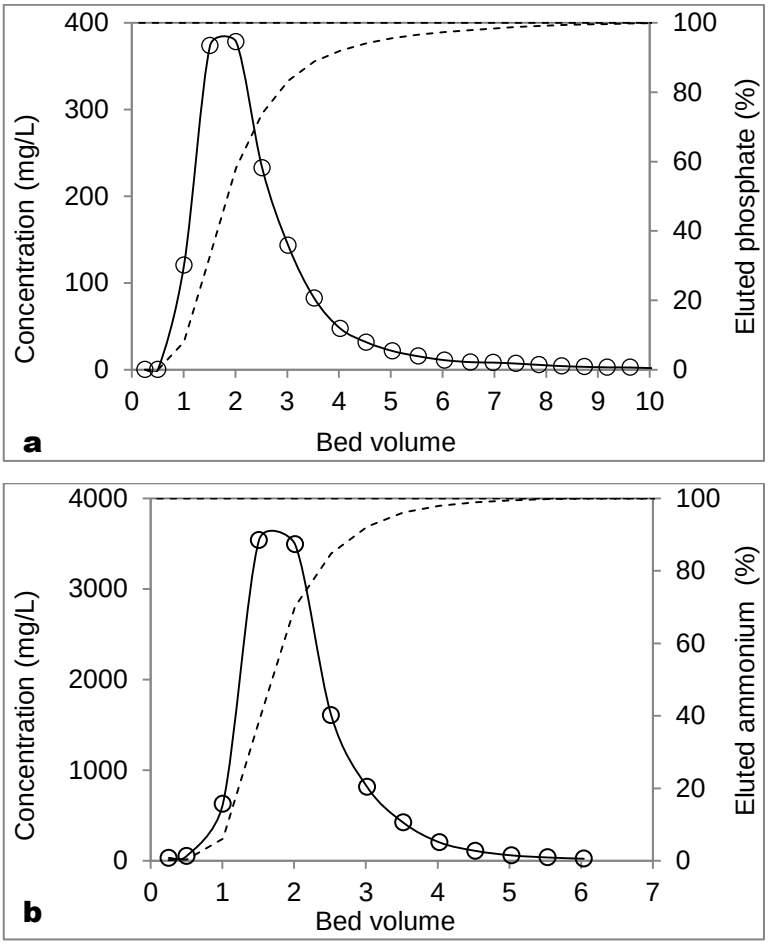

Figure 3.10. Column desorption profiles of a) phosphate and b) ammonium onto the hybrid hydrated aluminum oxide zeolite (Z-Al) using 1 M NaOH at EBHRT of 13 minutes.

3.4. Conclusions

The modification of a natural zeolite to produce a hybrid material containing hydrated aluminum oxide for phosphate recovery is not affecting its ammonium exchange capacity. Removal of phosphate is based on electrostatic interaction and the formation of inner sphere complexes with ≅Al-OH groups, while ammonium removal

occurs by means of ion exchange and complexation with the OH groups of the zeolite. Both phosphate and ammonium sorption by Z-Al were well described by the Langmuir isotherm. Sorption capacity of both ions was slightly reduced when competing ions were present. Regeneration of the loaded zeolite using alkaline solutions containing sodium (NaOH, $NaHCO_3$ and Na_2CO_3) provided higher recoveries ratios for ammonium than for phosphate. Concentration factors about 50 and 120 for phosphate and ammonium, respectively using NaOH as elution solution were achieved. A reduction of phosphate sorption capacity was observed in reuse (sorption-desorption cycle) experiments, indicating that their applications for sorption – desorption operation can be limited and suggesting the direct valorization of the loaded zeolites as soil amendment.

3.5. References

1. Zhang, M., et al., *Removal of ammonium from aqueous solutions using zeolite synthesized from fly ash by a fusion method.* Desalination, 2011. **271**(1–3): p. 111-121.
2. Guan, Q., et al., *Phosphate removal in marine electrolytes by zeolite synthesized from coal fly ash.* Fuel, 2009. **88**(9): p. 1643-1649.
3. Widiastuti, N., et al., *Removal of ammonium from greywater using natural zeolite.* Desalination, 2011. **277**(1–3): p. 15-23.
4. Malekian, R., et al., *Ion-exchange process for ammonium removal and release using natural Iranian zeolite.* Applied Clay Science, 2011. **51**(3): p. 323-329.
5. Chen, X., et al., *Synthesis of nano-zeolite from coal fly ash and its potential for nutrient sequestration from anaerobically digested swine wastewater.* Bioresource Technology, 2012. **110**(0): p. 79-85.
6. Xie, J., et al., *Synthesis of Zeolite/Aluminum Oxide Hydrate from Coal Fly Ash: A New Type of Adsorbent for Simultaneous Removal of Cationic and Anionic Pollutants.* Industrial & Engineering Chemistry Research, 2013. **52**(42): p. 14890-14897.
7. Xie, J., et al., *Synthesis and properties of zeolite/hydrated iron oxide composite from coal fly ash as efficient adsorbent to simultaneously retain cationic and anionic pollutants from water.* Fuel, 2014. **116**(0): p. 71-76.
8. Kim, K.S., J.O. Park, and S.C. Nam, *Synthesis of Iron-loaded Zeolites for Removal of Ammonium and Phosphate from Aqueous Solutions.* Environ Eng Res, 2013. **18**(4): p. 267-276.

9. Du, Q., et al., *Ammonia removal from aqueous solution using natural Chinese clinoptilolite.* Separation and Purification Technology, 2005. **44**(3): p. 229-234.
10. Leyva-Ramos, R., et al., *Ammonia exchange on clinoptilolite from mineral deposits located in Mexico.* Journal of Chemical Technology & Biotechnology, 2004. **79**(6): p. 651-657.
11. Król, M., et al., *Application of IR spectra in the studies of zeolites from D4R and D6R structural groups.* Microporous and Mesoporous Materials, 2012. **156**: p. 181-188.
12. Jiang, C., et al., *Adsorptive removal of phosphorus from aqueous solution using sponge iron and zeolite.* Journal of Colloid and Interface Science, 2013. **402**(0): p. 246-252.
13. Simsek, E.B., E. Özdemir, and U. Beker, *Zeolite supported mono- and bimetallic oxides: Promising adsorbents for removal of As(V) in aqueous solutions.* Chemical Engineering Journal, 2013. **220**: p. 402-411.
14. Jiménez-Cedillo, M.J., M.T. Olguín, and C. Fall, *Adsorption kinetic of arsenates as water pollutant on iron, manganese and iron–manganese-modified clinoptilolite-rich tuffs.* Journal of Hazardous Materials, 2009. **163**(2–3): p. 939-945.
15. Jiménez-Cedillo, M.J., et al., *Adsorption capacity of iron- or iron–manganese-modified zeolite-rich tuffs for As(III) and As(V) water pollutants.* Applied Clay Science, 2011. **54**(3–4): p. 206-216.
16. Alshameri, A., C. Yan, and X. Lei, *Enhancement of phosphate removal from water by TiO2/Yemeni natural zeolite: Preparation, characterization and thermodynamic.* Microporous and Mesoporous Materials, 2014. **196**(0): p. 145-157.
17. Lǔ, J., et al., *Adsorptive removal of phosphate by a nanostructured Fe–Al–Mn trimetal oxide adsorbent.* Powder Technology, 2013. **233**: p. 146-154.
18. Gómez-Hortigüela, L., et al., *Natural zeolites from Ethiopia for elimination of fluoride from drinking water.* Separation and Purification Technology, 2013. **120**: p. 224-229.
19. Vassileva, P. and D. Voikova, *Investigation on natural and pretreated Bulgarian clinoptilolite for ammonium ions removal from aqueous solutions.* Journal of Hazardous Materials, 2009. **170**(2-3): p. 948-953.

20. Tehrani, R.M.A. and A.A. Salari, *The study of dehumidifying of carbon monoxide and ammonia adsorption by Iranian natural clinoptilolite zeolite.* Applied Surface Science, 2005. **252**(3): p. 866-870.
21. Villanueva, M.E., et al., *Point of zero charge as a factor to control biofilm formation of Pseudomonas aeruginosa in sol-gel derivatized aluminum alloy plates.* Surface and Coatings Technology, 2014. **254**: p. 145-150.
22. Sarma, J. and S. Mahiuddin, *Specific ion effect on the point of zero charge of α-alumina and on the adsorption of 3,4-dihydroxybenzoic acid onto α-alumina surface.* Colloids and Surfaces A: Physicochemical and Engineering Aspects, 2014. **457**(0): p. 419-424.
23. Zebardast, H.R., et al., *Potentiometric titration of hematite and magnetite at elevated temperatures using a ZrO2-based pH probe.* Colloids and Surfaces A: Physicochemical and Engineering Aspects, 2014. **444**: p. 144-152.
24. Liu, Y., R. Naidu, and H. Ming, *Surface electrochemical properties of red mud (bauxite residue): Zeta potential and surface charge density.* Journal of Colloid and Interface Science, 2013. **394**: p. 451-457.
25. Khawmee, K., et al., *Surface charge properties of kaolinite from Thai soils.* Geoderma, 2013. **192**: p. 120-131.
26. Martinez, R.E., et al., *Surface charge and zeta-potential of metabolically active and dead cyanobacteria.* Journal of Colloid and Interface Science, 2008. **323**(2): p. 317-325.
27. Hieltjes, A.H.M. and L. Lijklema, *Fractionation of Inorganic Phosphates in Calcareous Sediments1.* J. Environ. Qual., 1980. **9**(3): p. 405-407.
28. APHA, A., WEF., *Standard methods for the examination of water and wastewater*, 2000, American Public Health Association, American Water Works Association, and Water Environment Federation.
29. Lei, L., X. Li, and X. Zhang, *Ammonium removal from aqueous solutions using microwave-treated natural Chinese zeolite.* Separation and Purification Technology, 2008. **58**(3): p. 359-366.
30. Doula, M.K., *Synthesis of a clinoptilolite–Fe system with high Cu sorption capacity.* Chemosphere, 2007. **67**(4): p. 731-740.
31. Valdés, H., S. Alejandro, and C.A. Zaror, *Natural zeolite reactivity towards ozone: The role of compensating cations.* Journal of Hazardous Materials, 2012. **227–228**(0): p. 34-40.

32. Margeta, K., et al., *Natural Zeolites in Water Treatment – How Effective is Their Use*, in *Water Treatment*, W. Elshorbagy and R.K. Chowdhury, Editors. 2013, InTech: Rijeka. p. 81-112.
33. Stumm, W., *Chemistry of the solid water interface: Processes at the mineral-water and water-particle interface in natural systems*, ed. W.I. Pubication1992: Wiley and Sons Inc.
34. Reháková, M., et al., *Removal of pyridine from liquid and gas phase by copper forms of natural and synthetic zeolites.* Journal of Hazardous Materials, 2011. **186**(1): p. 699-706.
35. Li, J., et al., *Studies on natural STI zeolite: modification, structure, adsorption and catalysis.* Microporous and Mesoporous Materials, 2000. **37**(3): p. 365-378.
36. Jin, F. and Y. Li, *A FTIR and TPD examination of the distributive properties of acid sites on ZSM-5 zeolite with pyridine as a probe molecule.* Catalysis Today, 2009. **145**(1–2): p. 101-107.
37. Alejandro, S., et al., *Oxidative regeneration of toluene-saturated natural zeolite by gaseous ozone: The influence of zeolite chemical surface characteristics.* Journal of Hazardous Materials, 2014. **274**(0): p. 212-220.
38. Alshameri, A., et al., *The investigation into the ammonium removal performance of Yemeni natural zeolite: Modification, ion exchange mechanism, and thermodynamics.* Powder Technology, 2014. **258**(0): p. 20-31.
39. Luan, Z. and J.A. Fournier, *In situ FTIR spectroscopic investigation of active sites and adsorbate interactions in mesoporous aluminosilicate SBA-15 molecular sieves.* Microporous and Mesoporous Materials, 2005. **79**(1–3): p. 235-240.
40. Cheng, X.-w., et al., *Studies on modification and structural ultra-stabilization of natural STI zeolite.* Microporous and Mesoporous Materials, 2005. **83**(1–3): p. 233-243.
41. Brunner, E., *Solid state NMR — a powerful tool for the investigation of surface hydroxyl groups in zeolites and their interactions with adsorbed probe molecules.* Journal of Molecular Structure, 1995. **355**(1): p. 61-85.
42. Foo, K.Y. and B.H. Hameed, *Insights into the modeling of adsorption isotherm systems.* Chemical Engineering Journal, 2010. **156**(1): p. 2-10.

43. Dzombak, D. and F. Morel, *Surface Complexation Modeling: Hydrous Ferric Oxide*1990, New York: John Wiley & Sons, Inc.
44. Blaney, L.M., S. Cinar, and A.K. SenGupta, *Hybrid anion exchanger for trace phosphate removal from water and wastewater.* Water Research, 2007. **41**(7): p. 1603-1613.
45. Sujana, M.G., et al., *Studies on fluoride adsorption capacities of amorphous Fe/Al mixed hydroxides from aqueous solutions.* Journal of Fluorine Chemistry, 2009. **130**(8): p. 749-754.
46. Su, Y., et al., *Strong adsorption of phosphate by amorphous zirconium oxide nanoparticles.* Water Research, 2013. **47**(14): p. 5018-5026.
47. Yan, L.-g., et al., *Adsorption of phosphate from aqueous solution by hydroxy-aluminum, hydroxy-iron and hydroxy-iron–aluminum pillared bentonites.* Journal of Hazardous Materials, 2010. **179**(1–3): p. 244-250.
48. Huang, H., et al., *Ammonium removal from aqueous solutions by using natural Chinese (Chende) zeolite as adsorbent.* Journal of Hazardous Materials, 2010. **175**(1–3): p. 247-252.
49. Onyango, M.S., et al., *Adsorptive Removal of Phosphate Ions from Aqueous Solution Using Synthetic Zeolite.* Industrial & Engineering Chemistry Research, 2007. **46**(3): p. 894-900.
50. Ning, P., et al., *Phosphate removal from wastewater by model-La(III) zeolite adsorbents.* Journal of Environmental Sciences, 2008. **20**(6): p. 670-674.
51. Weber, W.J. and J.C. Morris, *Kinetics of adsorption on carbon solution.* Journal of the Sanitary Engineering Division, 1963. **89**(2): p. 31-59.
52. Lin, L., et al., *Adsorption mechanisms of high-levels of ammonium onto natural and NaCl-modified zeolites.* Separation and Purification Technology, 2013. **103**(0): p. 15-20.
53. Helfferich, F.G., *Ion exchange*1962, New York: McGraw-Hill.
54. Valderrama, C., et al., *Kinetic evaluation of phenol/aniline mixtures adsorption from aqueous solutions onto activated carbon and hypercrosslinked polymeric resin (MN200).* Reactive and Functional Polymers, 2010. **70**(3): p. 142-150.
55. Moussavi, G., et al., *The investigation of mechanism, kinetic and isotherm of ammonia and humic acid co-adsorption onto natural zeolite.* Chemical Engineering Journal, 2011. **171**(3): p. 1159-1169.

56. Sprynskyy, M., et al., *Ammonium removal from aqueous solution by natural zeolite, Transcarpathian mordenite, kinetics, equilibrium and column tests.* Separation and Purification Technology, 2005. **46**(3): p. 155-160.
57. Huang, H., et al., *Simultaneous removal of nutrients from simulated swine wastewater by adsorption of modified zeolite combined with struvite crystallization.* Chemical Engineering Journal, 2014. **256**: p. 431-438.
58. Guo, J., C. Yang, and G. Zeng, *Treatment of swine wastewater using chemically modified zeolite and bioflocculant from activated sludge.* Bioresource Technology, 2013. **143**(0): p. 289-297.
59. Wahab, M.A., S. Jellali, and N. Jedidi, *Ammonium biosorption onto sawdust: FTIR analysis, kinetics and adsorption isotherms modeling.* Bioresource Technology, 2010. **101**(14): p. 5070-5075.
60. Wahab, M.A., et al., *Characterization of ammonium retention processes onto Cactus leaves fibers using FTIR, EDX and SEM analysis.* Journal of Hazardous Materials, 2012. **241–242**(0): p. 101-109.
61. Xu, Y.-H., T. Nakajima, and A. Ohki, *Adsorption and removal of arsenic(V) from drinking water by aluminum-loaded Shirasu-zeolite.* Journal of Hazardous Materials, 2002. **B92**: p. 275-287.

Chapter 4 Modification of a natural zeolite with Fe(III) for simultaneous phosphate and ammonium removal from aqueous solutions

Abstract

The incorporation of Fe(III) was performed in a natural clinoptilolite (Z-N) for simultaneous phosphate and ammonium removal. The existence of hydroxyl groups (≅Fe-OH) in the iron zeolite (Z-Fe) enhances the phosphate uptake from 0.6±0.1 mg-P/g in Z-N to 3.4±0.2 mg-P/g in Z-Fe. However, the ammonium sorption capacity slightly decreases from 33±2 mg-N/g in Z-N to 27±2 mg-N/g in Z-Fe. The equilibrium and kinetics sorption were well explained by the Langmuir isotherm and the intraparticle diffusion model, respectively. Both the phosphate and ammonium uptake were slightly affected by the coexistence of competing ions. The phosphate sorption capacity of iron zeolite was decreased in the regeneration cycles. The desorption using a 1 M NaOH solution under dynamic conditions provided higher enrichment factors for ammonium than phosphate.

Keywords: clinoptilolite; iron; phosphate; ammonium; sorption; kinetic

4.1. Introduction

Eutrophication, is a serious environmental problem associated with phosphate and ammonium overloading in surface waters due to municipal effluents and agricultural runoff [1]. Therefore, the implementation of wastewater purification technologies for both phosphate and ammonium removal is required [2, 3]. Natural and synthetic zeolites are crystalline microporous aluminosilicates that are widely used in separation and purification processes and a promising material for environmental applications [4] due to their high abundance, availability and low cost [5-7]. In addition, zeolites can be used as substrates for supporting and impregnating metallic hydroxides for oxyanion uptake applications (i.e., arsenic and phosphate) [8, 9]. Surface-modified adsorbents have become more prominent in recent years. In addition to granular media, such as granular ferric hydroxides (GFH) and granular activated carbon (GAC) that are used for anions adsorption, other iron composites have been used to confine iron oxide particles in the pores of the support. A convenient method to control aggregation and particle size involves the preparation of iron hydroxide particles (e.g., akaganeite) in a template, such as clay [10, 11], polymer [12, 13] or Fe-exchanged natural zeolite [14].

The modification of zeolites with Fe(III) is typically performed in two stages as follows: i) the conversion of the zeolite to the Na^+ form using NaCl, NaOH and NaOH/NaCl solutions and ii) the conversion of the sodium form of the zeolite (Z^-Na^+) to the Fe(III) form using typical $FeCl_3$ solutions. When the modification process is carried out under acidic conditions, Na^+ ions are exchanged by Fe(III) cationic species and, to a lesser extent, the formation of hydrated iron oxides [15, 16]. Under basic conditions, the formation of hydrated iron hydroxide particles is the main modification mechanism [17, 18]. In general, the mineral properties of the zeolite support are not modified. However, a slight increase in the surface area has been associated with the formation of hydrated mineral oxides occupying both the surface and channels of the porous structure of zeolitic material [19]. The application of Fe(III) modified zeolites as well as Al(III), Mn(II) or Zr(IV) for the removal of oxyanionic species has been primarily focused on the removal of toxic elements, such as As(III)/As(V) [18], and other anions, such as fluoride [20]. Most of these studies of modified zeolites have focused on the removal mechanism with little attention to their possible regeneration.

This study describes the modification of a natural zeolite (clinoptilolite) with Fe(III) to promote the formation of >FeOH surface groups on the zeolites structure to favour the simultaneous uptake of cationic (ammonium) and anionic ($H_2PO_4^-$/HPO_4^{2-}) species; to evaluate the sorption performance and the potential regeneration and re-use of the Z-Fe zeolite via sorption and desorption cycles for tertiary wastewater treatment applications. The objectives of this work are as follows: (i) to incorporate Fe(III) into natural zeolite, (ii) to characterize the modified zeolite, (iii) to study the influence of pH and concentration on the phosphate and ammonium sorption onto the modified zeolite, (iv) to determine the equilibrium and kinetic sorption parameters, (v) to determine the sorption selectivity of common ions in wastewater effluents and (vi) to evaluate its performance in sorption and desorption cycles via dynamic experiments.

4.2. Materials and methods

4.2.1. Incorporation of Fe(III) to the natural zeolite

A natural zeolite (Z-N) obtained from the Zeocem Company (Slovak Republic) was washed and dried at 80 °C for 24 hours. The experiments were performed in batch (particles < 200 μm) and fixed-bed (< 800 μm) configurations. Z-N was modified to the iron form using an adaptation of the method reported by Jiménez – Cedillo et al. [21]. The Z-N sample (30 g) was treated in 250 mL of NaCl (0.1 M) two consecutive times under reflux for 4 h to obtain the sodium form of the zeolite (Z-Na). Then, the Z-Na sample (30 g) was treated two consecutive times by refluxing in 250 mL of $FeCl_3$ (0.1 M) for 4 h to obtain the iron zeolite (Z-Fe). After treatment, the samples were washed until no chloride was detected using an $AgNO_3$ test followed by drying at 80 °C for 24 hours.

4.2.2. Physicochemical characterization of the zeolites

A powder X-ray diffractometer (D8 Advance A25 Bruker) was used for X-ray diffraction (XRD) characterization of the Z-N, Z-Na and Z-Fe samples. The chemical composition and morphology of the samples were determined using a field emission scanning electron microscope (JEOL JSM-7001F) coupled to an energy dispersive spectroscopy system (Oxford Instruments X-Max). The infrared absorption spectra were recorded on a Fourier transform FTIR 4100 (Jasco) spectrometer in a range of 4000 to 550 cm^{-1}. The nitrogen gas adsorption method was used to determine the specific surface area of the Z-N, Z-Na and Z-Fe samples on an automatic sorption

analyser (Micrometrics). The tests were replicated at least four times for each sample, and the average values are reported.

4.2.3. Equilibrium and kinetic batch sorption studies

The batch equilibrium sorption experiments were carried out using a standard methodology that has been previously reported [22]. Weighed amounts of the dry samples (particle size < 200 μm) were shaken overnight in 25 mL of a solution containing various phosphate (P) and ammonium (N) concentrations. The following types of experiments were performed:

i) Sorption capacity as a function of phosphate and ammonium concentration: The Z-N and Z-Fe samples (0.25 g) were equilibrated in solutions without pH adjustment using concentrations ranging 1 to 2000 mg-P/L and 10 – 5000 mg-N/L. Ranges of phosphate and ammonium concentrations were selected considering the expected values of a conventional biological secondary effluent or concentrated effluent from anaerobic digestion. A ratio of 2 to 5 of ammonium over phosphate concentration was used taking as reference the average values of the composition of the municipal wastewaters in Barcelona – Spain.

ii) Sorption capacity as a function of equilibrium pH: The Z-Fe (0.1 g) sample was added to 25 mg-P/L and 25 mg-N/L solutions (pH adjusted from 2 to 11).

iii) Sorption capacity as a function of phosphate and ammonium concentration in the presence of individual ions and mixtures of common competing ions present in wastewater effluents: By addition of the Z-Fe sample (0.1 g) to solutions (without pH adjustment) containing 25 mg-P/L, 25 mg-N/L and 25 mg/L of the competing ion. The ion concentrations were fixed at the average annual composition of the stream from a tertiary treatment including a reverse osmosis step at the El Prat wastewater treatment plant (Barcelona – Spain). The solution consisted of: chloride (625 mg/L), bicarbonate (325 mg/L), sulfate (200 mg/L), nitrate (30 mg/L), sodium (260 mg/L), calcium (160 mg/L), magnesium (50 mg/L) and potassium (40 mg/L). Finally, the Z-Fe sample (0.25 g) was equilibrated in a solution containing concentrations ranging from 1 to 2000 mg-P/L and 10 – 5000 mg-N/L with the mixed ion solutions.

iv) Batch kinetic sorption experiments: The Z-Fe (0.1 g) sample was equilibrated in a solution containing 20 mg-N/L and 10 mg-P/L. The tubes were withdrawn sequentially at specific time intervals. All of the tests were performed at 200 rpm and room temperature (21±1 °C) in triplicate, and the average values are reported. The samples were centrifuged for 10 min and filtered (45 μm) prior to analysis. The

concentrations of the phosphate and ammonium ions were determined in the initial and remaining aqueous solution. In addition, the loaded zeolite samples were examined by field scanning electron microscopy, and the mineral phases were identified by X-Ray diffraction.

4.2.4. Phosphate speciation in the loaded Z-Fe samples by fractionation assays.

The fractionation of phosphorus immobilized in loaded Z-Fe was performed based on a modified three sequential step extraction protocol [23]. The Z-Fe sample (0.25 g) was equilibrated in 25 mL of a 25 mg-P/L solution. The loaded sample was washed and dried prior to the extraction trials. The loosely bound phosphorus fraction (LB-P) was determined by two consecutive extractions of the Z-Fe loaded sample (0.25 g) in 20 mL of 1 M NH_4Cl (pH 7). The iron and aluminum fraction ($Fe^{+}Al$)-P was determined by two consecutive extractions in 20 mL of 0.1 M NaOH followed by extraction in 1 M NaCl. Finally, the phosphorus linked to the calcium and magnesium compounds ($Ca^{+}Mg$)-P was determined by two consecutive extractions in 20 mL of 0.5 M HCl. The residual phosphorus (R-P) was calculated based on the mass balance between the phosphorus adsorbed and the extracted fractions. The tests were performed at 200 rpm in triplicate at 21±1 °C, and the average data are reported.

4.2.5. Phosphate and ammonium batch desorption studies

The Z-Fe sample (0.5 g < 200 μm) was added to 25 mL of a solution containing 25 mg-P/L and 25 mg-N/L. The loaded sample was washed and dried followed by equilibration in 25 mL of the elution solution: (i.e., NaOH (1 M), $NaHCO_3$ (0.1 M), Na_2CO_3 (0.1 M) and $NaHCO_3$/Na_2CO_3 (0.1 M)). The tests were performed in two sorption – desorption cycles at 200 rpm in triplicate at 21±1 °C, and average values are reported.

4.2.6. Phosphate and ammonium sorption and desorption column studies

The Z-Fe samples (<800 μm) were packed in a glass column (15 mm x 100 mm). The expected values of the effluent streams from secondary treatment at the El Prat wastewater treatment plant (Barcelona – Spain) were considered for the feed composition (i.e., phosphate (12.5 mg/L), ammonium (25 mg/L), chloride (312.5 mg/L), bicarbonate (162.5 mg/L), sulfate (10 mg/L), nitrate (15 mg/L), sodium (130 mg/L), calcium (80 mg/L), magnesium (25 mg/L) and potassium (20 mg/L)). The sorption under dynamic conditions was evaluated in the presence and absence of

competing ions with a countercurrent flow rate of 1.85 mL/min. Then, Z-Fe was saturated in the absence of competing ions and regenerated using a 1 M NaOH solution at a flow rate of 0.5 mL/min.

4.2.7. Analytical methods

Standard methods were used for phosphate (P) and ammonium (N) determination [24]. The vanadomolybdophosphoric acid colorimetric method (4500-P C) allowed for P quantification, and the ammonia-selective electrode method (4500-NH3 D) was employed for N determination. The ions were determined using a Thermo Scientific Ionic Chromatograph (Dionex ICS-1100 and ICS-1000).

4.3. Results and discussion

4.3.1. Characterization of modified Fe(III) zeolite

The XRD patterns of Z-N, Z-Na and Z-Fe indicated that clinoptilolite as the main crystalline phase, which coexisted with quartz and albite. The Z-Na sample was an intermediate stage in the zeolite modification to the iron form due to the easy sodium removal in ion exchange applications [25]. The existence of akaganeite (β-FeOOH) as the crystalline iron phase was observed in Z-Fe, which is in contrast to the reports of amorphous iron oxide species forming on natural zeolite surfaces [8, 21, 26]. The Z-Na and Z-Fe spectra exhibited the zeolite characteristic reflections (i.e., 2θ at 9.92°, 11.23°, 17.36°, 22.52° and 32.08°), which did not change. The small changes in the intensity of the reflections observed in the Z-Fe spectra resulted from the occupation of cation exchange sites by iron ions due to the $FeCl_3$ treatment. In addition, the specific surface area (19.8±0.3 m^2/g) of Z-N and Z-Fe was the same.

The FSEM-EDX analysis indicated that the chemical composition of clinoptilolite consisted of O, Na, Mg, Al, Si, K, Ca, Ti and Fe as the main elements (Table 4.1).

Element	Z-N	Z-Na	Z-Fe
O	57.8 ± 2.6	60.3 ± 1.4	57.4 ± 3.4
Na	0.3 ± 0.0	1.5 ± 0.1	0.4 ± 0.8
Mg	0.4 ± 0.1	0.4 ± 0.0	- ± -
Al	5.3 ± 0.2	5.3 ± 0.0	3.3 ± 1.4
Si	29.7 ± 1.7	29.1 ± 1.5	23.3 ± 3.7
Cl	< loq*	< loq*	1.1 0.2
K	2.9 ± 0.5	1.8 ± 0,2	1.0 ± 0.2
Ca	1.9 ± 0.3	1.1 ± 0,1	0.6 ± 1.0
Ti	0.2 0.2	< loq*	< loq*

Fe	1.6	±	0.4	0.5	±	0,0	12.8	± 2.4

*loq: limit of quantification

Table 4.1. Chemical composition (wt. %) of the zeolitic materials: natural zeolite (Z-N), sodium zeolite (Z-Na) and iron zeolite (Z-Fe).

In the Z-Na sample, the increase in the Na^+ content was due to the cationic exchange reaction between the Mg^{2+}, K^+ and Ca^{2+} ions. The iron content in Z-Fe exhibited an eight-fold increase due to ion exchange between K^+, Mg^{2+}, and Ca^{2+}. In addition, it is important to note the existence of chloride (1.1%) in the modified zeolite, which is consistent with previously reported results for natural or synthetic zeolites [15, 22]. Unfortunately, no discussion has been provided in these previous studies. The presence of chloride in the sample is associated with the presence of Fe-Cl complexes (e.g., $FeCl^{2+}$ and $FeCl_2^+$), which are the predominant species in the $FeCl_3$ solutions used to modify the zeolites. The modification process of the zeolite can be described by exchange reactions involving Fe-Cl complexes (Eq. (1-3)) even though it could not be discarded the exchange with Fe^{+3} ions.

$$>ZO^-Na^+ + FeCl_2^+ \leftrightarrow \ >ZO^- FeCl_2^+ + Na^+ \quad (1)$$

$$2(>ZO^-Na^+) + FeCl^{+2} \leftrightarrow \ (>ZO^-)_2(FeCl^{+2}) + 2\ Na^+ \quad (2)$$

$$3(>ZO^-Na^+) + Fe^{+3} \leftrightarrow \ (>ZO^-)_3Fe^{+3} + 3\ Na^+ \quad (3)$$

where $>ZO^-$ represents the zeolitic structure.

A network of crystal clusters with a homogeneous size distribution was identified in the FSEM image of the Z-N sample. The crystals of clinoptilolite displayed the characteristic plate-like morphology with large cavities and entries in to the channels inside the zeolite framework [27]. Notably, some lamellar crystals and small particles covered the surface of Z-Na and Z-Fe, confirming that sodium and iron modification was achieved in clinoptilolite.

The FTIR spectra of Z-N, Z-Na and Z-Fe displayed peaks between 798 cm^{-1} and 547 cm^{-1} that correspond to the stretching bridges of the Al-O-Si and Si-O-Si groups. The stretching vibration of the Si–O groups corresponds to the band at ~1100 cm^{-1}, and the deformation vibration of water was located at ~1630 cm^{-1}. The hydroxyl groups of the zeolitic structure are associated with the peaks in the range from 3700 cm^{-1} to 3100 cm^{-1} [4, 28]. The Z-N and Z-Na spectra exhibited minimal differences, which is typical for ion exchange between cations with a similar valence [29]. The Z-Fe spectra exhibit some changes in comparison to Z-N due to the ion exchange with the

trivalent Fe(III). The new bands located at 1396 cm^{-1}, 1455 cm^{-1} and 1541 cm^{-1} as well as the shift at 3396 cm^{-1} are related to the presence of the surface iron hydroxide groups (≅FeOH) [30, 31]. The formation of (≅FeOH) is caused by the modification step due to the strong acidity of the Fe(III) species even at low pH values, promoting the formation of $Fe(OH)_2^+$ and $Fe(OH)^{2+}$ (e.g., $(>ZO^-)_2(FeOH^{2+})$ or $>ZO^-FeOH_2^+$). In addition, a fraction of Fe(III) will be in the ≅ Fe-OH form (e.g., $(Fe(OH)_3(s))$.

4.3.2. Phosphate and ammonium equilibrium isotherms

The equilibrium uptake for phosphate and ammonium (q_e) was calculated using Eq. 4.

$$\boldsymbol{q_e = (C_o - C_e) \times \frac{v}{w}} \quad (4)$$

where C_o (mg/L) and C_e (mg/L) represent the initial and equilibrium concentrations, respectively, v (L) is the aqueous solution volume and w (g) is the mass of the zeolite. The phosphate and ammonium equilibrium sorption was evaluated according to the Langmuir (Eq. 5) and Freundlich (Eq. 6) isotherms:

$$\boldsymbol{\frac{C_e}{q_e} = \frac{1}{K_L . q_m} + \frac{C_e}{q_m}} \quad (5)$$

$$\boldsymbol{\log q_e = \log K_F + \frac{1}{n} log\ C_e} \quad (6)$$

where q_m (mg/g) is the maximum sorption capacity, K_L (L/mg) is the Langmuir sorption equilibrium constant and K_F ((mg/g)/$(mg/L)^{1/n}$) is the Freundlich equilibrium sorption constant.

The Langmuir isotherm provided a better description of the phosphate and ammonium equilibrium sorption ($R^2 \geq 0.99$) compared with the Freundlich isotherm (Table 4.2 and Figure 4.1), which only describes the experimental data at low concentrations levels. These results suggest that the availability of specific and equal affinity sites on the zeolite for monolayer and homogenous sorption or/and ion exchange. The phosphate maximum sorption capacity exhibited a six-fold increase in Z-Fe (3.4±0.2 mg-P/g) compared with Z-N (0.6±0.1 mg-P/g). In contrast, a decrease in ammonium capacity from 33±2 mg-N/g in Z-N to 27±2 mg-N/g in Z-Fe was observed.

		Langmuir			Freundlich		
		q_m (mg/g)	K_L (L/mg)	R^2	K_F ((mg/g)/$(mg/L)^{1/n}$)	1/n	R^2
Z-N	Phosphate	0.6	0.01	0.99	0.02	0.47	0.97

	Ammonium	33	0.006	0.99	1.84	0.36	0.94
Z-Fe	Phosphate	3.4	0.02	0.99	0.59	0.25	0.71
	Ammonium	27	0.004	0.99	0.80	0.46	0.96

Table 4.2. Isotherm parameters for phosphate and ammonium sorption on natural zeolite (Z-N) and iron zeolite (Z-Fe).

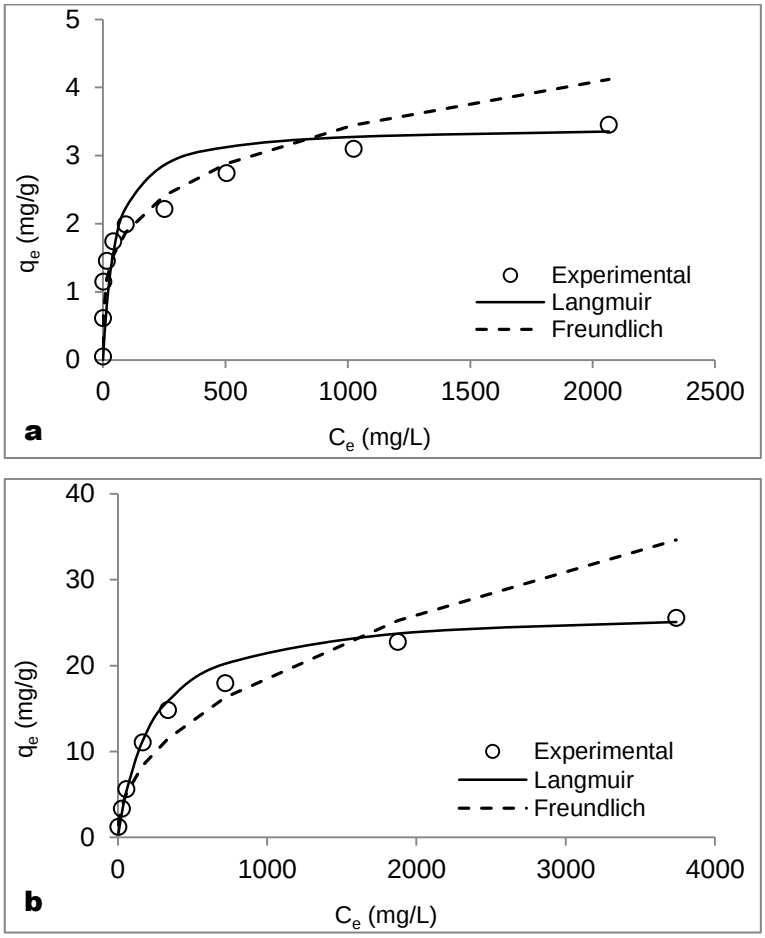

Figure 4.1. Experimental and theoretical equilibrium isotherms for a) phosphate and b) ammonium removal by iron zeolite (Z-Fe) at constant equilibrium pH 3.1±0.2.

The phosphate removal was not dependent on the pH in the range of 2 to 11 (Figure 4.2). The sorption mechanism of the phosphate oxyanion (H_2PO^{4-} - HPO_4^{2-} - PO_4^{3-}) is associated with the formation of monodentate and bidentate complexes with the hydroxyl surface groups of both of the exchanged iron complexes on the cation exchange positions or on the hydrated iron oxides (≅FeOH groups) inside the zeolite micropores (specific adsorption), which is represented by Eq. 7 [32-34]; or by means of columbic forces depending of the pH_{pzc} (non-specific adsorption), as shown in Eqs. 8 and 9 [35].

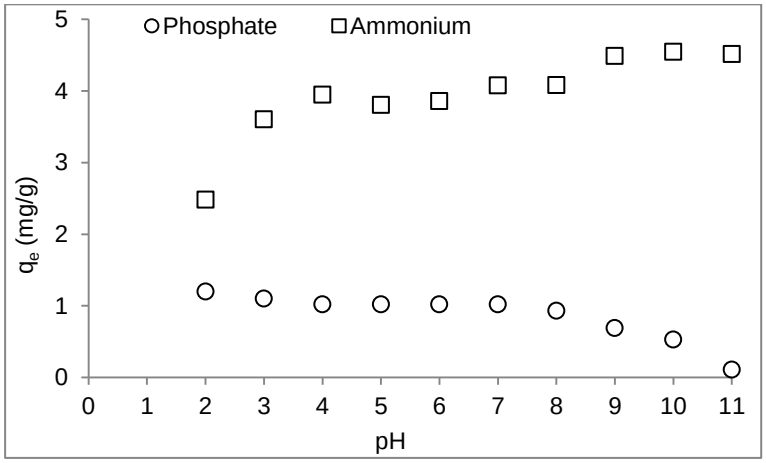

Figure 4.2. Effect of pH on the phosphate and ammonium removal by iron zeolite (Z-Fe).

$$\mathrm{H_2PO_4^-} \quad \mathrm{Z-Fe-}\overset{\overset{OH}{|}}{\underset{\underset{O}{\|}}{O-P-OH}} \quad + OH^- \quad Monodentate$$

$$Z-Fe-OH + \xrightarrow[pH \geq pH_{PZC}]{Complexation} \mathrm{Z-Fe} \begin{matrix} O \\ O \end{matrix} > P \leqslant \begin{matrix} OH \\ O \end{matrix} + OH^- \quad \begin{matrix} Bidentate \\ Mononuclear \end{matrix} \qquad (7)$$

$$\mathrm{HPO_4^{2-}} \quad \mathrm{Z-Fe-O \atop Z-Fe-O} > P \leqslant \begin{matrix} OH \\ O \end{matrix} + 2OH^- \quad \begin{matrix} Bidentate \\ Binuclear \end{matrix}$$

$$Z-Fe-OH \xrightarrow[pH < pH_{PZC}]{Protonation} Z-Fe-OH^{2+} \xrightarrow[\mathrm{H_2PO_4^-/HPO_4^{2-}}]{Electrostatic\ attraction} \begin{matrix} Z-Fe-OH^{2+} \ldots \mathrm{H_2PO_4^-} \\ Z-Fe-OH^{2+} \ldots \mathrm{HPO_4^{2-}} \end{matrix} \qquad (8)$$

$$Z-Fe-OH \xrightarrow[pH \gg pH_{PZC}]{Hydroxilation} Z-Fe-O^- + H_2O \qquad (9)$$

The reduction of the P sorption capacity above a pH of 8, indicates the acid-base properties of the hydrated iron oxides formed during the impregnation processes with a pH_{PCZ} close to 8. This behaviour is in agreement with published data for the akaganeite minerals [36] and ion-exchange resins impregnated with hydrated iron oxides [37, 38].

The electrostatic interactions of the surface groups of Z-Fe (Eq. 7 and 9) are responsible for the lowest ammonium sorption at acidic pH values (near pH 2) due to competition with H^+ ions. The NH_4^+ sorption pH dependence exhibited an unexpected increase even above a pH of 9.3 when it is converted to NH_3, and then, the removal values could not be explained by the exchange reaction defined by Eq. 10 [39].

However, Liu et al. [20] reported Fe(III) removal of NH_3 due to a complexation reaction with Fe atoms as $\cong FeOH_n(NH_3)_m$.

$Z\text{-}Na^+ + NH_4^+ \leftrightarrow Na^+ + Z\text{-}NH_4^+$ (10)

4.3.3. Effect of competing ions on phosphate and ammonium sorption

The phosphate sorption exhibited a slight improvement in the presence of Mg^{2+} (6 %) > K^+ (5 %) > Na^+ (3 %) and Ca^{2+} (1 %), which it has been reported for a synthetic zeolite due to the effect of a precipitation reaction involving the formation of $Mg/NH_4/PO_4$ and Ca/PO_4 minerals [40]. However, no mineralogical phase was identified by XRD analysis of the loaded iron samples due to their content being below the limit of detection. An important decrease in the ammonium removal was promoted by K^+ (18 %) > Ca^{2+} (16 %) > Na^+ (10 %) > Mg^{2+} (4 %), which is in agreement with the behaviour reported for a synthetic zeolite [5] even though the ion-exchange coefficients are favoured for NH_4^+ ions over $K^+/Na^+/Ca^{2+}$ and Mg^{2+}. The cation mixture decreases by 16% and 38 % for the phosphate and ammonium uptakes, respectively.

The phosphate and ammonium sorption capacity has a variation of less 5 % in the presence of chloride and sulfate as reported for other zeolites (Figure 4.3) [5, 39]. Therefore, there is no competition between these species for the same binding sites due to outer-sphere complexation [40, 41]. Notably, a reduction in the phosphate removal was promoted by the coexistence of HCO_3^-, which is consistent with the selectivity reported for a modified zeolite [42]. The combination of anions decreases the phosphate and ammonium uptake by 8 % and 14 %, respectively.

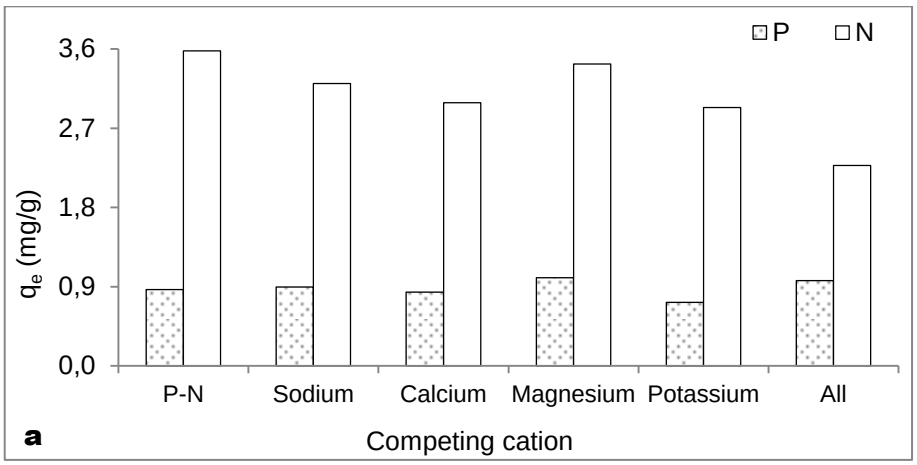

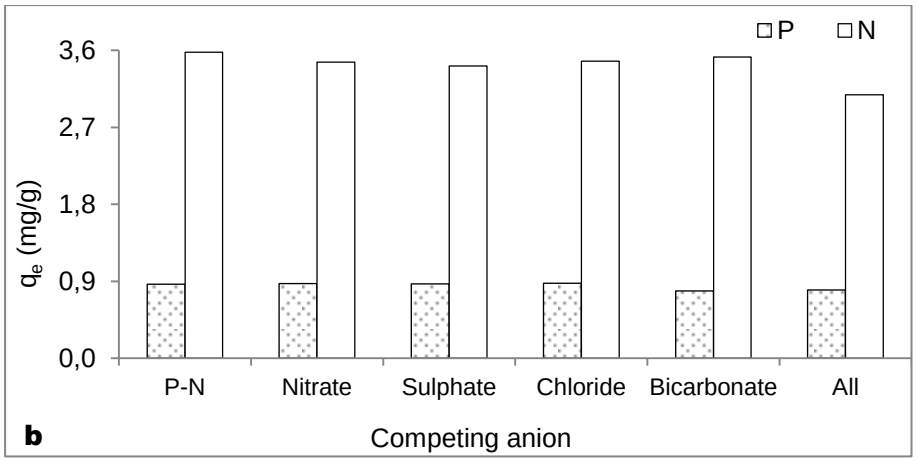

Figure 4.3. Individually effect of a) cations and b) anions for phosphate (P) and ammonium (N) removal by iron zeolite (Z-Fe).

The Langmuir isotherm ($R^2 \geq 0.99$) provided a better description of the phosphate and ammonium equilibrium sorption in the presence of competing ions compared with the Freundlich isotherm (Table 4.3, Figure 4.4). The ammonium sorption capacity decreased in the presence of ions at 23 mg-N/g and at 25mg-N/g with coexisting anions and cations. Similarly, decrease in the phosphate uptake capacity was observed in the presence of ions and anions at 3.1 mg-P/g and in the presence of cations at 3.3 mg-P/g.

	Langmuir			Freundlich		
	q_m (mg/g)	K_L (L/mg)	R^2	K_F ((mg/g)/(mg/L)$^{1/n}$)	1/n	R^2
Phosphate	3.4	0.02	0.99	0.59	0.25	0.71
P-Anions	3.1	0.01	0.99	0.35	0.31	0.81
P-Cations	3.3	0.02	0.99	0.54	0.26	0.80
P-Ions	3.1	0.02	0.99	0.53	0.24	0.98
Ammonium	27	0.004	0.99	0.80	0.46	0.96
N-Anions	25	0.003	0.99	0.69	0.45	0.97
N-Cations	25	0.002	0.98	0.45	0.49	0.99
N-Ions	23	0.002	0.99	0.46	0.47	0.99

Table 4.3. Isotherm parameters for phosphate and ammonium sorption by iron zeolite (Z-Fe) in the presence of competing ions.

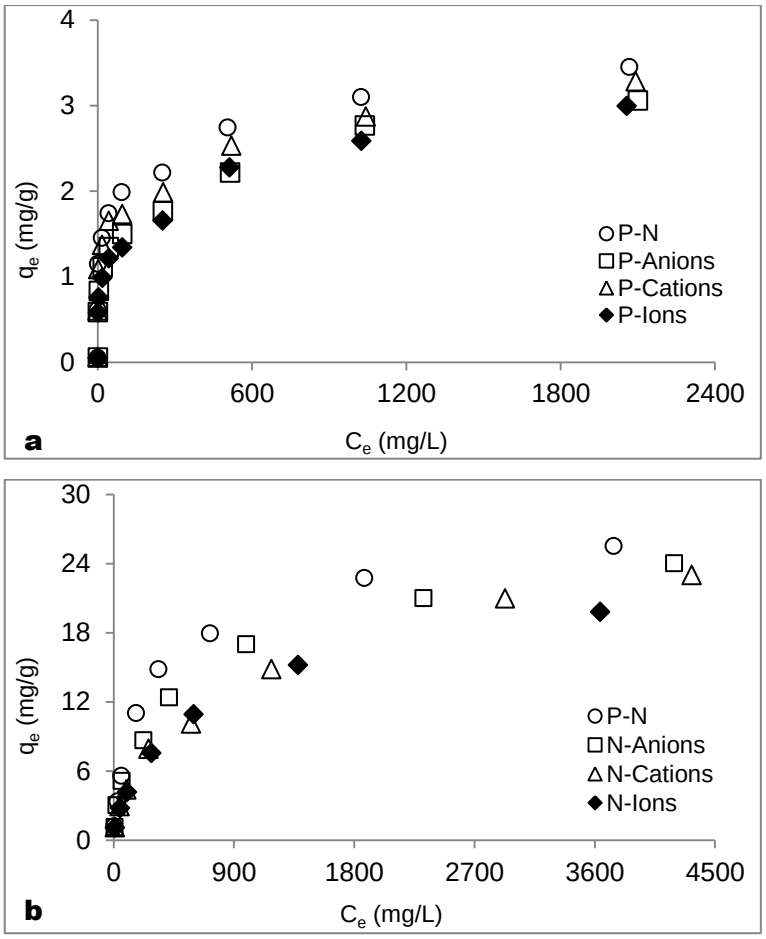

Figure 4.4. Equilibrium capacity for a) phosphate and b) ammonium recovery by the iron zeolite (Z-Fe) in presence of competing ions.

4.3.4. Phosphate and ammonium sorption kinetics

The sorption kinetics of both the phosphate and ammonium ions for Z-Fe are comparable to those reported for zeolitic materials (Figure 4.5). Equilibrium was reached within 200 minutes which is in agreement with the behaviour of a Fe (III) natural modified zeolite [43], and the phosphate sorption rates were lower compared with those of the ammonium ions, which is due to ion exchange between NH_4^+ and Na^+ ions being faster than phosphate ion complexation on the zeolite surface (≅FeOH).

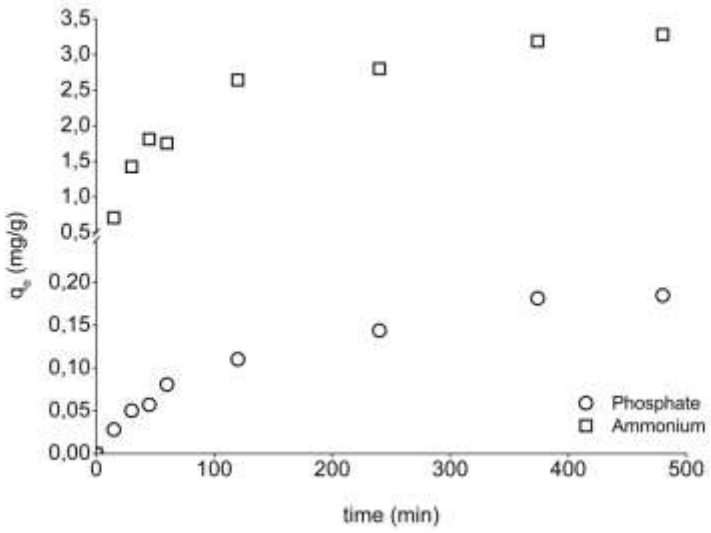

Figure 4.5. Evolution of phosphate and ammonium sorption uptake versus time for iron zeolite (Z-Fe) in batch experiments at 21±1 ºC.

The intraparticle diffusion model reported by Weber and Morris [44] (Eq. 11) was employed to describe the sorption mechanisms of the zeolite assuming it was promoted by diffusion in the spherical adsorbent and convective diffusion in the adsorbate solution.

$$q_t = k_t\, t^{1/2} + A \qquad (11)$$

where k_t ($mg.g^{-1}.h^{-1/2}$) is the intraparticle diffusion rate constant and A (mg/g) describes the thickness of the boundary layer (i.e., the higher the value of A, the greater the boundary layer effect). The sorption process is controlled by intraparticle diffusion when the sorption uptake (q_t) as a function of $t^{1/2}$ yields a straight line. In contrasts, when two or more steps influence the sorption process, the data result in multi-linear plots.

The fitting of the kinetic data to the intraparticle diffusion model revealed two linear steps. Therefore, film diffusion followed by particle diffusion may be used to describe the phosphate and ammonium sorption [45]. In addition, the phosphate and ammonium sorption were evaluated based on the film diffusion (D_f) and particle diffusion (D_p) mechanisms corresponding to the homogenous particle diffusion model (HPDM) (Figure 4.6) [46, 47]. The effective particle diffusivity calculates the sorption on the spherical particles using Eq. 12:

$$-\ln\left(1-\left(\frac{q_t}{q_e}\right)^2\right)=\frac{2\,\pi^2 D_p}{r^2}t \qquad (12)$$

When the rate of sorption is controlled by liquid film diffusion, this rate can be expressed as shown in Eq. 13:

$$-\ln\left(1-\left(\frac{q_t}{q_e}\right)\right)=\frac{D_f C_s}{h\,r\,C_z}t \qquad (13)$$

where q_t and q_e are the solute loadings on the adsorbent phase at time t and equilibrium (mg/g), respectively, C_s (mg/L) and C_z (mg/kg) are the ion concentrations in solution and in the zeolite, respectively, r is the average radius of the zeolite particles ($1x10^{-4}$ m), t is the contact time (min) and h is the thickness of film around the zeolite particle ($1x10^{-5}$ m for a poorly stirred solution) [48].

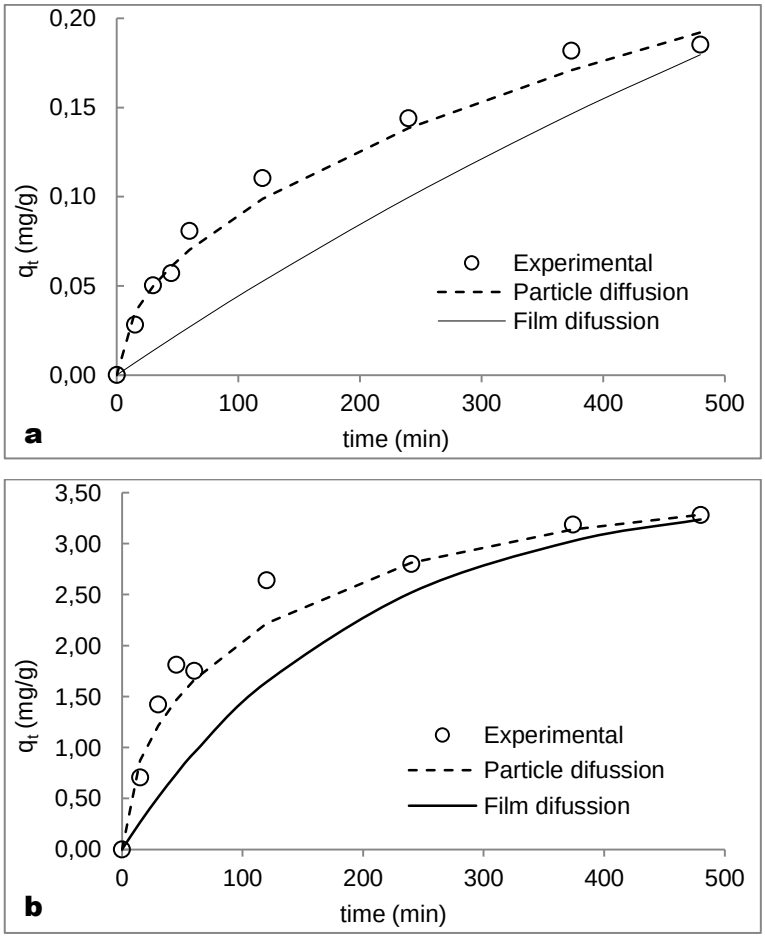

Figure 4.6. Experimental and theoretical sorption kinetics of a) phosphate and b) ammonium ions for Z-Fe.

Both the phosphate and ammonium sorption exhibited higher values of D_f than those found for D_p. Therefore, particle diffusion was the rate-limiting step, and monolayer molecular sorption occurred on the surface of zeolite (Table 4.4), which is consistent

with the results reported for ammonium sorption on natural zeolites at low initial ammonium concentrations [45, 48, 49].

Model	Kinetic parameters	Phosphate	Ammonium
Intraparticle diffusion	k_{t1} ($mg \cdot g^{-1} \cdot h^{-1/2}$)	0.1	1.9
	R^2	0.99	0.97
	k_{t2} ($mg \cdot g^{-1} \cdot h^{-1/2}$)	0.1	0.5
	R^2	0.89	0.96
Film diffusion	D_f ($m^2 \cdot s^{-1}$)	$4.6x10^{-11}$	$1.2x10^{-09}$
	R^2	0.92	0.95
Particle diffusion	D_p ($m^2 \cdot s^{-1}$)	$1.6x10^{-13}$	$2.1x10^{-12}$
	R^2	0.98	0.98

Table 4.4. Kinetic parameters for phosphate and ammonium removal by iron zeolite (Z-Fe).

Based on FSEM – EDAX analysis, the loaded Z-Fe possessed a surface covered by several lamellar particles, and the existence of phosphorus but not nitrogen was observed, which may be due to the content being below the limit of quantification. After sorption, the zeolite surface exhibited a compact crystalline framework. The loaded zeolite spectra exhibited changes in the bands at 3392 cm^{-1}, 1455 cm^{-1} and 1040 cm^{-1} due to the hydroxyl groups (Fe(OH)) of the zeolite surface participating in the complexation reactions with the phosphate and ammonium ions [9, 50, 51]. Therefore, the increase in phosphate removal at the expense of a slight reduction in ammonium sorption occurred on Z-N and Z-Fe due to binding site competition, as it was reported by a natural zeolite in the aluminum form [52].

4.3.5. Phosphorus speciation in the loaded Z-Fe samples

The L-B and R-P were the minor fractions of the immobilized phosphorous at 4±2 % and 3±2 %, respectively (Table 4.5), which is in agreement with previous results using a synthetic zeolite [53]. The 54±8 % phosphorus was associated with the iron and aluminum hydroxides. This result suggests that the Fe-OH groups of the hydrated iron oxides in Z-Fe are primarily responsible for phosphate removal, which is in accordance to the report of a synthetic zeolite [54]. In addition, 39±6 % of phosphorus was immobilized by calcium and magnesium (Ca+Mg)-P compounds. Chemical precipitation encouraged phosphate uptake but no mineral phase was determine by XRD analysis due to the concentrations being below the limit of quantification.

q_e	LB-P		(Fe+Al)-P		(Ca+Mg)-P (mg/g)		R-P	
(mg/g)	(mg/g)	%	(mg/g)	%	(mg/g)	%	(mg/g)	%
0.98	0.03	4±2	0.53	54±8	0.39	39±6	0.03	3±2

Table 4.5. Speciation of phosphate immobilized on the iron zeolite (Z-Fe) associated to the chemical forms: LB-P; (Fe+Al)-P; (Ca+Mg)-P; R-P.

4.3.6. Phosphate and ammonium batch desorption

Higher recovery ratios were obtained for ammonium than phosphate from the loaded zeolite using NaOH, $NaHCO_3$, Na_2CO_3 and mixtures of $NaHCO_3$/Na_2CO_3 in the first sorption – desorption cycle (Table 4.6)

Elution solution	Desorption (%)	
	Phosphate	Ammonium
1 M NaOH	64±4	92±6
0.1 M $NaHCO_3$	49±4	52±4
0.1 M Na_2CO_3	74±5	91±6
0.1 $NaHCO_3$/0.1 MNa_2CO_3	73±5	66±4

Table 4.6. Simultaneous phosphate and ammonium desorption efficiency from loaded Z-Fe in batch experiments at 21±ºC.

The partial phosphate desorption was due to complexation between hydrated iron oxide groups and phosphate and the formation of Ca-Mg phosphate mineral phases. All of the regenerated Z-Fe samples exhibited a larger decrease in phosphate uptake compared with ammonium removal capacity in the subsequent sorption cycles. Therefore, in operational terms, the sorption capacity obtained in the impregnation step was lost. Previous studies of Fe-loaded zeolites do not discuss general regeneration cycles and reuse, and loading capacity losses have not been previously reported. Therefore, the reuse of the modified zeolite will require re-impregnation after cycling, or the loaded zeolites could be potentially used for improvement of soil quality.

4.3.7. Simultaneous phosphate and ammonium uptake in dynamic assays

The breakthrough curves of ammonium (25 mg/L) and phosphate (12.5 mg/L) sorption by Z-Fe with and without competing ions are shown in Figure 4.7. The ammonium maximum sorption capacity at column saturation (C/C_0=0.95) was 26 mg-N/g at 306 BV, and in the presence of competing ions, the ammonium maximum

sorption capacity decreased to 15 mg-N/g at 257 BV. In addition, the phosphate maximum sorption capacity decreased from 2.7 mg P/g at 167 BV to 1.1 mg-P/g at 122 BV in the presence of coexisting ions.

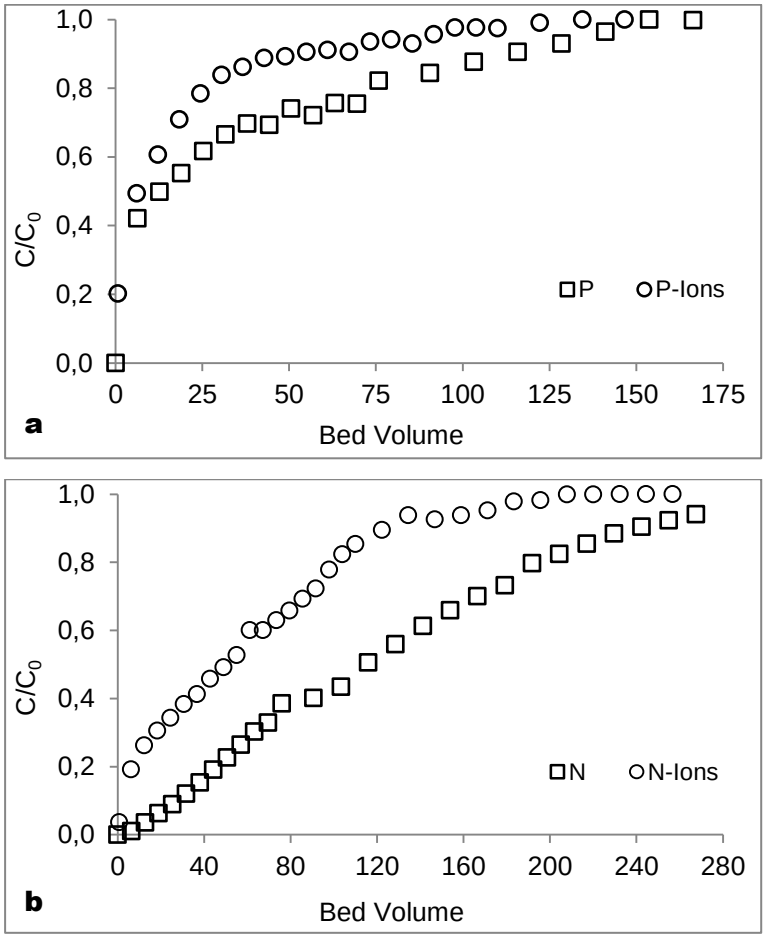

Figure 4.7. Breakthrough curves of a) phosphate and b) ammonium uptake by iron zeolite (Z-Fe) at flow rate of 1.8 mL/min.

The profiles of the ammonium and phosphate desorption in a NaOH solution (Figure 4.8) indicated a recovery of 88±3 % of the eluted phosphate and 92±2 % of the eluted ammonium at 4 BV. The highest concentrations were determined to be 131 mg-P/L and 3834 mg-P/L. Under these conditions, enrichment factors of 40 and 80 were achieved for phosphate and ammonium, respectively.

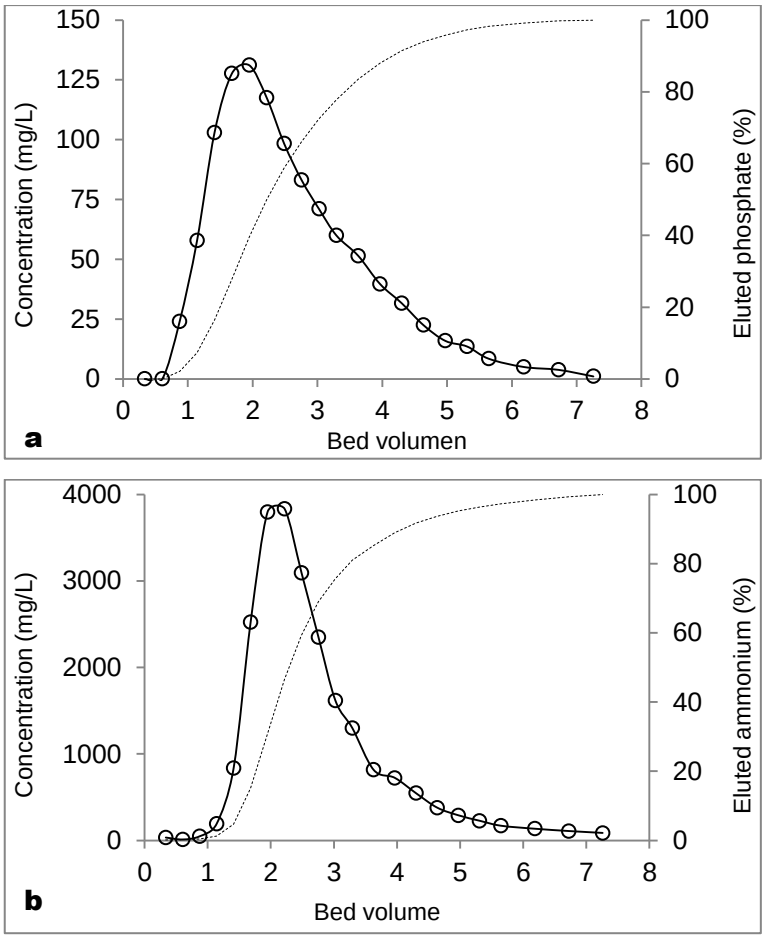

Figure 4.8. Desorption profiles of a) phosphate and b) ammonium from loaded iron zeolite (Z-Fe) using 1 M NaOH at 0.5 mL/min.

4.4. Conclusions

In this study, a simple modification process of an iron zeolite (Fe(III)) resulted in simultaneous cationic and anionic sorption. The enhancement of the phosphate uptake slightly affected the ammonium exchange capacity of the modified zeolite. The ammonium sorption primarily occurred by ion exchange and complexation with the (ZO^-) groups of the zeolitic structure and a combination of electrostatic interactions, chemical precipitation and inner sphere complexation with ≅Fe-OH functional groups act as the sorption mechanism for phosphate uptake. The coexistence of competing ions slightly affected the phosphate and ammonium sorption uptake onto Z-Fe. In the dynamic experiments, the desorption using 1 M NaOH provided enrichment factors of 39 and 80 for phosphate and ammonium, respectively. However, the sorption – desorption operation revealed a reduction in the anionic and cationic uptake capacity. Therefore, re-impregnation steps are

required after reuse cycles, or based on the reusability limitations, the loaded zeolites have the potential for use as additives to improve soil quality.

4.5. References

1. Zamparas, M., et al., *A novel bentonite-humic acid composite material Bephos™ for removal of phosphate and ammonium from eutrophic waters.* Chemical Engineering Journal, 2013. **225**(0): p. 43-51.
2. Yin, H. and M. Kong, *Simultaneous removal of ammonium and phosphate from eutrophic waters using natural calcium-rich attapulgite-based versatile adsorbent.* Desalination, 2014. **351**: p. 128-137.
3. Villanueva, M.E., et al., *Point of zero charge as a factor to control biofilm formation of Pseudomonas aeruginosa in sol-gel derivatized aluminum alloy plates.* Surface and Coatings Technology, 2014. **254**: p. 145-150.
4. Król, M., et al., *Application of IR spectra in the studies of zeolites from D4R and D6R structural groups.* Microporous and Mesoporous Materials, 2012. **156**: p. 181-188.
5. Zhang, M., et al., *Removal of ammonium from aqueous solutions using zeolite synthesized from fly ash by a fusion method.* Desalination, 2011. **271**(1–3): p. 111-121.
6. Alshameri, A., et al., *The investigation into the ammonium removal performance of Yemeni natural zeolite: Modification, ion exchange mechanism, and thermodynamics.* Powder Technology, 2014. **258**(0): p. 20-31.
7. Malekian, R., et al., *Ion-exchange process for ammonium removal and release using natural Iranian zeolite.* Applied Clay Science, 2011. **51**(3): p. 323-329.
8. Jiménez-Cedillo, M.J., et al., *Adsorption capacity of iron- or iron–manganese-modified zeolite-rich tuffs for As(III) and As(V) water pollutants.* Applied Clay Science, 2011. **54**(3–4): p. 206-216.
9. Huang, H., et al., *Simultaneous removal of nutrients from simulated swine wastewater by adsorption of modified zeolite combined with struvite crystallization.* Chemical Engineering Journal, 2014. **256**: p. 431-438.
10. Haque, N., et al., *Iron-modified light expanded clay aggregates for the removal of arsenic(V) from groundwater.* Microchemical Journal, 2008. **88**(1): p. 7-13.

11. Villalba, J.C., V.R.L. Constantino, and F.J. Anaissi, *Iron oxyhydroxide nanostructured in montmorillonite clays: Preparation and characterization.* Journal of Colloid and Interface Science, 2010. **349**(1): p. 49-55.
12. Iesan, C.M., et al., *Evaluation of a novel hybrid inorganic/organic polymer type material in the Arsenic removal process from drinking water.* Water Research, 2008. **42**(16): p. 4327-4333.
13. Cumbal, L., et al., *Polymer supported inorganic nanoparticles: characterization and environmental applications.* Reactive and Functional Polymers, 2003. **54**(1–3): p. 167-180.
14. Jeon, C.-S., et al., *Adsorption characteristics of As(V) on iron-coated zeolite.* Journal of Hazardous Materials, 2009. **163**(2–3): p. 804-808.
15. Li, Z., et al., *Combination of hydrous iron oxide precipitation with zeolite filtration to remove arsenic from contaminated water.* Desalination, 2011. **280**(1–3): p. 203-207.
16. Bilici Baskan, M. and A. Pala, *Removal of arsenic from drinking water using modified natural zeolite.* Desalination, 2011. **281**(0): p. 396-403.
17. Li, Z., et al., *Removal of arsenic from water using Fe-exchanged natural zeolite.* Journal of Hazardous Materials, 2011. **187**(1–3): p. 318-323.
18. Šiljeg, M., et al., *Structure investigation of As(III)- and As(V)-species bound to Fe-modified clinoptilolite tuffs.* Microporous and Mesoporous Materials, 2009. **118**(1–3): p. 408-415.
19. Dávila-Jiménez, M.M., et al., *In situ and ex situ study of the enhanced modification with iron of clinoptilolite-rich zeolitic tuff for arsenic sorption from aqueous solutions.* Journal of Colloid and Interface Science, 2008. **322**(2): p. 527-536.
20. Liu, H., et al., *The transformation of ferrihydrite in the presence of trace Fe(II): The effect of the ammonia, amine and the coordination ions of Fe(III).* Journal of Solid State Chemistry, 2010. **183**(3): p. 542-546.
21. Jiménez-Cedillo, M.J., M.T. Olguín, and C. Fall, *Adsorption kinetic of arsenates as water pollutant on iron, manganese and iron–manganese-modified clinoptilolite-rich tuffs.* Journal of Hazardous Materials, 2009. **163**(2–3): p. 939-945.

22. Kim, K.S., J.O. Park, and S.C. Nam, *Synthesis of Iron-loaded Zeolites for Removal of Ammonium and Phosphate from Aqueous Solutions.* Environ Eng Res, 2013. **18**(4): p. 267-276.
23. Hieltjes, A.H.M. and L. Lijklema, *Fractionation of Inorganic Phosphates in Calcareous Sediments1.* J. Environ. Qual., 1980. **9**(3): p. 405-407.
24. APHA, A., WEF., *Standard methods for the examination of water and wastewater*, 2000, American Public Health Association, American Water Works Association, and Water Environment Federation.
25. Lei, L., X. Li, and X. Zhang, *Ammonium removal from aqueous solutions using microwave-treated natural Chinese zeolite.* Separation and Purification Technology, 2008. **58**(3): p. 359-366.
26. Doula, M.K., *Synthesis of a clinoptilolite–Fe system with high Cu sorption capacity.* Chemosphere, 2007. **67**(4): p. 731-740.
27. Margeta, K., et al., *Natural Zeolites in Water Treatment – How Effective is Their Use*, in *Water Treatment*, W. Elshorbagy and R.K. Chowdhury, Editors. 2013, InTech: Rijeka. p. 81-112.
28. Reháková, M., et al., *Removal of pyridine from liquid and gas phase by copper forms of natural and synthetic zeolites.* Journal of Hazardous Materials, 2011. **186**(1): p. 699-706.
29. Li, J., et al., *Studies on natural STI zeolite: modification, structure, adsorption and catalysis.* Microporous and Mesoporous Materials, 2000. **37**(3): p. 365-378.
30. Luan, Z. and J.A. Fournier, *In situ FTIR spectroscopic investigation of active sites and adsorbate interactions in mesoporous aluminosilicate SBA-15 molecular sieves.* Microporous and Mesoporous Materials, 2005. **79**(1–3): p. 235-240.
31. Jin, F. and Y. Li, *A FTIR and TPD examination of the distributive properties of acid sites on ZSM-5 zeolite with pyridine as a probe molecule.* Catalysis Today, 2009. **145**(1–2): p. 101-107.
32. Lǔ, J., et al., *Adsorptive removal of phosphate by a nanostructured Fe–Al–Mn trimetal oxide adsorbent.* Powder Technology, 2013. **233**: p. 146-154.
33. Dzombak, D. and F. Morel, *Surface Complexation Modeling: Hydrous Ferric Oxide*1990, New York: John Wiley & Sons, Inc.

34. Simsek, E.B., E. Özdemir, and U. Beker, *Zeolite supported mono- and bimetallic oxides: Promising adsorbents for removal of As(V) in aqueous solutions.* Chemical Engineering Journal, 2013. **220**: p. 402-411.
35. Sujana, M.G., et al., *Studies on fluoride adsorption capacities of amorphous Fe/Al mixed hydroxides from aqueous solutions.* Journal of Fluorine Chemistry, 2009. **130**(8): p. 749-754.
36. Chitrakar, R., et al., *Phosphate adsorption on synthetic goethite and akaganeite.* Journal of Colloid and Interface Science, 2006. **298**(2): p. 602-608.
37. You, X., et al., *Phosphate removal from aqueous solution using a hybrid impregnated polymeric sorbent containing hydrated ferric oxide (HFO).* Journal of Chemical Technology & Biotechnology, 2015: p. n/a-n/a.
38. Blaney, L.M., S. Cinar, and A.K. SenGupta, *Hybrid anion exchanger for trace phosphate removal from water and wastewater.* Water Research, 2007. **41**(7): p. 1603-1613.
39. Huang, H., et al., *Ammonium removal from aqueous solutions by using natural Chinese (Chende) zeolite as adsorbent.* Journal of Hazardous Materials, 2010. **175**(1–3): p. 247-252.
40. Guan, Q., et al., *Phosphate removal in marine electrolytes by zeolite synthesized from coal fly ash.* Fuel, 2009. **88**(9): p. 1643-1649.
41. Onyango, M.S., et al., *Adsorptive Removal of Phosphate Ions from Aqueous Solution Using Synthetic Zeolite.* Industrial & Engineering Chemistry Research, 2007. **46**(3): p. 894-900.
42. Ning, P., et al., *Phosphate removal from wastewater by model-La(III) zeolite adsorbents.* Journal of Environmental Sciences, 2008. **20**(6): p. 670-674.
43. Huo, H., et al., *Ammonia-nitrogen and phosphates sorption from simulated reclaimed waters by modified clinoptilolite.* Journal of Hazardous Materials, 2012. **229–230**(0): p. 292-297.
44. Weber, W.J. and J.C. Morris, *Kinetics of adsorption on carbon solution.* Journal of the Sanitary Engineering Division, 1963. **89**(2): p. 31-59.
45. Lin, L., et al., *Adsorption mechanisms of high-levels of ammonium onto natural and NaCl-modified zeolites.* Separation and Purification Technology, 2013. **103**(0): p. 15-20.
46. Helfferich, F.G., *Ion exchange*1962, New York: McGraw-Hill.

47. Valderrama, C., et al., *Kinetic evaluation of phenol/aniline mixtures adsorption from aqueous solutions onto activated carbon and hypercrosslinked polymeric resin (MN200).* Reactive and Functional Polymers, 2010. **70**(3): p. 142-150.
48. Moussavi, G., et al., *The investigation of mechanism, kinetic and isotherm of ammonia and humic acid co-adsorption onto natural zeolite.* Chemical Engineering Journal, 2011. **171**(3): p. 1159-1169.
49. Sprynskyy, M., et al., *Ammonium removal from aqueous solution by natural zeolite, Transcarpathian mordenite, kinetics, equilibrium and column tests.* Separation and Purification Technology, 2005. **46**(3): p. 155-160.
50. Guo, J., C. Yang, and G. Zeng, *Treatment of swine wastewater using chemically modified zeolite and bioflocculant from activated sludge.* Bioresource Technology, 2013. **143**(0): p. 289-297.
51. Wahab, M.A., et al., *Characterization of ammonium retention processes onto Cactus leaves fibers using FTIR, EDX and SEM analysis.* Journal of Hazardous Materials, 2012. **241–242**(0): p. 101-109.
52. Guaya, D., et al., *Simultaneous phosphate and ammonium removal from aqueous solution by a hydrated aluminum oxide modified natural zeolite.* Chemical Engineering Journal, 2015. **271**: p. 204-213.
53. Xie, J., et al., *Synthesis and properties of zeolite/hydrated iron oxide composite from coal fly ash as efficient adsorbent to simultaneously retain cationic and anionic pollutants from water.* Fuel, 2014. **116**(0): p. 71-76.
54. Wu, D., et al., *Simultaneous removal of ammonium and phosphate by zeolite synthesized from fly ash as influenced by salt treatment.* Journal of Colloid and Interface Science, 2006. **304**(2): p. 300-306.

Chapter 5 Simultaneous nutrients removal by using a hybrid inorganic sorbent impregnated with hydrated manganese oxide

Abstract

A natural zeolite (Z-N) and its hybrid form (Z-Mn) prepared by impregnation with hydrated manganese oxide have been evaluated for the simultaneous removal of ammonium and phosphate from aqueous solutions. The ammonium sorption capacity reported by Z-Mn was 23±2 mg $N\text{-}NH_4^+$/g; while the phosphate uptake reached 5.6±0.2 mg $P\text{-}PO_4^{3-}$/g at pH 7.5. Both ammonium and phosphate uptake were slightly affected by coexisting ions commonly found in wastewater effluents. The Mn(II) activated zeolite (Z-Mn) improved the phosphate sorption capacity, in the pH range 7 to 9, by formation of surface complexes of P(V) anions with the precipitated Mn(II) hydrated oxides or by formation of mineral phases as Mn(II)--NH_4-PO_4 (e.g., ($NH_4MnPO_4 \cdot H_2O$)) which was detected by XRD analysis. The soil availability test from loaded zeolites reported higher ammonium than phosphate availability. The desorption of ammonium and phosphate from the loaded zeolites using 1 M NaOH solution in dynamic experiments provided higher recoveries and enrichment factors of ammonium than phosphate.

Key words: clinoptilolite; manganese; sorption; hybrid sorbent; phosphate and ammonium recovery, hydrated manganese oxide

5.1. Introduction

Nitrogen and phosphorus compounds are the major threats to natural water receiving bodies as they provide suitable conditions for a quickly and excessive growing of aquatic organisms promoting its deterioration. Nitrogen and phosphorus compounds in water environment are found mainly as inorganic species as ammonium and phosphate, respectively [1, 2], and in less extension organic based N and P organic forms. New technologies are being studying for the effective discharge reduction of ammonium and phosphate to natural receiving water bodies. Zeolites have been identified as the most efficient ion exchangers for ammonium removal especially from wastewater solutions where the relative high presence of dissolved organic matter inabilities the application of organic polymers due to fouling phenomena [3]. However, zeolites shown a moderate ammonium capacity (from 0.3 to 2.1 mmol/g) when compared with synthetic cation exchange resins (e.g., 4 to 6 mmol/g for sulphonic resins) [4, 5] and their application to tertiary urban or industrial effluents (30 to 100 mg $N\text{-}NH_4^+$/L) provides low service volume and accordingly a higher regeneration cost [6]. Then, proposals have been addressed to: a) find low cost non-regenerable ammonium sorbent and then loaded ammonium sorbent could be used for agronomical application as could be improvement of soil quality in forest and degraded areas and b) improve properties to achieve the simultaneous ammonium and phosphate recovery to enhance their fertilizing properties. Taking zeolites as reference ammonium sorbent; a modification process of the zeolite to facilitate the sorption or the formation of P(V) mineral phases needs to be developed. In general oxyanions (e.g. As(V), P(V)) sorption could be achieved by hydrated metal oxides (HMOs). Polyvalent metal oxides, namely, Al(III), Fe(III), and Zr(IV) are known to sorb oxyanions through formation of inner-sphere complexes or Lewis acid-base (LAB) interactions [7, 8]. Anionic species, such as chloride, sulfate or nitrate, exhibit poor sorption towards these metal oxides and can only form outer-sphere complexes with the metal oxides [9]. Application of granular Fe-HMO has been mainly restricted to remove low levels of As(V)/As(III) as single use sorbents to be disposed when exhausted due to the sorbates toxicity [10, 11]. However, when applied to non-toxic species as P(V), the loading capacities of granular Fe-HMO have tried to be implemented by increasing surface reactivity using HMO nanoparticles or by supporting them onto templates, such as clays [12], polymers [13] or zeolites [14].

Manganese oxides, widely applied to remove heavy metals from water [15], have similar loading capacities for P(V) oxyanions but with weak complexation properties than Al and Fe oxides that could be suitable to develop a material providing neither efficient regeneration or high P(V) availability if applied as soil amendments.

The aim of this study is to evaluate the modification of a natural zeolite by impregnation with hydrated manganese oxide to produce a hybrid sorbent and then assess its sorption performance for the simultaneous ammonium and phosphate removal. The specific objectives of this work are:

(i) Characterize the natural and manganese modified hybrid sorbent.

(ii) study the effect of pH and competing ions (potassium, magnesium, calcium, sodium, bicarbonate, chloride, sulfate and nitrate) on the ammonium and phosphate sorption by natural and manganese modified hybrid sorbent.

(iii) study the effect of the initial concentration of ammonium and phosphate from a solutions without and with competing ions (potassium, magnesium, calcium sodium, bicarbonate, chloride, sulphate, nitrate) on the sorption by the natural zeolite and manganese modified hybrid sorbent considering isotherms models.

(iv) Evaluate the ammonium and phosphate sorption as a function of time by the natural zeolite and manganese modified hybrid sorbent considering kinetic models.

(v) Evaluate the release of the ammonium and phosphate from the natural zeolite and manganese modified hybrid sorbent after the sorption process in a batch and dynamic systems

(vi) Propose the mechanisms of interaction of ammonium and phosphate with the components of the natural zeolite and manganese modified hybrid sorbent.

5.2. Materials and methods

5.2.1. Preparation of Na- and Mn- modified natural zeolites

A natural zeolite (Z-N) from the Zeocem Company (Slovak Republic) was used in batch (particles < 200 μm) and fixed-bed (< 800 μm) configurations. Z-N was modified to the manganese form (Z-Mn) by using an adaptation of the method reported by Jiménez – Cedillo et al. [16]. Z-N sample (30 g) was first treated in 250 mL of NaCl (0.1 M) and once in the sodium form Z-Na sample (30 g) was treated in 250 mL of $MnCl_2$ (0.1 M) by two consecutive times under reflux for 4 h obtaining Z-Mn. After treatment, samples were washed until no chloride was detected by the $AgNO_3$ test and dried at 80 °C for 24 hours.

5.2.2. Characterization before and after ammonium and phosphate sorption

The chemical composition and morphology of the samples were determined by a Field Emission Scanning Electron Microscope (JEOL JSM-7001F) coupled to an Energy Dispersive Spectroscopy system (Oxford Instruments X-Max). The test was replicated at least four times for each sample and the average values are reported. A powder X-ray Diffractometer (D8 Advance A25 Bruker) was used for X-ray diffraction (XRD) characterization of zeolitic samples. The infrared absorption spectra were recorded with a Fourier Transform FTIR 4100 (Jasco) spectrometer in the range of 4000 – 550 cm^{-1}. The nitrogen gas adsorption method was used for the specific surface area determination of solid samples on an automatic sorption analyzer (Micrometrics). The tests were replicated at least four times for each sample and the average values are reported. Also, Z-N and Z-Mn samples (0.1 g) were equilibrated in 25 mL of solutions for different ionic strengths (deionized water; 0.01, 0.05 and 0.1 M NaCl) for 24 hours at 200 rpm and 21±1 °C. The point of zero charge (PZC) was determined by the pH drift method in the range of pH 2 to 11 [17]. Tests were performed in triplicate for each sample and the average values are reported.

5.2.3. Ammonium and phosphate batch sorption studies

Batch equilibrium sorption experiments were carried out using standard methodology described elsewhere [18]. Weighted amounts of dry samples (particle size < 200 µm) were shaken overnight with 25 mL of aqueous solutions containing different phosphate and ammonium concentration. The solutions were prepared by dissolving sodium phosphate ($NaH_2PO_4.2H_2O$) and ammonium chloride (NH_4Cl) in deionized water, respectively. The following types of experiments were performed.

5.2.4. Effect of pH on sorption

Z-Mn (0.1 g) sample was added to 25 mg P-PO_4^{3-}/L and 25 mg N-NH4+/L solutions (pH adjusted from 2 to 11).

5.2.5. Effect of competing ions

The Z-Mn sample (0.1 g) was added to solutions (without pH adjustment) containing 25 mg P-PO_4^{3-}/L, 25 mg N- NH_4^+/L and 25 mg/L of the corresponding typical coexisting ions present in wastewater effluents.

5.2.6. Isotherms of ammonium and phosphate from a solutions without competing ions and with competing ions

The Z-N and Z-Mn samples (0.25 g) were equilibrated in solutions at pH 4.6±0.2 (without pH adjustment) and at pH 7.5±0.3 (with pH adjustment according to the

expected treated wastewater conditions) using concentrations ranging 1 to 2000 mg $P\text{-}PO_4^{3-}$/L and 10 – 5000 mg $N\text{-}NH_4^{+}$/L.

The effect of the combination of ions was evaluated through equilibration of Z-Mn sample (0.25 g) in solution containing concentrations ranging from 1 to 2000 mg $P\text{-}PO_4^{3-}$/L and 10 – 5000 mg $N\text{-}NH_4^{+}$/L. The composition of the solution was: sodium (260 mg/L), calcium (160 mg/L), magnesium (50 mg/L), potassium (40 mg/L), chloride (625 mg/L), bicarbonate (325 mg/L), sulfate (200 mg/L) and nitrate (30 mg/L). The ions concentrations were fixed taking as reference the average annual composition of the stream from a tertiary treatment at the El Prat wastewater treatment plant (Barcelona – Spain).

5.2.7. Kinetic of the ammonium and phosphate sorption

The Z-Mn (0.1 g) sample was equilibrated in solution containing 15 mg $N\text{-}NH_4^{+}$/L and 5 mg $P\text{-}PO_4^{3-}$/L (pH 6.4 and pH 7.5) at 200 rpm and room temperature (21±1 °C). Tubes were withdrawn sequentially at given times. All tests were performed by triplicate and the average values are reported. Samples were centrifuged for 10 min and filtered (45 µm) before analysis. The concentrations of ammonium and phosphate ions were determined at the initial and remaining aqueous solution. Also the loaded zeolites samples were examined by field scanning electron microscope and mineral phases were identified by X-Ray Diffractometry.

5.2.8. Release of the ammonium and phosphate from manganese modified zeolite

5.2.8.1. In a batch system

Z-Mn sample (0.5 g < 200 µm) was equilibrated in 25 mL of solution containing 25 mg $P\text{-}PO_4^{3-}$/L and 25 mg $N\text{-}NH_4^{+}$/L. The loaded sample was washed and dried; for being equilibrated into 25 mL of elution solutions: NaOH (1 M), $NaHCO_3$ (0.1 M), Na_2CO_3 (0.1 M), $NaHCO_3/Na_2CO_3$ (0.1 M). Tests were performed by triplicate (average values are reported) in two sorption – desorption cycles at 200 rpm and at 21±1 °C.

5.2.8.2. In a dynamic system.

Z-Mn samples (<800 µm) were packed in a glass column (15mm x 100mm). The sorption in continuous conditions was evaluated in presence and absence of competing ions through countercurrent flow rate of 1.9 mL/min. After, Z-Mn was saturated in absence of competing ions it was regenerated using 1 M NaOH solution at flow rate of 0.5 mL/min. The expected values of effluents streams from secondary

treatment at the El Prat wastewater treatment plant (Barcelona – Spain) were considering for the feed composition: phosphate (12.5 mg/L), ammonium (25 mg/L), chloride (312.5 mg/L), bicarbonate (162.5 mg/L), sulfate (10 mg/L), nitrate (15 mg/L), sodium (130 mg/L), calcium (80 mg/L), magnesium (25 mg/L) and potassium (20 mg/L).

5.2.9. Sequential chemical fractionation of phosphorus

An adaptation of the sequential extraction protocol modified from Hieltjes and Lijklema [19] was used for the fractionation of immobilized phosphorus in loaded zeolite. Z-Mn sample (0.25 g) was equilibrated in 25 mL of 25 mg P-PO_4^{3-}/L solution. The first stage involves two consecutive extractions in 20 mL of 1 M NH_4Cl (pH 7) for the loosely bound phosphorus fraction (LB-P) determination. The iron and aluminum fraction (Fe+Al+Mn)-P was extracted two consecutive times in 20 mL of 0.1 M NaOH followed by extraction in 1 M NaCl. Finally, two consecutive extractions in 20 mL of 0.5 M HCl determined the phosphorus bound to calcium, magnesium and manganese compounds (Ca+Mg+Mn)-P. The residual phosphorus (R-P) was calculated by the mass balance between the phosphorus adsorbed and the extracted fractions. Tests were performed at 200 rpm by triplicate at 21±1 °C and average data are reported.

5.2.10. Ammonium and phosphate analysis

Standard Methods were used for phosphate (P) and ammonium (N) quantification [20]. The P concentration was analyzed by the vanadomolybdophosphoric acid colorimetric method (4500-P C) and N was determined by ammonia-selective electrode method (4500-NH3 D). Also, it was used a Thermo Scientific Ionic Chromatograph (Dionex ICS-1100 and ICS-1000) for ions determination.

5.3. Results and discussions

5.3.1. Characterization of modified zeolite before and after ammonium and phosphate sorption

The chemical composition for clinoptilolite included O, Na, Mg, Al, Si, K, Ca and Fe (Table 5.1). The FSEM – EDX data and the analysis of aqueous phase (data not reported) suggested the occurrence of ion exchange reactions when manganese form of zeolite were obtained by the releasing of Na^+, K^+, Mg^{2+} and Ca^{2+} ions. Then, the modification of the Z-Na to Z-Mn could be described as a partial cation exchange reaction described by Eq. 1-2:

$$2\ (\cong ZO^-Na^+/K^+) + Mn^{2+} \leftrightarrow (\cong ZO^-)_2Mn^{2+} + 2Na^+/K^+ \qquad (1)$$

$$2\ (\cong ZO^-)Ca^{2+}/Mg^{2+} + Mn^{2+} \leftrightarrow (\cong ZO^-)_2Mn^{2+} + Ca^{2+}/Mg^{2+} \quad (2)$$

Element	Z-N	Z-Na	Z-Mn	Loaded Z-Mn
O	57.8±2.6	60.3±1.4	59.8±2.6	58.9±3.2
Na	0.3±0.0	1.5±0.1	1.2±1.5	0.4±0.1
Mg	0.4±0.1	0.4±0.0	0.1±0.1	0.1±0.1
Al	5.3±0.2	5.3±0.0	6.3±1.9	5.3±0.3
Si	29.7±1.7	29.1±1.5	27.4±1.7	32.7±2
P	<lq*	<lq*	<lq*	0.3±0.1
Cl	<lq*	<lq*	<lq*	<lq*
K	2.9±0.5	1.8±0.2	1.4±0.5	0.9±0.5
Ca	1.9±0.3	1.1±0.1	1.3±0.9	0.3±0.1
Ti	0.2±0.2	<lq*	<lq*	<lq*
Mn	<lq*	<lq*	1.6±1.1	0.3±0.14
Fe	1.60±0.4	0.5±0.0	0.9±0.5	0.9±0.5

lq*: limit of quantification

Table 5.1. Chemical composition (FSEM – EDX, wt. %) of Natural zeolite (Z-N), zeolite in sodium form (Z-Na), zeolite in manganese form (Z-Mn) and loaded zeolite in manganese form (Loaded Z-Mn).

Clinoptilolite revealed the typically networks of crystal clusters plate-like morphology, as can be seen in FSEM-EDAX analysis. The Z-N sample was characterized by porosity while in Z-Na and Z-Mn samples some crystals covered the surface. Then, the measured reduction of the specific surface area of 19.8±0.8 m^2/g for Z-N to 17.6±0.9 m^2/g in Z-Mn is a consequence of the interaction of compensating cations and water molecues coordinated in the zeolite framework [21].

The Z-N, Z-Na and Z-Mn were mainly composed by clinoptilolite and traces of quarts and albite and no important changes were identified by the occupation of Mn^{2+} ions in the exchange sites of the zeolitic structure. The absence of crystalline phases was confirmed in Z-Mn as it was reported for a natural zeolite in the iron and manganese form [22, 23]. Moreover, the pH_{pzc} of Z-Mn sample was 6.1±0.6, which is in agreement with those values reported for a natural MnO_2 (pH_{pzc} 5.5) and for Mn(II) and Mn(IV) hydroxy/oxides and some natural MnO_2(s) (pH_{pzc} 4.0±0.8) [24, 25].

However it was slightly far from 7.0 and 8.7 described for β-MnO_2(s) and crystalline MnO_2, respectively [26, 27].

The FTIR spectra of Z-N, Z-Na and Z-Mn exhibited bands between 798 cm^{-1} and 547 cm^{-1}, at ~1100 cm^{-1} and at ~1630 cm^{-1} corresponding to the deformation vibration of OH, Al-O-Si and Si-O-Si groups, stretching vibration of Si–O groups and the deformation vibration of water, respectively. Some differences between Z-N and Z-Mn spectra were found in the bands from 3700 cm^{-1} to 3100 cm^{-1} which correspond to the hydroxyl groups of the zeolitic structure [28, 29], and the zeolitic water responsible for sorption behaviour [30]. New bands were found in Z-Mn at 1396 cm^{-1}, 1455 cm^{-1} and 1541 cm^{-1} and at 3747 cm^{-1} which correspond to the bridging hydroxyl groups (Si-OH-Mn) [31, 32]; then this fact suggested the existence of hydrated oxide manganese covering the clinoptilolite surface Z-Mn as it was determined by the SEM images.

5.3.2. Ammonium and phosphate sorption

5.3.3. Effect of pH on ammonium and phosphate sorption

The ammonium and phosphate ions sorption on adsorbent surfaces occurs through specific and/or nonspecific interactions. The nonspecific sorption through coulombic forces is associated with the pH_{pzc} of the sorbent while the specific sorption implies ligand exchange reactions [33].

The ammonium sorption by Z-Mn increases from pH 2 until 4 and then is maintained constant until pH 10 (Figure 5.1). The existence of positive charges on Z-Mn below pH_{Ppzc} promotes competition for the ammonium removal while above the pH_{pzc} the ammonium (NH_4^+) sorption is governed by the electrostatic interaction with the deprotonated surface groups ($\cong MO^-$). Thus, the decrease of ammonium sorption at pH 11 is associated with the decrease of the NH_4^+ concentration as it is converted to the NH_3. The analysis of aqueous phase (data not reported) and the SEM analysis confirmed the release of Na^+ and in less degree of K^+, Mg^{2+} and Ca^{2+} in the loaded Z-Mn. Additionally, energy dispersive X-ray spectroscopy used as semi quantitative technique revealed an important reduction of manganese content in the loaded ammonium and phosphate Z-Mn zeolite after the ammonium sorption (Table 5.1). So ammonium also could be exchanged by Mn2+ cations from the zeolite network. Then, the ion exchange reaction on a manganese zeolite is a chemical process involving valence forces through the sharing or exchange of electrons between zeolite sites with negative charge and ammonium cations as described by Eq. 3 [34]:

$(\cong ZO^-)_2Mn^{2+} + 2NH_4^+ \leftrightarrow\ 2(\cong ZO^-NH_4^+) + Mn^{2+}$ (3)

A low phosphate sorption capacity was reported between pH 2 and pH 6 (Figure 5.1), which is mainly governed by coulombic forces interaction where the surface of hydrated manganese oxide groups of Z-Mn were possitively-charged below pH_{pzc}= 5.4 as described by Eq. 4.

$\cong MnOH^+ + H_2PO_4^- \leftrightarrow (\cong MnOH^+H_2PO_4^-)$ (4)

where ≅MnOH represents the surface groups of the hydrated manganese oxide precipitated on the zeolite structure.

Contrary, the phosphate sorption capacity increased from pH 7 to pH 9 in Z-Mn charged negatively; then the sorption of the expected phosphate oxyanion forms, $H_2PO_4^-$ and HPO_4^{2-} were mainly achieved by ligand exchange complexation with the hydroxyl surface groups [35] through inner sphere complexation [36] as described by Eq. 5.

$\cong MnOH + H_2PO_4^-/HPO_4^{2-} \leftrightarrow\ \cong MnH_2PO_4^-/HPO_4^{2} + OH^-$ (5)

Sorption experiments were also characterized for the formation of precipitates on the surface of the Z-Mn between pH 7 to 9, and it was detected visually with a change of zeolite from pale grey to browner colour. The XRD patterns of the loaded Z-Mn samples revealed the existence of new crystalline phase ammonium manganese phosphate hydrate oxide ($NH_4MnPO_4 \cdot H_2O$). Then, precipitation is an additional mechanism proposed for phosphate sorption on Z-Mn due to the formation of some (P(V) – Mn^{2+} – NH_4^+ - Ca^+/ Mg^{2+}/ Na^+/ K^+ complexes [37] as described by Eq. 6 -7:

$(\cong ZO^-)_2Mn^{2+} + HPO_4^{2-} + 2Na^+ \leftrightarrow 2\ (\cong ZO^-Na^+) + MnHPO_4(s) + H^+$ (6)

$(\cong ZO^-)_2Mn^{2+} + HPO_4^{2-} + 2Na^+ + NH_4^+ \leftrightarrow\ 2\ (\cong ZO^-Na^+) + NH_4MnPO_4(s) + H^+$ (7)

It should be mention that the Na and Mn contents on Z-Mn are in the same order of magnitude (Table 5.1).

Above pH 10 the conversion of HPO_4^{2-} into PO_4^{3-} form promotes the reduction of phosphate sorption capacity by effect of repulsion with the negative charges of the surface. Furthermore, in these pH conditions the formation of the mixed metal ($Mn/NH_4/PO_4$) mineral is not favoured as it was described for the $MnHPO_4(s)$ and $Mn_3(PO_4)_2(s)$.

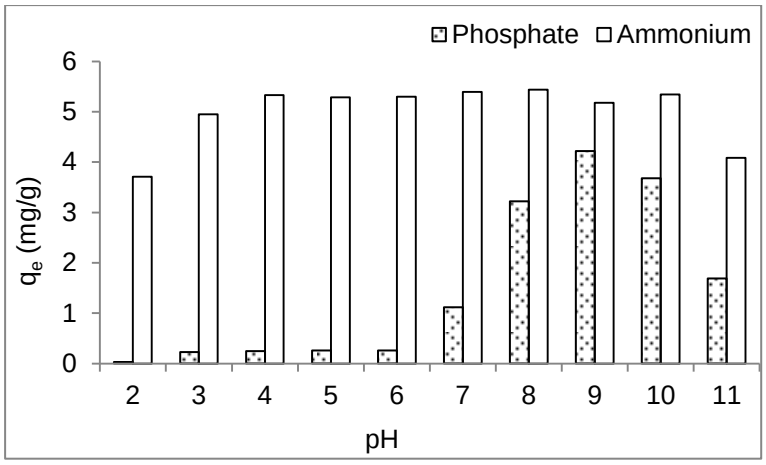

Figure 5.1. Effect of pH on the ammonium and phosphate sorption capacity by Z-Mn.

5.3.4. Effect of the competing ions

The ammonium and phosphate removal was evaluated in the presence of common cationic species in wastewater effluents (Figure 5.2). The ammonium uptake by Z-Mn was affected by the presence of Ca^{2+} (20 %) > K^{+} (14 %) > Na^{+} (10 %) > Mg^{2+} (7 %); as was reported for other natural zeolites [34]. Contrary, the phosphate sorption was slightly improved as it was reported for MnO_2 surfaces in combination of alkaline earth cations [37]; however, although detected by FSEM-EDAX, the XRD analysis did not reveal the precipitation of Ca^{2+}/ Mg^{2+}-phosphate species [38].

The ammonium and phosphate sorption was not affected by the individual competing anions. It is in accordance with the effects reported for ammonium removal in the presence of chloride and sulfate interferences [5, 34]; while the outer-sphere complexation of these species result in the permanent availability of phosphate bonding sites [9]. It is noteworthy to mention the significant increase of phosphate sorption in the presence of HCO_3^{-} and all anions by the effect of solution (~7), which enhance the phosphate sorption on manganese sorbents [37]. Otherwise, a reduction of 14 % of ammonium sorption capacity was found in the multi anions solution.

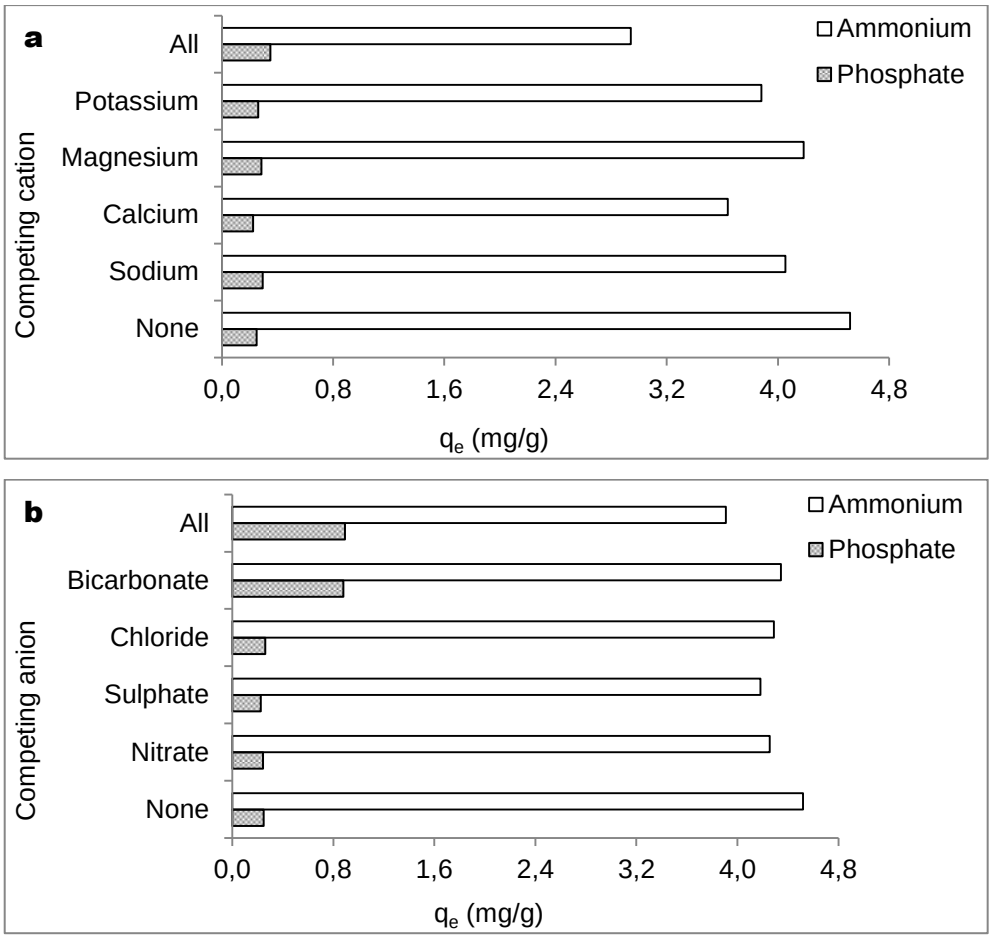

Figure 5.2. Individually effect of a) cations and b) anions on ammonium (N) and phosphate (P) uptake by manganese zeolite (Z-Mn).

5.3.5. Isotherms of ammonium and phosphate from a solutions without competing ions and with competing ions

The equilibrium uptake for ammonium and phosphate (q_e) was calculated by Eq. 8.

$$\boldsymbol{q_e = (C_o - C_e) \times \frac{v}{w}} \quad (8)$$

where C_o (mg/L) and C_e (mg/L) represents the initial and equilibrium concentration, respectively; v (L) is the aqueous solution volume and w (g) is the mass of zeolite. The ammonium and phosphate equilibrium sorption was evaluated according to Langmuir (Eq. 9) and Freundlich (Eq. 10) isotherms.

$$\boldsymbol{\frac{C_e}{q_e} = \frac{1}{K_L . q_m} + \frac{C_e}{q_m}} \quad (9)$$

$$\boldsymbol{\log q_e = \log K_F + \frac{1}{n} log\ C_e} \quad (10)$$

where q_m (mg/g) is the maximum sorption capacity and K_L (L/mg) is the Langmuir sorption equilibrium constant. K_F ((mg/g)/(mg/L)$^{1/n}$) is the Freundlich equilibrium sorption constant.

The equilibrium data of ammonium and phosphate sorption by Z-Mn was better described by the Langmuir isotherm (Figure 5.3). Thus, monolayer and homogenous sorption or/and ion exchange at specific and equal affinity sites available on the zeolites surface is supposed to occur.

			Langmuir			Freundlich		
pH_{eq}	Zeolite	Ion specie	q_m (mg/g)	K_L (L/mg)	R^2	K_F ((mg/g)/(mg/L)$^{1/n}$)	1/n	R^2
	Z-N	Phosphate	0.6±0.1	0.01	0.99	0.02	0.47	0.97
		Ammonium	33±2	0.006	0.99	1.84	0.36	0.94
4.6±0.2	Z-Mn	Phosphate	2.8±0.4	0.01	0.99	0.30	0.32	0.96
		Ammonium	31±3	0.009	0.99	2.63	0.34	0.85
7.5±0.3	Z-Mn	Phosphate	5.6±0.3	0.01	0.99	0.95	0.34	0.65
		Ammonium	23±2	0.010	0.99	2.50	0.29	0.93

Table 5.2. Isotherm parameters for ammonium and phosphate sorption on Z-N and Z-Mn.

The Z-N reported maximum sorption capacities of 33±2 mg N-NH_4^+/g and 0.6±0.1 mg P-PO_4^{3-}/g for ammonium and phosphate, respectively; as it was described in a previous study [39]. The ammonium sorption capacity decreased from 31±3 mg N-NH_4^+/g (at pH 4.6) to 23±2 mg N-NH_4^+/g (pH 7.5) (Table 5.2); while the phosphate removal capacity increased from 2.8±0.4 mg P-PO_4^{3-}/g (at pH 4.6) up to 5.6±0.3 mg P-PO_4^{3-}/g (pH 7.5). The increase of phosphate removal between pH 6 and 9 has been reported is due to the effect of the transition metal ions Mn^{2+} by combination between the hydrous manganese (IV) oxide (HMO) and alkaline earth cations [37]; as it was confirmed by the XRD patterns of the loaded Z-Mn samples (Ammonium Manganese Phosphate Hydrate Oxide, $NH_4MnPO_4 \cdot H_2O$). The existence of phosphorous and nitrogen was confirmed in loaded zeolite Z-Mn, and the surface was covered by a solid crystalline framework. However, it could not be discarded the presence of Mn-PO_4 minerals (e.g., $MnHPO_4$(s), $Mn_3(PO_4)_2$(s)). The FTIR spectra revealed important changes in bands at 3747 cm^{-1}, 1016 cm^{-1} and 1435 cm^{-1}; which correspond to the hydroxyl groups complexated with ammonium and phosphate [40, 41]. This fact could explain that the increase of the phosphate removal leads to the

slight reduction of the ammonium sorption capacity as it occurred in natural and in modified zeolite forms.

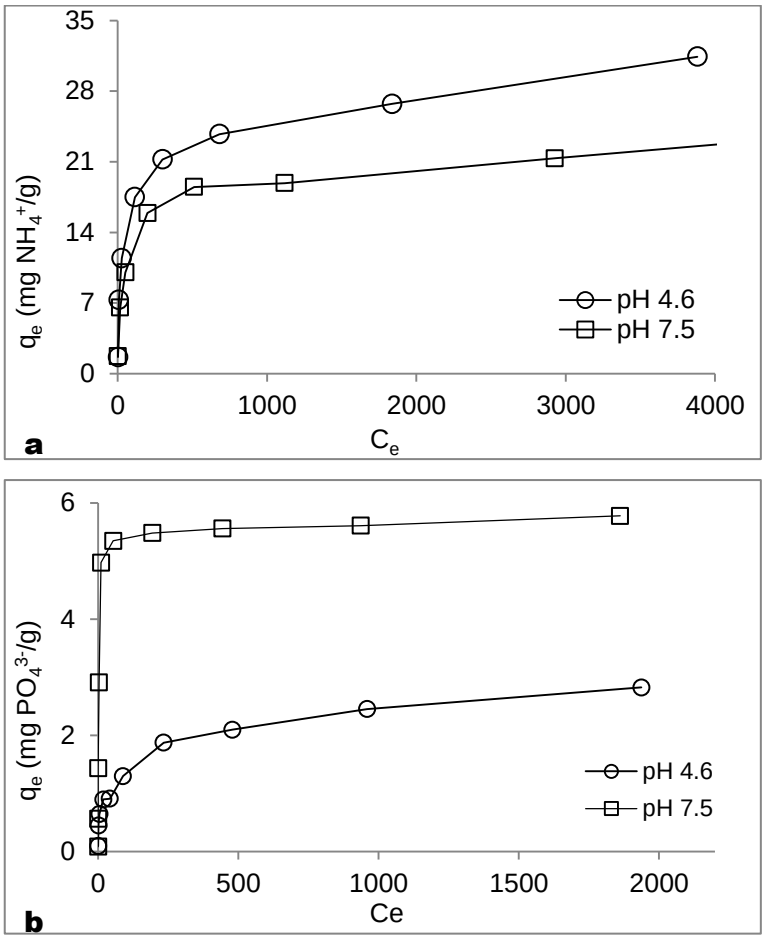

Figure 5.3. Experimental equilibrium isotherms for a) ammonium and b) phosphate removal by manganese zeolite (Z-Mn) at 21±1°C. Sorption experiments were carried at constant equilibrium pH 4.6±0.2 and 7.5±0.3.

The experimental data of ammonium and phosphate equilibrium sorption on Z-Mn in the presence of mixtures of anions and cations were also better described by the Langmuir isotherm. The phosphate uptake capacity was slightly reduced in the presence of ions (3.3±0.3 mg P-PO_4^{3-}/g at pH 5.1 ±0.2) and cations (2.7±0.2 mg P-PO_4^{3-}/g at pH 5.1 ±0.2) while in the presence of anions it was increased to 3.6±0.3 mg P-PO_4^{3-}/g (pH 6.5±0.2) as the pH increases (Table 5.3). Similar effect was reported for ammonium uptake in the presence of cations mixture (26±2 mg N-NH_4^+/g) > cations and anions mixture (27±2 mg N-NH_4^+/g) > anions mixture (27±3 mg N-NH_4^+/g).

pH_{eq}	Ion specie	Langmuir	Freundlich

		q_m (mg/g)	K_L (L/mg)	R^2	K_F ((mg/g)/(mg/L)$^{1/n}$)	1/n	R^2
4.6±0.2	Phosphate	2.8±0.4	0.01	0.99	0.30	0.32	0.96
6.5 ±0.2	P-Anions	3.6±0.3	0.01	0.99	0.82	0.31	0.48
5.1 ±0.2	P-Cations	2.7±0.2	0.01	0.99	0.44	0.24	0.99
5.1 ±0.2	P-Ions	3.3±0.3	0.01	0.99	0.49	0.38	0.82
4.6 ±0.2	Ammonium	31±3	0.009	0.99	2.63	0.34	0.85
6.5 ±0.2	N-Anions	27±3	0.013	0.99	2.03	0.36	0.86
5.1 ±0.2	N-Cations	26±2	0.008	0.99	1.20	0.42	0.79
5.1 ±0.2	N-Ions	27±2	0.005	0.99	0.82	0.47	0.89

Table 5.3. Isotherm parameters for ammonium and phosphate sorption on manganese zeolite Z-Mn in the presence of competing ions.

5.3.6. Kinetic of the ammonium and phosphate sorption

The sorption kinetics of both the ammonium and phosphate ions on Z-Mn, revealed that equilibrium was reached within 200 minutes (Figure 5.4). The phosphate sorption capacities were lower at pH 6.2 compared with that obtained at pH 8.0; while the opposite effect was revealed in ammonium ions.

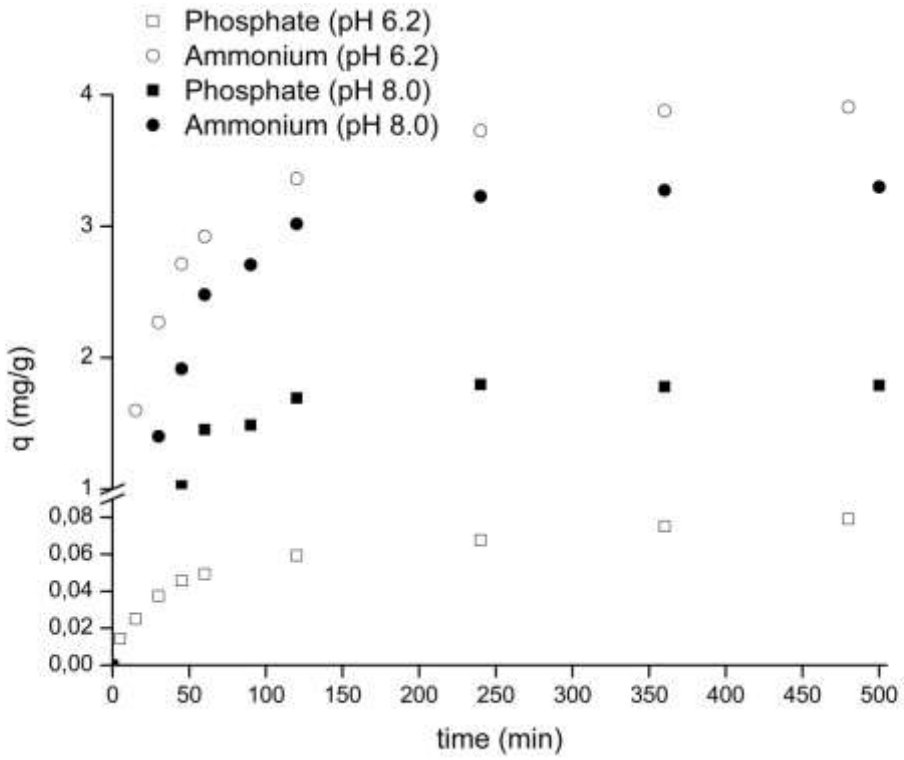

Figure 5.4. Evolution of ammonium and phosphate sorption uptake versus time for Z-Mn at 21 ±1 ºC.

The ammonium and phosphate equilibrium sorption kinetics were well described by the intraparticle diffusion model (Eq. 11) [42]; which considers diffusion in the spherical adsorbent and also that convective diffusion in the adsorbate solution governed the sorption mechanisms.

$$q_t = k_t\, t^{1/2} + A \qquad (11)$$

where k_t (mg.g^{-1}.h$^{-1/2}$) is the intraparticle diffusion rate constant and A (mg/g) is a constant providing information about the thickness of the boundary layer. Two linear regions were identified and characterized by the diffusion rate constants kt_1 and kt_2, which suggested the ammonium and phosphate sorption process, may be described by film diffusion followed by particle diffusion process [43].

The homogenous particle diffusion model (HPDM) was also evaluated for the ammonium and phosphate sorption onto zeolites [44, 45]. If particle diffusion controls (Dp) the sorption rate is described using Eq. 12:

$$-\ln\left(1-\left(\frac{q_t}{q_e}\right)^2\right) = \frac{2\,\pi^2 D_p}{r^2}\,t \qquad (12)$$

When the rate of sorption is controlled by liquid film diffusion, this rate can be expressed as shown in Eq. 13:

$$-\ln\left(1-\left(\frac{q_t}{q_e}\right)\right)=\frac{D_f C_s}{h\, r\, C_z}t \qquad (13)$$

where q_t and q_e are the solute loadings on the adsorbent phase at time t and equilibrium (mg/g), respectively, C_s (mg/L) and C_z (mg/kg) are the ion concentrations in solution and in the zeolite, respectively, r is the average radius of the zeolite particles ($1x10^{-4}$ m), t is the contact time (min) and h is the thickness of film around the zeolite particle ($1x10^{-5}$ m for a poorly stirred solution) [46]. D_p is the diffusion coefficient in the zeolite phase ($m^2.s^{-1}$) and D_f ($m^2.s^{-1}$) is the diffusion in the film phase surrounding the zeolite particles.

Kinetic experimental data for ammonium and phosphate sorption on Z-Mn were fitted to the equations 11, 12 and 13 and best-fit of D_p and D_f values as well as the linear regression analysis are summarized in Table 5.4. Higher R^2 values were found for particle diffusion, thus, monolayer molecular sorption occurred on the surface of zeolite, which is in concordance with data previously reported for ammonium sorption on natural zeolites at low initial ammonium concentrations [43].

Model	Kinetic parameters	Ammonium		Phosphate	
		pH 6.4±0.2	pH 8.0±0.2	pH 6.2±0.2	pH 8.0±0.2
Intraparticle diffusion	k_{t1} ($mg\cdot g^{-1}\cdot h^{-1/2}$)	3.1	2.2	0.05	1.22
	R^2	0.99	0.99	0.99	0.97
	k_{t2} ($mg\cdot g^{-1}\cdot h^{-1/2}$)	0.5	0.3	0.02	0.09
	R^2	0.91	0.93	0.99	0.68
HPDF Film diffusion	D_f ($m^2\cdot s^{-1}$)	$1.9x10^{-9}$	$1.8x10^{-9}$	$7.8x10^{-11}$	$4.5x10^{-9}$
	R^2	0.91	0.84	0.94	0.78
HPDM Particle diffusion	D_p ($m^2\cdot s^{-1}$)	$3.0x10^{-12}$	$8.8x10^{-12}$	$1.7x10^{-12}$	$9.5x10^{-12}$
	R^2	0.96	0.98	0.99	0.98

Table 5.4. Kinetic parameters for ammonium and phosphate removal on Z-Mn at 21 ±1 ºC.

5.3.7. Release of the ammonium and phosphate from manganese modified zeolite

5.3.7.1. In a batch system

Availability of ammonium and phosphate was studied in both strong moderate alkaline solutions bicarbonate and free bicarbonate solutions. Ammonium ion was efficiently desorbed in strong basic solutions (pH> 12 as 1M NaOH 0.1 M and 0.1 M Na_2CO_3) and partially removed by slightly basic solutions (e.g. pH> 8 as 0.1 M $NaHCO_3$, 0.1 M $NaHCO_3$/0.1 M Na_2CO_3 (pH= 10.3)) (Table 5.5).

Elution solution	Desorption (%)	
	Ammonium	Phosphate
1 M NaOH (pH>13)	89±4	90±3
0.1 M $NaHCO_3$ (pH=8.3)	41±4	34±3
0.1 M Na_2CO_3 (pH=11.8)	83±4	33±3
0.1 M $NaHCO_3$/0.1 M Na_2CO_3 (pH=10.3)	64±4	72±3

Table 5.5. Simultaneous ammonium and phosphate desorption efficiency from loaded Z-Mn at 21±ºC.

In concentrated Na^+ and OH^- containing solutions Eq 3 is reversed as NH_4^+ ions are additionally converted to NH_3 as described by Eq. 14.

$$ZO^-NH_4^+ + Na^+ + OH^- \cong \leftrightarrow \cong ZO^-Na^+ + NH_3 + H_2O \quad (14)$$

However only partial recoveries are measured in more diluted solutions or at pH values where the formation of NH_3 is not favoured.

Phosphate is only efficiently desorbed in 1M NaOH solutions and partially desorbed in the $NaHCO_3$/Na_2CO_3 mixtures. Partial desorption of phosphate could be explained when using $NaHCO_3$, Na_2CO_3 and $NaHCO_3$/ Na_2CO_3 solutions by Eqs. 15 and 16:

$$\cong MnOH^+H_2PO_4^- + 2OH^- \leftrightarrow \cong MnO^- + PO_4^{3-} + 2H_2O \quad (15)$$

$$\cong MnH_2PO_4^-/HPO_4^{2-} + OH^- \leftrightarrow \cong MnO^- + PO_4^{3-} \quad (16)$$

The desorption of more stable phosphate species (e.g., mineral phases found on the zeolite structure) and only favoured in strongly basic solutions are described by Eqs. 17 and 18.

$$MnHPO_4(s) + OH^- \leftrightarrow \cong MnO^- + PO_4^{3-} + H_2O \quad (17)$$

$$NH_4MnPO_4(s) + OH^- \leftrightarrow + PO_4^{3-} + Mn^{2+} + NH_3 + H_2O \quad (18)$$

In the subsequent sorption cycles the regenerated Z-Mn samples ($NaHCO_3$, Na_2CO_3 and $NaHCO_3$/ Na_2CO_3) shown a strong decrease in phosphate uptake in comparison with the ammonium removal capacity. No previous studies have been reported about a modified zeolite Z-Mn for ammonium and phosphate removal considering the regeneration step. However, the results obtained in this study suggest that zeolite should be impregnated after each regeneration cycle or could be used for the improvement of soil quality.

5.3.7.2. In a dynamic system

The ammonium maximum sorption capacity at column saturation (C/C_0=0.95) was 28 mg N-NH_4^+/g at 416 BV (pH 6.0) and 21 mg N-NH_4^+/g at 424 BV (pH 8.0), while in the presence of competing ions, the ammonium maximum sorption capacity decreased to 17 mg N-NH_4^+/g at 400 BV (pH 7.0) (Figure 5.5). In addition, the phosphate maximum sorption capacity increased from 0.4 mg P-PO_4^{3-}/g at 167 BV (pH 6.0) to 7.4 mg P- PO_4^{3-}/g at 167 BV (pH 8.0), while in the presence of coexisting ions it was 5.2 mg P-PO_4^{3-}/g at 400 BV (pH 7.0).

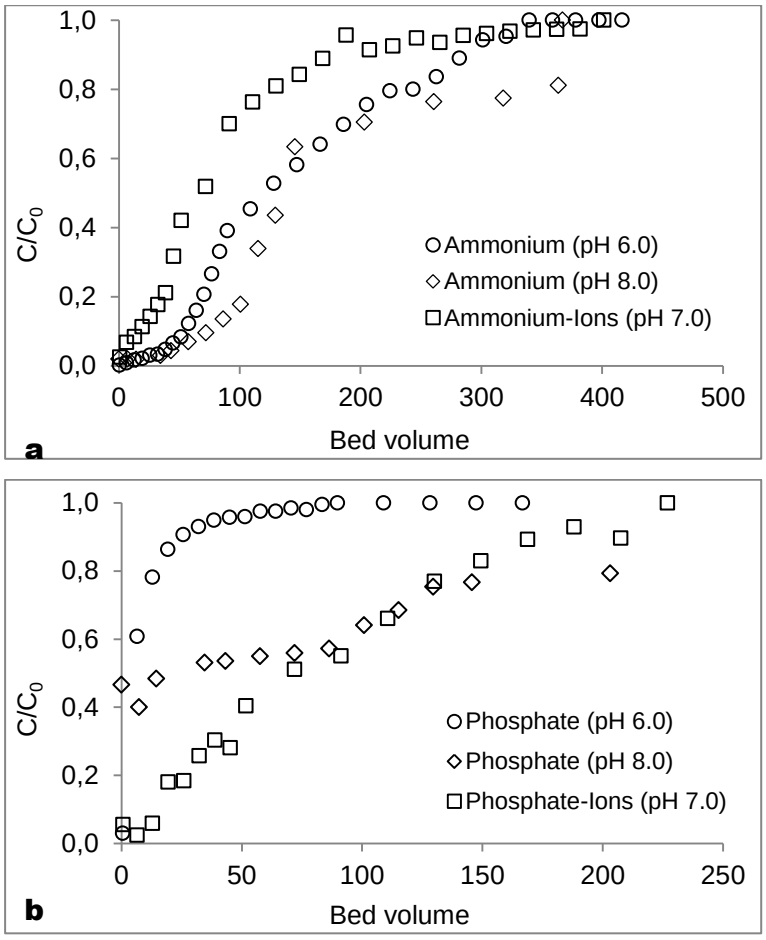

Figure 5.5. Breakthrough curves of a) ammonium and b) phosphate uptake by manganese zeolite (Z-Mn) at flow rate of 1.8 mL/min.

After desorption experiments it was recovered 90 % of ammonium and 60 % of the phosphate within 2.5 BV (Figure 5.6). The maximum concentrations were found 3475 mg N-NH_4^+/L and 2.6 mg P-PO_4^{3-}/L. Under these conditions, enrichment factors of 57 and 18 were achieved for ammonium and phosphate, respectively. It is important to point out that manganese and ammonium phosphates are listed as fertilizers and indeed, the zeolites can release nutrients at slow rate, which indicates that results obtained in this study are promising in view of the application of loaded zeolite in N and P from wastewater effluents.

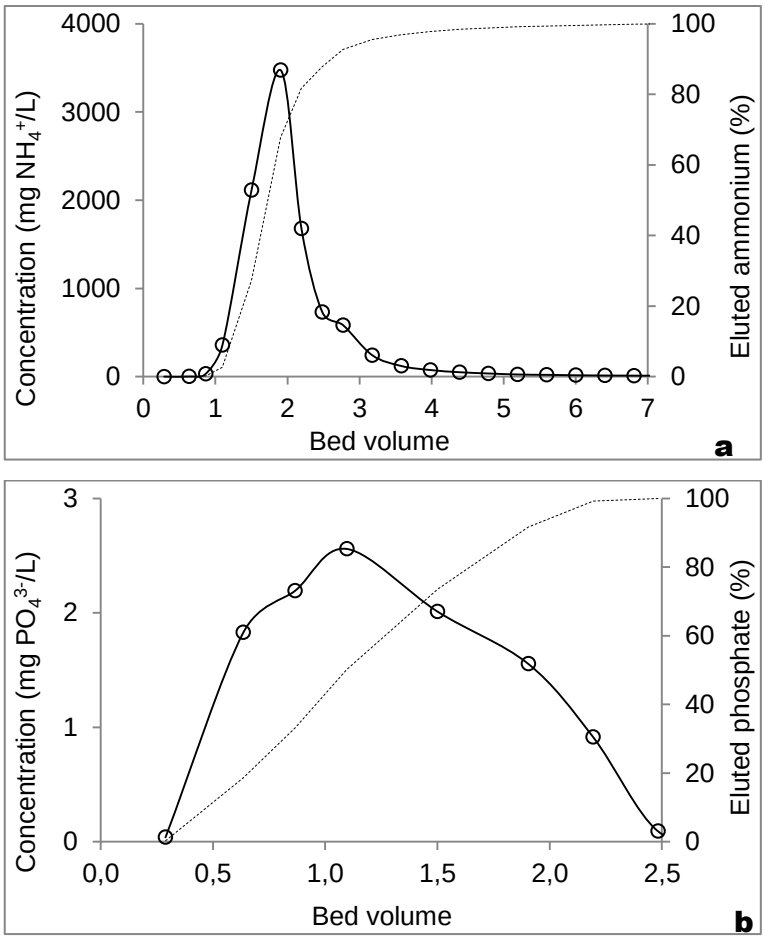

Figure 5.6. Desorption profiles of a) ammonium and b) phosphate from loaded manganese zeolite (Z-Mn) using 1 M NaOH at 0.4 mL/min.

5.3.8. Fractionation of immobilized phosphorus in loaded Z-Mn

The residual phosphorus (R-P) and loosely bound phosphorus fraction (LB-P) were found to be 2±1 % and 8±3 %, respectively. The 74±5 % of P was bounded to Al, Fe, Mn hydroxides (Fe+Al+Mn)-P, this fact suggests the participation of hydrated manganese oxide groups in the phosphate immobilization trough ligand exchange

complexation. Additionally, the 16±3 % of phosphorus was bounded to calcium, magnesium and manganese (Ca+Mg+Mn)-P fraction. Also the chemical precipitation with cationic species was identified by the XRD analysis.

5.4. Conclusions

A hybrid sorbent prepared by impregnation of a natural zeolite by hydrated manganese oxide was prepared in order to remove ammonium and phosphate simultaneously from aqueous solutions. It was observed that ammonium and phosphate sorption capacity were 23 mg/g and 5.6 mg/g, respectively at pH 7.5. The ammonium sorption occurred mainly by ion exchange and complexation due to the hydroxyl groups of the modified zeolite (Z-Mn). Moreover, the phosphate removal was accomplished by a combination of electric interactions, inner sphere complexation with ≅Mn-OH functional groups and chemical precipitation (predominantly in the pH range 7 to 9). The XRD analysis of the mineralogical phases precipitated revealed the formation of ammonium manganese phosphate hydrate oxide ($NH_4MnPO_4 \cdot H_2O$). Leaching tests using moderate alkaline bicarbonate solutions shown high availability for both ammonium and phosphate providing a potential use of loaded samples as controlled nutrient release for soil amendments. When evaluated for reuse, the desorption in dynamic conditions and using 1 M NaOH as elution solution provided enrichment factors of 57 and 18 for ammonium and phosphate, respectively.

5.5. References

1. Millar, G.J., et al., *Equilibrium studies of ammonium exchange with Australian natural zeolites.* Journal of Water Process Engineering, 2016. **9**: p. 47-57.
2. Yuan, X., et al., *Acid–base properties and surface complexation modeling of phosphate anion adsorption by wasted low grade iron ore with high phosphorus.* Journal of Colloid and Interface Science, 2014. **428**(0): p. 208-213.
3. Zhao, D. and A.K. Sengupta, *Ultimate removal of phosphate from wastewater using a new class of polymeric ion exchangers.* Water Research, 1998. **32**(5): p. 1613-1625.
4. Gefenienė, A., D. Kaušpėdienė, and J. Snukiškis, *Performance of sulphonic cation exchangers in the recovery of ammonium from basic and slight acidic solutions.* Journal of Hazardous Materials, 2006. **135**(1–3): p. 180-187.

5. Zhang, M., et al., *Removal of ammonium from aqueous solutions using zeolite synthesized from fly ash by a fusion method.* Desalination, 2011. **271**(1–3): p. 111-121.
6. Alshameri, A., et al., *An investigation into the adsorption removal of ammonium by salt activated Chinese (Hulaodu) natural zeolite: Kinetics, isotherms, and thermodynamics.* Journal of the Taiwan Institute of Chemical Engineers, 2014. **45**(2): p. 554-564.
7. Yamani, J.S., et al., *Enhanced arsenic removal using mixed metal oxide impregnated chitosan beads.* Water Research, 2012. **46**(14): p. 4427-4434.
8. Zhu, J., et al., *Fe3O4 and MnO2 assembled on honeycomb briquette cinders (HBC) for arsenic removal from aqueous solutions.* Journal of Hazardous Materials, 2015. **286**(0): p. 220-228.
9. Onyango, M.S., et al., *Adsorptive Removal of Phosphate Ions from Aqueous Solution Using Synthetic Zeolite.* Industrial & Engineering Chemistry Research, 2007. **46**(3): p. 894-900.
10. Pan, B., et al., *Development of polymer-based nanosized hydrated ferric oxides (HFOs) for enhanced phosphate removal from waste effluents.* Water Research, 2009. **43**(17): p. 4421-4429.
11. German, M., H. Seingheng, and A.K. SenGupta, *Mitigating arsenic crisis in the developing world: Role of robust, reusable and selective hybrid anion exchanger (HAIX).* Science of The Total Environment, 2014. **488–489**(0): p. 547-553.
12. Haque, N., et al., *Iron-modified light expanded clay aggregates for the removal of arsenic(V) from groundwater.* Microchemical Journal, 2008. **88**(1): p. 7-13.
13. Cumbal, L., et al., *Polymer supported inorganic nanoparticles: characterization and environmental applications.* Reactive and Functional Polymers, 2003. **54**(1–3): p. 167-180.
14. Jeon, C.-S., et al., *Adsorption characteristics of As(V) on iron-coated zeolite.* Journal of Hazardous Materials, 2009. **163**(2–3): p. 804-808.
15. Mustafa, S., M.I. Zaman, and S. Khan, *pH effect on phosphate sorption by crystalline MnO2.* Journal of Colloid and Interface Science, 2006. **301**(2): p. 370-375.
16. Jiménez-Cedillo, M.J., M.T. Olguín, and C. Fall, *Adsorption kinetic of arsenates as water pollutant on iron, manganese and iron–manganese-*

modified clinoptilolite-rich tuffs. Journal of Hazardous Materials, 2009. **163**(2–3): p. 939-945.

17. Villanueva, M.E., et al., *Point of zero charge as a factor to control biofilm formation of Pseudomonas aeruginosa in sol-gel derivatized aluminum alloy plates.* Surface and Coatings Technology, 2014. **254**: p. 145-150.
18. Kim, K.S., J.O. Park, and S.C. Nam, *Synthesis of Iron-loaded Zeolites for Removal of Ammonium and Phosphate from Aqueous Solutions.* Environ Eng Res, 2013. **18**(4): p. 267-276.
19. Hieltjes, A.H.M. and L. Lijklema, *Fractionation of Inorganic Phosphates in Calcareous Sediments1.* J. Environ. Qual., 1980. **9**(3): p. 405-407.
20. APHA, A., WEF., *Standard methods for the examination of water and wastewater*, 2000, American Public Health Association, American Water Works Association, and Water Environment Federation.
21. Valdés, H., S. Alejandro, and C.A. Zaror, *Natural zeolite reactivity towards ozone: The role of compensating cations.* Journal of Hazardous Materials, 2012. **227–228**(0): p. 34-40.
22. Doula, M.K., *Synthesis of a clinoptilolite–Fe system with high Cu sorption capacity.* Chemosphere, 2007. **67**(4): p. 731-740.
23. Jiménez-Cedillo, M.J., et al., *Adsorption capacity of iron- or iron–manganese-modified zeolite-rich tuffs for As(III) and As(V) water pollutants.* Applied Clay Science, 2011. **54**(3–4): p. 206-216.
24. Ouvrard, S., M.-O. Simonnot, and M. Sardin, *Reactive Behaviour of Natural Manganese Oxides toward the Adsorption of Phosphate and Arsenate.* Industrial & Engineering Chemistry Research, 2002. **41**(11): p. 2785-2791.
25. Kosmulski, M., *Compilation of PZC and IEP of sparingly soluble metal oxides and hydroxides from literature.* Advances in Colloid and Interface Science, 2009. **152**(1–2): p. 14-25.
26. Mustafa, S., M.I. Zaman, and S. Khan, *Temperature effect on the mechanism of phosphate anions sorption by β-MnO2.* Chemical Engineering Journal, 2008. **141**(1–3): p. 51-57.
27. Zaman, M.I., et al., *Effect of phosphate complexation on Cd2+ sorption by manganese dioxide (β-MnO2).* Journal of Colloid and Interface Science, 2009. **330**(1): p. 9-19.

28. Król, M., et al., *Application of IR spectra in the studies of zeolites from D4R and D6R structural groups.* Microporous and Mesoporous Materials, 2012. **156**: p. 181-188.
29. Reháková, M., et al., *Removal of pyridine from liquid and gas phase by copper forms of natural and synthetic zeolites.* Journal of Hazardous Materials, 2011. **186**(1): p. 699-706.
30. Alshameri, A., et al., *The investigation into the ammonium removal performance of Yemeni natural zeolite: Modification, ion exchange mechanism, and thermodynamics.* Powder Technology, 2014. **258**(0): p. 20-31.
31. Luan, Z. and J.A. Fournier, *In situ FTIR spectroscopic investigation of active sites and adsorbate interactions in mesoporous aluminosilicate SBA-15 molecular sieves.* Microporous and Mesoporous Materials, 2005. **79**(1–3): p. 235-240.
32. Cheng, X.-w., et al., *Studies on modification and structural ultra-stabilization of natural STI zeolite.* Microporous and Mesoporous Materials, 2005. **83**(1–3): p. 233-243.
33. Sujana, M.G., et al., *Studies on fluoride adsorption capacities of amorphous Fe/Al mixed hydroxides from aqueous solutions.* Journal of Fluorine Chemistry, 2009. **130**(8): p. 749-754.
34. Huang, H., et al., *Ammonium removal from aqueous solutions by using natural Chinese (Chende) zeolite as adsorbent.* Journal of Hazardous Materials, 2010. **175**(1–3): p. 247-252.
35. Simsek, E.B., E. Özdemir, and U. Beker, *Zeolite supported mono- and bimetallic oxides: Promising adsorbents for removal of As(V) in aqueous solutions.* Chemical Engineering Journal, 2013. **220**: p. 402-411.
36. Su, Y., et al., *Strong adsorption of phosphate by amorphous zirconium oxide nanoparticles.* Water Research, 2013. **47**(14): p. 5018-5026.
37. Kawashima, M., et al., *Phosphate adsorption onto hydrous manganese(IV) oxide in the presence of divalent cations.* Water Research, 1986. **20**(4): p. 471-475.
38. Yao, W. and F.J. Millero, *Adsorption of Phosphate on Manganese Dioxide in Seawater.* Environmental Science & Technology, 1996. **30**(2): p. 536-541.

39. Guaya, D., et al., *Simultaneous phosphate and ammonium removal from aqueous solution by a hydrated aluminum oxide modified natural zeolite.* Chemical Engineering Journal, 2015. **271**: p. 204-213.
40. Wahab, M.A., et al., *Characterization of ammonium retention processes onto Cactus leaves fibers using FTIR, EDX and SEM analysis.* Journal of Hazardous Materials, 2012. **241–242**(0): p. 101-109.
41. Huang, H., et al., *Simultaneous removal of nutrients from simulated swine wastewater by adsorption of modified zeolite combined with struvite crystallization.* Chemical Engineering Journal, 2014. **256**: p. 431-438.
42. Weber, W.J. and J.C. Morris, *Kinetics of adsorption on carbon solution.* Journal of the Sanitary Engineering Division, 1963. **89**(2): p. 31-59.
43. Lin, L., et al., *Adsorption mechanisms of high-levels of ammonium onto natural and NaCl-modified zeolites.* Separation and Purification Technology, 2013. **103**: p. 15-20.
44. Helfferich, F.G., *Ion exchange*1962, New York: McGraw-Hill.
45. Valderrama, C., et al., *Kinetic evaluation of phenol/aniline mixtures adsorption from aqueous solutions onto activated carbon and hypercrosslinked polymeric resin (MN200).* Reactive and Functional Polymers, 2010. **70**(3): p. 142-150.
46. Moussavi, G., et al., *The investigation of mechanism, kinetic and isotherm of ammonia and humic acid co-adsorption onto natural zeolite.* Chemical Engineering Journal, 2011. **171**(3): p. 1159-1169.

Chapter 6 Recovery of ammonium and phosphate from treated urban waste water by using potassium clinoptilolite impregnated hydrated metal oxides as N-P-K fertilizer

Abstract

A natural clinoptilolite in its potassium form (KNC) was modified by impregnation of hydrated metal oxides (HMO) of aluminium (III) (KAlC), iron (III) (KFeC) and manganese (IV) (KMnC) for the simultaneous ammonium and phosphate recovery from urban wastewaters. The resulting pH_{pzc} of the HMOs on the modified zeolites (7.3±0.3 for KAlC, 6.4±0.4 for KFeC and 6.9±0.3 for KMnC) are suitable for phosphate sorption at pH of treated urban wastewaters (6-8).The sorption capacity for phosphate for KAlC and KFeC zeolites is higher at the lower pH range while for KMnC is higher at the upper pH range. Differences were associated to the intrinsic complexing properties of the MOH groups to form outer and inner sphere MOH-phosphate complexes. The maximum phosphate sorption capacity for the three zeolites were 6.8 mg-P/g for KAlC, 7.2 mg-P/g for KFeC and 8.2 mg-P/g for KMnC. Contrary maximum ammonium sorption capacity is kept constant between pH 4 to 9 for the tree zeolites as the main sorption mechanism is the ion-exchange reaction with K^+ ions of the zeolite. The maximum ammonium sorption capacity for the three zeolites ranged from 29 to 33 mg-N/g. These differences on the nature of the sorption processes are also reflected in a much faster sorption kinetic for ammonium than for phosphate although for both species the rate determining step was ions diffusion on the zeolite particles. Modified zeolites shown high selectivity towards ammonium and phosphate in the presence of the dissolved organic matter as well as other ionic species present in the treated wastewaters. Finally, phosphorous (P) fractionation assays of the loaded zeolites confirmed a high phosphate bioavailability if these are applied as phosphate slow release fertilizers in soil applications.

Keywords: potassium clinoptilolite; nutrients recovery; hydrated metal oxides; sorption; NPK fertilizer

6.1. Introduction

Ammonia nitrogen (NH_4^+-N) and orthophosphate phosphorous (PO_4^{3-} -P) are the major polluting species of aqueous environmental compartments [1]. These nutrients are discharged into surface water bodies from treated municipal wastewaters, or from run-off of bio-fertilizers applied in agriculture by effect of the rain drainage leading to eutrophication [2]. Currently, phosphate is becoming a major economical concern because its natural deposits are diminishing due to the continuous growth of the world population. Then, urban, industrial and farming wastewaters and sludge streams with phosphorous (P) contents below 1% (w/w) are considered P secondary resources that need to be mined [3]. There are already a variety of technologies for P recovery from wastewaters. These technologies differ by the origin of the used resources (wastewater, sludge, sludge liquor, sludge ash), the applied process (precipitation, wet chemical extraction, and thermal treatment) and the P-recovery ratio. P could be recovered simultaneously with ammonium from concentrated streams of urban wastewater (e.g. anaerobic digestion side streams) by chemical precipitation of struvite [4]. Few efforts have been directed for the recovery from diluted streams where few techniques for phosphate removal are available [5]. Chemical precipitation and coagulation processes are not cost effective and polymeric ion exchangers are not applicable due to potentially high contents of dissolved and particulate organic matter. Thus, phosphate removal/recovery solutions have been focused to the use of low-cost adsorbents with high removal efficiency in terms of equilibrium (sorption capacity) and kinetics. Moreover, simultaneous removal of ammonium and phosphate from diluted streams (e.g., treated waste waters from the conventional activated sludge reactors) can be achieved using inorganic adsorbents like natural zeolites [6]. The ammonium removal is favoured by the high cation exchange capacity of natural zeolites [7, 8], however they exhibited poor performance for anions removal (e.g., phosphate) [9]. So, a modification stage of the zeolitic material [10] by incorporating neither cations forming low solubility phosphate minerals (e.g., Ba (II), Ca (II), Mg (II)) [11]; or by incorporating hydrated metal oxides (e.g., Fe, Al, Mn) with complexing properties (inner and outer sphere complexes with phosphate ions) is needed. The resulting exhausted sorbents could be used in agriculture and in agronomical applications to improve soil properties in both physical and chemical terms as potential fertilizer as they will provide P and N. The methodology to modify a granular natural zeolite in

sodium form into the Al (III), Fe (II)) and Mn (II) forms to be used in sorption and desorption cycles was described in previous studies [12, 13]. Therefore, the aim of this work is to evaluate the simultaneous removal of ammonium and phosphate from treated urban wastewater using impregnated aluminium, iron and manganese forms of a powder natural zeolite in its potassium form. The specific objectives proposed are: i) to evaluate the use of powder natural potassium zeolites impregnated with hydrated metal oxides to recover phosphate and ammonium from treated wastewaters and ii) to evaluate the P availability of the loaded N,P,K zeolites for soil quality improvement by using Phosphorous fractionation tests of the loaded zeolites.

6.2. Materials and methods

6.2.1. Preparation of metal hydrated oxide impregnated zeolites

A natural zeolite (NC) (Zeocem Company from the Slovak Republic) was ground until particles were below 74 μm. Then, three different samples of 50 g of NC were treated separately in a 250 mL glass reactor with 0.1 M $AlCl_3$, 0.1 M $FeCl_3$ and 0.1 M $MnCl_2$. After 20 minutes of agitation, the pH of the solutions was adjusted to pH 7±0.5 using 0.1 M KOH (KNC). Then, samples were treated two consecutive times by refluxing in 250 mL of KCl (0.1 M) for 3 h to obtain the aluminium/potassium (KAlC), iron/potassium (KFeC) and manganese/potassium (KMnC) forms of NC zeolite. After treatment, samples were washed until no chloride was detected using an $AgNO_3$ test followed by drying at 80 °C for 24 hours.

6.2.2. Characterization of potassium-metal hydrated oxide impregnated zeolites

A powder X-ray Diffractometer (D8 Advance A25 Bruker) was used for X-ray diffraction (XRD) characterization of KAlC, KFeC, KMnC samples. The phase purity and crystallinity of the powder samples was analysed by X-ray diffraction with λ CuKα radiation (λ= 1.54056 Å)) at a scanning rate time of 19.2 and 57.6 s, steep angle of 0.015° and 2θ in range of 4-60°.

The chemical composition and morphology of the samples were determined by a Field Emission Scanning Electron Microscope (JEOL JSM-7001F) coupled to an Energy Dispersive Spectroscopy system (Oxford Instruments X-Max). The infrared absorption spectra were recorded with a Fourier Transform FTIR 4100 (Jasco) spectrometer in the range of 4000 – 550 cm^{-1}. The nitrogen gas adsorption method was used for the specific surface area determination of KAlC, KFeC, KMnC samples

by using an automatic sorption analyser (Micrometrics). The tests were replicated at least four times for each sample and the average values are reported.

6.2.3. Point of cero charge of potassium-metal hydrated oxide impregnated zeolites

Samples of impregnated zeolites (KAlC, KFeC, KMnC) were equilibrated with aqueous solutions at different ionic strengths (25 mL of deionized water; 0.01, 0.05 and 0.1 M NaCl) at 200 rpm and 21±1 °C. The pH drift method was used for point of zero charge (PZC) determination in the range of pH 2 to 11 [14]. Tests were performed in triplicate for each sample and the average values are reported.

6.2.4. Ammonium and phosphate sorption equilibrium studies

Ammonium and phosphate solutions were prepared by dissolving appropriated amounts of ammonium chloride (NH_4Cl) and sodium phosphate ($NaH_2PO_4.2H_2O$) in deionized water. KAlC, KFeC, KMnC samples (0.1 g) were equilibrated in 25 mL of aqueous solutions containing 25 mg $N\text{-}NH_4^+$/L and 25 mg $P\text{-}PO_4^{3-}$/L (pH adjusted from 2 to 11). The tests were replicated three times for each sample and the average values are reported. Experiments using the effluent from secondary treatment at the El Prat wastewater treatment plant (WWTP) (Barcelona – Spain), at its average pH of 7.5±0.5, were also carried out in triplicate. The chemical composition of the used treated wastewater is shown in Table 6.1.

6.2.5. Ammonium and phosphate sorption kinetic studies

Weighted amounts of impregnated zeolite samples (6 g of KAlC, KFeC, KMnC) were equilibrated in 500 mL of the effluent stream from the secondary treatment at the El Prat WWTP (composition shown in Table 6.1). Experiments were performed at 500 rpm and at room temperature (21±1 °C). Samples (10 mL) were withdrawn at given times for determining the total ammonium and phosphate ions concentrations at the initial and remaining aqueous solution. Tests were performed in triplicate for each sample and the average values are reported. Samples were filtered (0.2 μm) before analysis.

ICP - MS elements											
	Na	Ca	S	K	Mg	Sr	Al	Si	Fe	Ba	
mg/L	246	127	82	36	35	1	0.2	0.03	0.03	0.02	
	Li	B	Ti	V	Cr	Mn	Co	Ni	Cu	Zn	As
μg/L	19	258	6	12	1	3.	2	29	45	61	3
	Se	Rb	Sr	Mo	Sn	Sb	Ba	W	Pb	U	

µg/L	3	16	1091	15	0.3	4	19	3	0.2	2

Organic and inorganic carbon content					
	NPOC	NT	TOC	TC	IC
mg/L	12	296	11	50	42

Major ionic species				
	NH_4^+	PO_4^{3-}	NO_3^-	Cl^-
mg/L	30	14	51	542

Table 6.1. Chemical composition of the effluent stream from the secondary treatment at the El Prat WWTP (Barcelona, Spain) used for kinetic studies.

Standard methods for phosphate and ammonium quantification [15] were used. The P concentration was determined by the vanadomolybdophosphoric acid colorimetric method (4500-P C) and N concentration was determined by ammonia-selective electrode method (4500-NH3 D). A Thermo Scientific Ionic Chromatograph (Dionex ICS-1100 and ICS-1000) for ions quantification was also used. The non-purgeable organic carbon (NPOC), total carbon (TC), total organic carbon (TOC), inorganic carbon (IC) and total nitrogen (NT) were determined by a total organic carbon analyser (Shimadzu, TOC-V_{CPH}). Finally, the concentration of trace elements in the treated wastewater effluent was performed by Inductively Coupled Plasma Mass Spectrometry (ICP-MS) at CSIC, Barcelona - Spain.

6.2.6. Sequential chemical fractionation of phosphorous on loaded zeolites samples

The modified zeolites were loaded in a solution containing 500 mg/L of ammonium and phosphate ions, and then they were filtered and dried for the sequential chemical fractionation of phosphorus by an adaptation of the Hedley method [16]. The sequential P extraction was performed to classify and quantify P fractions of the loaded potassium modified zeolites. Samples (0.5 g of KAlC, KFeC, KMnC) were added to 20 mL of each extracting solution 0.5 M $NaHCO_3$ (pH 8.5), 0.1 M NaOH and 1.0 M HCl. The tubes were shaken for 16 h and then the suspensions were centrifuged at 8000 rpm for 10 min and filtered (0.45 µm). The supernatant was collected and stored for analysis and the remaining soil was re-suspended for subsequent extractions. An aliquot of the $NaHCO_3$ and NaOH extracts was acidified to precipitate extracted organic matter and the supernatant was analysed for total inorganic phosphorus content (P_i). Another aliquot of the extracts was digested with

acidified ammonium persulfate in an autoclave at 120 kPa and 121 °C (60 min and 90 min for the $NaHCO_3$ and the NaOH extract, respectively) to convert organic into inorganic form; total phosphorus content (P_t) in the digest was analysed spectrophotometrically. The organic phosphorus content (P_o) in $NaHCO_3$ and NaOH extracts was calculated as the difference between P_t and P_i contents of the respective extracts. Residual P content in soil samples was determined after digestion with H_2SO_4/H_2O_2. The P concentration in all extracts and digestion solutions was determined spectrophotometrically at 882 nm [17]. Among the P fractions, $NaHCO_3$-P is considered to be labile whereas NaOH-P, HCl-P and residual P are referred to as non-labile [18, 19].

6.2.7. Kinetic data treatment of ammonium and phosphorous removal

Zeolites are characterized by a highly regular porous structure with cavities and interconnected channels that can be penetrated by specific ions while others are excluded. Hence, two different types of pores exist: micropores in the crystals and macropores in the binding network. The Homogeneous Diffusion Model (HDM) and the Shell Progressive Model (SPM) [20] were selected to describe phosphate and ammonium removal by HMO impregnated potassium zeolites. In the HDM model the zeolite is considered as a quasi-homogeneous media and the sorption diffusion rate controlling step on the spherical particles leads to:

i) if particle diffusion (D_p (m^2 s^{-1})) controls the sorption rate as described by Eq. 1:

$$-\ln(1-X(t)^2) = \frac{2\,\pi^2 D_p}{r^2}t \qquad (1)$$

ii) if liquid film diffusion (D_f (m^2 s^{-1})) controls the sorption rate is described by Eq. 2:

$$-\ln\big(1-X(t)\big) = \frac{D_f C}{h\,r\,C_z}t \qquad (2)$$

Where X(t) is the fractional attainment of sorption equilibrium (q_t/q_e) on the zeolite phase at time t, C_s and C_z (mg kg^{-1}) are the concentrations of solute in solution and in the zeolite, respectively; r is the average radius of zeolite particles ($4x10^{-4}$ m), t is the contact time (min or s); and h is the thickness of film around the zeolite particle ($1x10^{-5}$ m for poorly stirred solution) [21] In the SPM, as the porosity of the zeolite is considered small and thus practically impervious to the fluid reactant and the sorption process is described by a concentration profile of the solution containing phosphate

and ammonium ions advancing into a spherical zeolite particle partially saturated [20]. The sorption rate controlling steps on the zeolite particles leads to:

(a) if it is controlled by the fluid film (K_F (m s^{-1})) described by Eq. 3:

$$X(t) = \frac{3C_{so}K_F}{a_s r C_{zo}}\ t \qquad (3)$$

(b) if it is controlled by the diffusion though the particle sorption layer (D_p (m^2 s^{-1})), described by Eq. 4:

$$\left[3 - 3(1 - X(t))^{2/3} - 2X(t)\right] = \frac{6D_p C_{so}}{a_s r^2 C_{zo}}\ t \qquad (4)$$

(c) if it is controlled by the chemical reaction (k_s (m.mol.L^{-1} s^{-1})), described by Eq. 5:

$$\left[1 - (1 - X(t))^{1/3}\right] = \frac{k_s C_{so}}{r}\ t \qquad (5)$$

Where C_{so} and C_{zo} are the concentration of solute in bulk solution and at the zeolite unreacted core, respectively (mg L^{-1}) and a_s is the stoichiometric coefficient.

All experimental data were treated graphically and compared to all fractional attainment of equilibrium functions (F(X) = f (t)) defined previously for both models HDM and SPM.

6.3. Results and discussion

6.3.1. Zeolites characterization

The natural zeolite was mainly identified as clinoptilolite and traces of cristobalite and mordenite were also identified by XDR analysis (Figure 6.1).

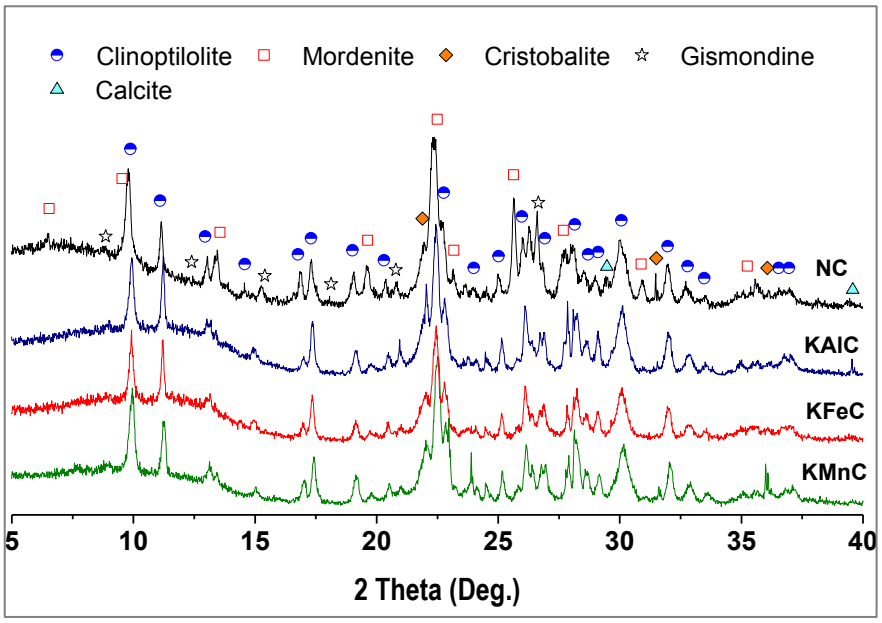

Figure 6.1. X-ray diffractograms of NC, KAlC, KFeC and KMnC.

The natural zeolite does not exhibited a highly pure and crystalline nature. It was not observed any significant attenuation of the peak intensity of the modified forms of NC zeolite revealing the absence of changes on the structure of the raw NC after the modification with aluminium, iron and manganese hydrated oxides. The absence of new mineralogical phases and also of significant shift in peaks position of the modified samples suggested that K^+ and remaining non-precipitated Al^{3+}, Fe^{3+} and Mn^{2+} ions are not modifying the raw zeolite structure (NC) [22]. The chemical composition of the natural and modified zeolites are collected in Table 6.2. The three modified zeolites revealed a reduction in the sodium, magnesium and calcium content that was accompanied by the slight increase of potassium content, in comparison with the natural zeolite. Clinoptilolite plate-like morphology that was characterized by networks of crystal clusters with cavities and entries to the channels inside the framework [23]. The surfaces of the modified zeolites were covered of small particles and crystals uniformly distributed which is in accordance with reported studies [24]. The FTIR analysis of the parent zeolite NC and its aluminium, iron and manganese forms revealed a slight variation in the intensity of the peaks in the range from 3700 cm^{-1} to 2951 cm^{-1}, at 1630 cm^{-1} and at 1012 cm^{-1} was observed in the three modified zeolites in comparison to the parent zeolite. The range of bands from 3700 cm^{-1} to 2951 cm^{-1} was assigned to the hydroxyl region of the zeolite structure: SiO–H groups, AlO–H groups, bridging hydroxyls, and H-bonded species [25]. The decrease of the intensity of these bridging Si(OH)Al groups was attributed to the substitution of protons for positively charged M species (e.g. Al (III), Fe (III) and Mn (II)). Then, these changes could be attributed to the formation of Al^{3+}–OH, Fe^{3+}–OH and Mn^{2+}–OH hydroxyl sites, which generated the variation of intensity in the band of deformation vibration of water band at ~1630 cm^{-1} [26]. The change of intensity in the peak at ~1012 cm^{-1} also suggested the structural changes promoted by the incorporation of transition metal ions into the zeolite structure [27]. Additionally, the appearance of new peaks below the 1558 cm^{-1} peak when the Al^{3+}, Fe^{3+} and Mn^{2+} are exchanged, can be associated to the amount of Brønsted and Lewis acid sites variation [22].

Sample	O	Na	Mg	Al	Si	K	Ca	Fe	Mn
NC	57.9±3	0.3±0.1	0.4±0.1	5.3±0.4	29.7±2	2.9±1	1.9±0.3	1.6±0.2	-
KAlC	46.6±1	<loq*	<loq*	5.6±1	14.7±2	3.4±1	<loq*	<loq*	-
KFeC	42.4±3	<loq*	<loq*	2.7±0.3	15.6±3	3.4±1	<loq*	8.9±1	-

KMnC	47.8±3	<loq*	<loq*	3.8±1	21.9±5	3.4±1	<loq*	<loq*	1.6±0.2

*loq: limit of quantification

Table 6.2. Relative atomic percentages measured by EDX of natural and potassium modified zeolites by impregnation with HMO (Al, Fe and Mn).

The acid–base characterization measured a pH_{pzc} of 5.2±0.4 for parent zeolite in comparison to modified zeolites pH_{pzc} (7.3±0.4 for KAlC, 6.4±0.4 for KFeC and 6.9±0.4 for KMnC). The pH_{pzc} provides information about the sorbent surface charge, and then a slight increase of the point of zero charge after modification can be attributed to the surface nature of the impregnated HMO. It was reported in previous studies that metal hydrated oxides developed a surface charge with water contact [28] and its interfacial behaviour is promoted by the dissociation of functional groups on the active sites of the sorbent [29]. The values of pH_{pzc} determined for modified zeolites are in agreement with those reported for an aluminium hydroxide γ-AlOOH (HAO) with 7.26 [30], for an iron hydroxide supported on a modified zeolite with 6.23 [31], and for manganese oxide Mn_2O_3 with 6.7 [32]. The development of negative charges is obtained for solutions with pH above pH_{pzc}, while pH below pH_{pzc} characterise positive charges development. The pH_{pzc} in modified zeolites KAlC, KFeC and KMnC revealed the existence of positive charges near below the common pH of treated domestic wastewater (pH ~7), favouring the adsorption of orthophosphate anions [33].

6.3.2. Ammonium and phosphate sorption as function of pH

The removal of ammonium can be described by an ion-exchange reaction with potassium ions as it is described by Eq. 6.

$$Z\text{-}K^+ + NH_4^+ \leftrightarrow K^+ + Z\text{-}NH_4^+ \qquad (6)$$

where Z^- represents the ionogenic groups of the zeolite structure.

The selectivity of the exchange process is considered mainly affected by the ionic charge and ionic radius. Although the Stokes hydration ionic radius for both ions is similar (130 nm) the differences in selectivity for the exchange of K^+/NH_4^+ is enough to assure a high removal efficiency for ammonium [34].

The influence of pH on ammonium sorption capacity of the potassium modified forms KAlC, KFeC and KMnC is plotted in Figure 6.2. A similar behaviour of the ammonium sorption capacity as a function of pH was obtained for NC. The repulsion of ammonium ions with the positive charges existing on the surface of the modified

sorbents was observed below the pH_{pzc} in the acid range from pH 2 to pH 4. Then, the maximum values of ammonium sorption capacity were reached between pH 4 to 7 which is near below the pH_{pzc} of the sorbents. However, above pH_{pzc} it was observed a progressive reduction of ammonium sorption capacity since at pH 7 starts the decrease of the NH_4^+ ion concentration due to its conversion into the non-protonated form (NH_3) [35].

The aluminium and iron hydrated oxide forms revealed similar pH dependence behaviour on phosphate sorption. The highest value of sorption capacity is below the pH_{pzc} of these sorbents; so the presence of positive charges favoured the anion sorption. However, the reduction of phosphate capacity at pH 2 seems to be connected to the conversion of charged phosphate species (e.g. $H_2PO_4^-$) to non-charge H_3PO_4. In the range from pH 4 to 11, near and above the pH_{pzc} of these zeolitic modified sorbents, the decrease of phosphate sorption was attributed to the existence of negative surface charged species. Moreover, for the manganese zeolite, low values of phosphate sorption in the pH range from 2 to 6 were measured, and then suddenly increased from pH 7 to pH 10. The phosphate oxyanions ($H_2PO_4^-$ - HPO_4^{2-}) sorption ocurred through chemical reaction via complexes formation with HMO functional groups (≅MOH). According to these removal patterns observed, the phosphate sorption in the expected pH range (Eq. 7 to 9) could be explained as follow:

- Formation of outer-sphere complexes with $\cong MOH_2^+$ surface groups, described by Eq. 7:

$$\cong MOH_2^+X^- + (H_2PO_4^-/HPO_4^{2-}) \leftrightarrow \cong MOH_2^+(H_2PO_4^-/HPO_4^{2-}) + X^- \quad (7)$$

- Formation of inner-sphere complexes with ≅MOH surface groups, described by Eq. 8:

$$\cong MOH + H_2PO_4^-/HPO_4^{2-} \leftrightarrow \cong MH_2PO_4^-/HPO_4^{2-} + OH^- \quad (8)$$

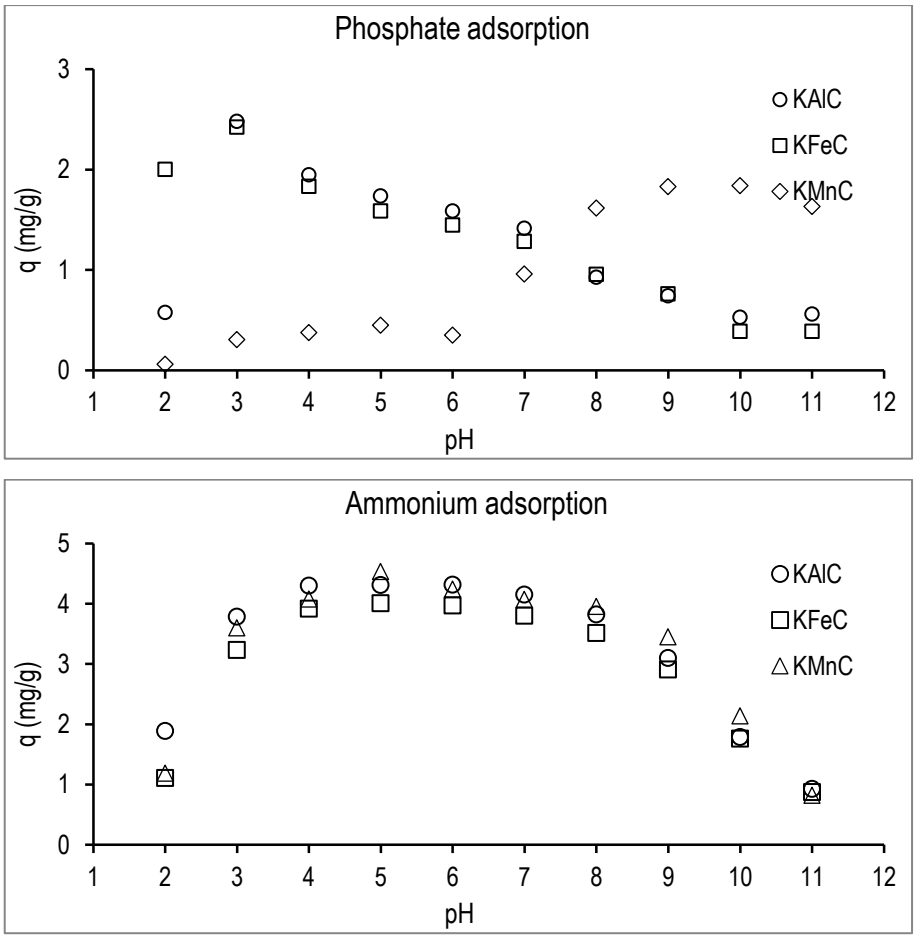

Figure 6.2. Effect of pH on the removal of ammonium and phosphate on modified zeolites KAlC, KFeC and KMnC.

6.3.3. Kinetic of phosphate and ammonium sorption

Kinetic sorption data for ammonium and phosphate for KAlC, KFeC and KMnC zeolites are shown in Figure 6.3. The ammonium sorption rates are comparable for the three modified zeolites which reached the equilibrium in only 15 minutes; whereas the phosphate sorption rates were lower and more than 60 minutes were needed to reach equilibrium. It can suggest that the ion exchange reaction between NH_4^+/K^+ (Eq. 6) occurred faster than complexation reactions of phosphate ions (Eq. 8 and 9). It can be explained due to the better access of the ammonium cations to the negative sites in comparison to the access of the surface hydroxide groups on the zeolite particles.

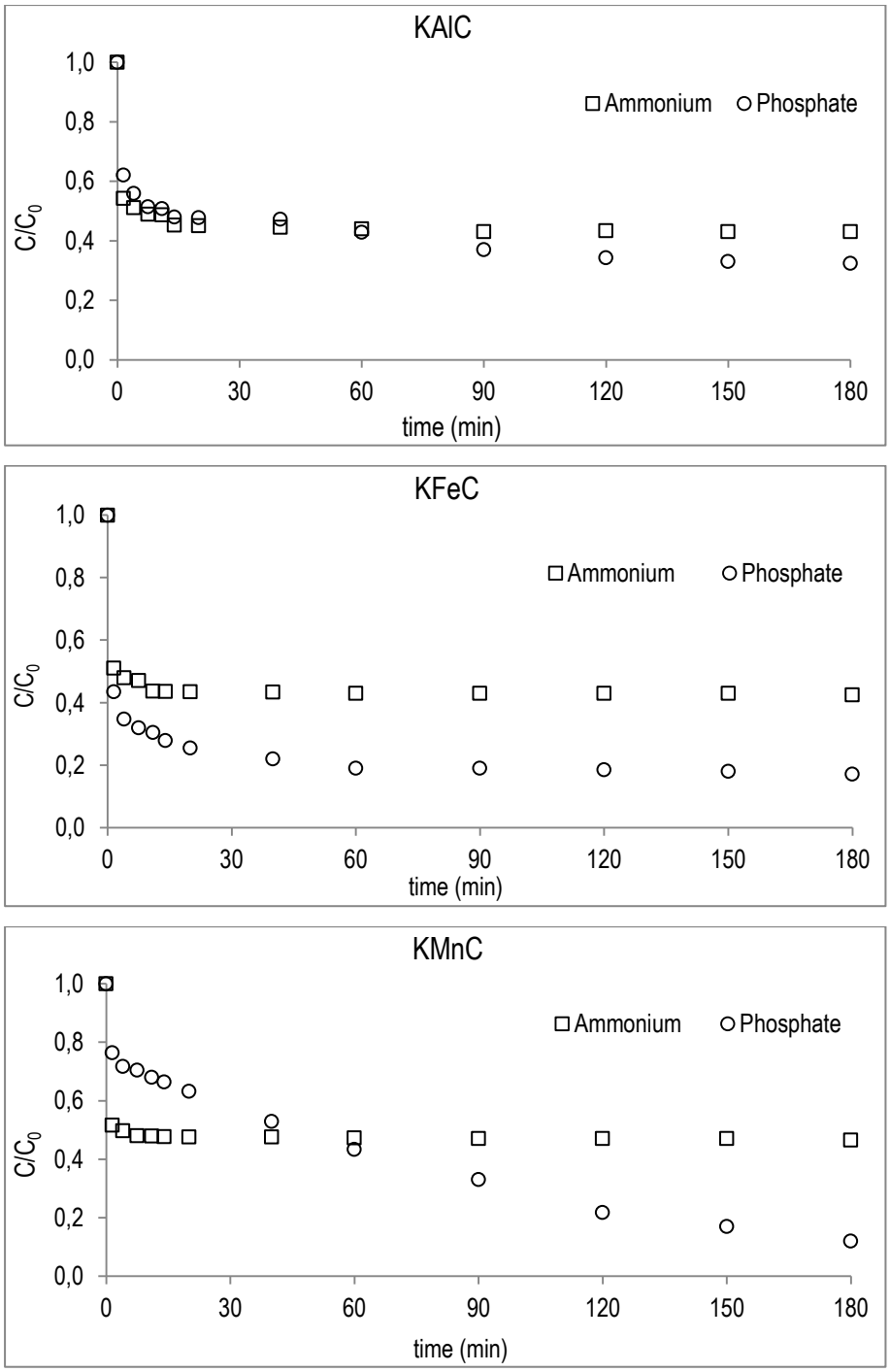

Figure 6.3. Ammonium and phosphate kinetic adsorption curves of KAlC, KFeC and KMnC zeolites in treated wastewater effluent sample.

The KMnC zeolite exhibited a lower phosphate sorption rate than KAlC and KFeC zeolites; and indeed the sorption capacity showed an increase of removal from 57% up to 78% (50% relative increase) after 30 minutes. This behaviour indicates that the main sorption mechanism involved in phosphate uptake for KMnC zeolite is also involving precipitation reactions.

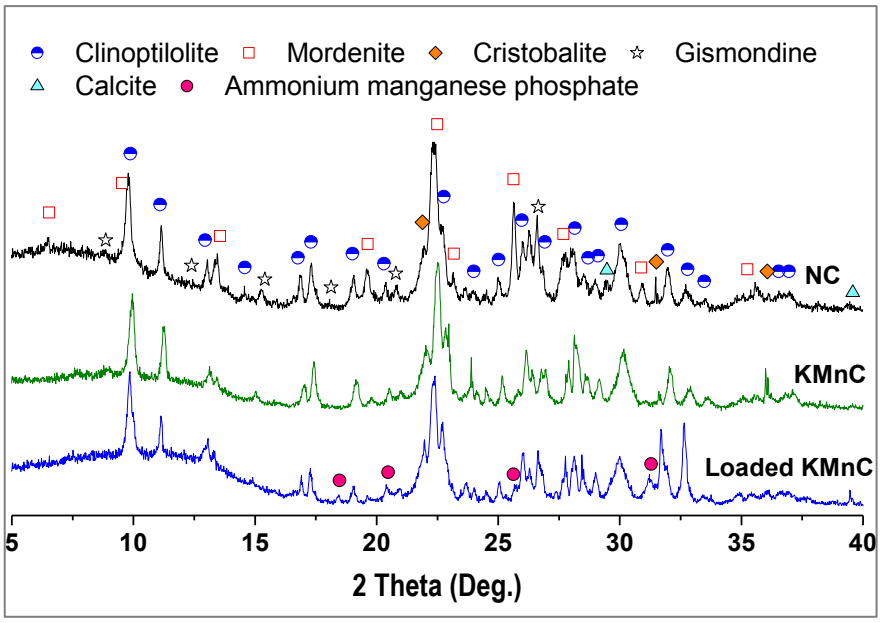

Figure 6.4. X-ray diffractograms of NC, KMnC and loaded KMnC. (ammonium manganese phosphate ($NH_4MnPO_4 \cdot H_2O$)).

The chemical precipitation of a new crystalline phase was revealed and identified as ammonium manganese hydrogen phosphate ($NH_4MnPO_4 \cdot H_2O$) through the XRD patterns of the loaded modified potassium manganese clinoptilolite (KMnC) as shown in Figure 6.4. In the case of KAlC and KFeC neither phosphate-Al nor phosphate-Fe phases were identified after sorption tests.

Analysis of the fractional equilibrium attainment functions (F(X) = f (t)) by using both HDM and SPM models (Eq. 1-5) indicated that sorption rate control of ammonium and phosphate ions is particle diffusion. A first stage of NH_4^+ and $HPO_4^{2-}/H_2PO_4^-$ diffusion from the solution to the external surface of zeolite is followed by a sorption stage along the zeolite internal surface. The linear regression analyses of the rate control equations for ammonium and phosphate sorption onto modified zeolites are summarized in Table 6.3. The R^2 values are closer to 1 for D_p than for D_f attributing to particle diffusion as the rate-limiting step for both ions.

		HPDM				SPM					
		$-\ln(1-X^2)$		$-\ln(1-X)$		X		$[3-3(1-X)^{2/3}-2X]$		$[1-(1-X)^{1/3}]$	
		R^2	D_f ($m^2 \cdot s^{-1}$)	R^2	D_p ($m^2 \cdot s^{-1}$)	R^2	K_F ($m \cdot s^{-1}$)	R^2	D_p ($m^2 \cdot s^{-1}$)	R^2	k_s ($m \cdot s^{-1}$)
KFeC	Phosphate	0.97	$1.1\ 10^{-13}$	0.86	$1.1\ 10^{-8}$	0.83	$2.9\ 10^{-10}$	0.97	$6.8\ 10^{-14}$	0.84	$4.6\ 10^{-10}$
KMnC		0.98	$2.2\ 10^{-14}$	0.91	$1.4\ 10^{-8}$	0.94	$7.4\ 10^{-10}$	0.99	$2.2\ 10^{-14}$	0.93	$2.1\ 10^{-10}$
KAlC		0.99	$1.1\ 10^{-13}$	0.93	$2.9\ 10^{-8}$	0.72	$8.3\ 10^{-9}$	0.98	$5.0\ 10^{-14}$	0.84	4.910^{-10}

KFeC	Ammonium	0.99	$1.1\ 10^{-12}$	0.92	$3.7\ 10^{-8}$	0.79	$3.2\ 10^{-9}$	0.98	$4.6\ 10^{-13}$	0.87	$7.9\ 10^{-10}$
KMnC		0.98	$5.7\ 10^{-13}$	0.86	$2.1\ 10^{-8}$	0.79	$1.2\ 10^{-10}$	0.97	$2.6\ 10^{-13}$	0.86	$1.4\ 10^{-10}$
KAlC		0.99	$2.6\ 10^{-13}$	0.89	$1.4\ 10^{-8}$	0.75	$2.3\ 10^{-9}$	0.99	$2.1\ 10^{-13}$	0.87	$3.5\ 10^{-10}$

Table 6.3. Kinetic parameters for ammonium and phosphate removal by modified zeolites using both HPDM and SPM models.

The effective diffusion coefficients in the range of 10^{-14}-10^{-12} m^2s^{-1} for both ions are common with chemisorption systems [36] and similar to those reported with powder synthetic zeolites used for ammonium or phosphate removal. The effective diffusion coefficients for ammonium ions are higher than for phosphate ions due to the different internal structure of the sites responsible for the sorption mechanism, ion-exchange for ammonium, and surface complexation for phosphate ions. Onyango et al. [37] reported effective diffusion coefficients in the order of 10^{-15} to 10^{-14} m^2/s for phosphate removal with synthetic zeolites impregnated with Al (III) hydrated oxides.
Sorption selectivity patterns of ammonium and phosphate in front of sodium, calcium, magnesium, chloride, sulphate and nitrate, major ions present in the treated wastewaters, for the impregnated zeolites are plot in Figure 6.5. For the three zeolites, the concentration ratio (C/C_0) decreases with time. A different trend was observed for K^+ as the concentration in solution increased due to the exchange with Na^+/Mg^{2+} and also for Ca^{2+} as expected according to Eq. 6. The selectivity order of K-zeolites for monovalent cations is as follows, NH_4^+>K^+>Na. The exchanged amount of Ca^{2+} and Mg^{2+} are higher compared to that of monovalent cations, especially for KAlC and KFeC zeolites. The three impregnated potassium zeolites were very selective for the simultaneous ammonium and phosphate sorption as it was reported for aluminium and iron impregnated zeolites [12, 13], taking into account the ions present in the treated wastewaters that were not sorbed. It should be pointing out that the KMnC zeolite showed the highest selectivity.

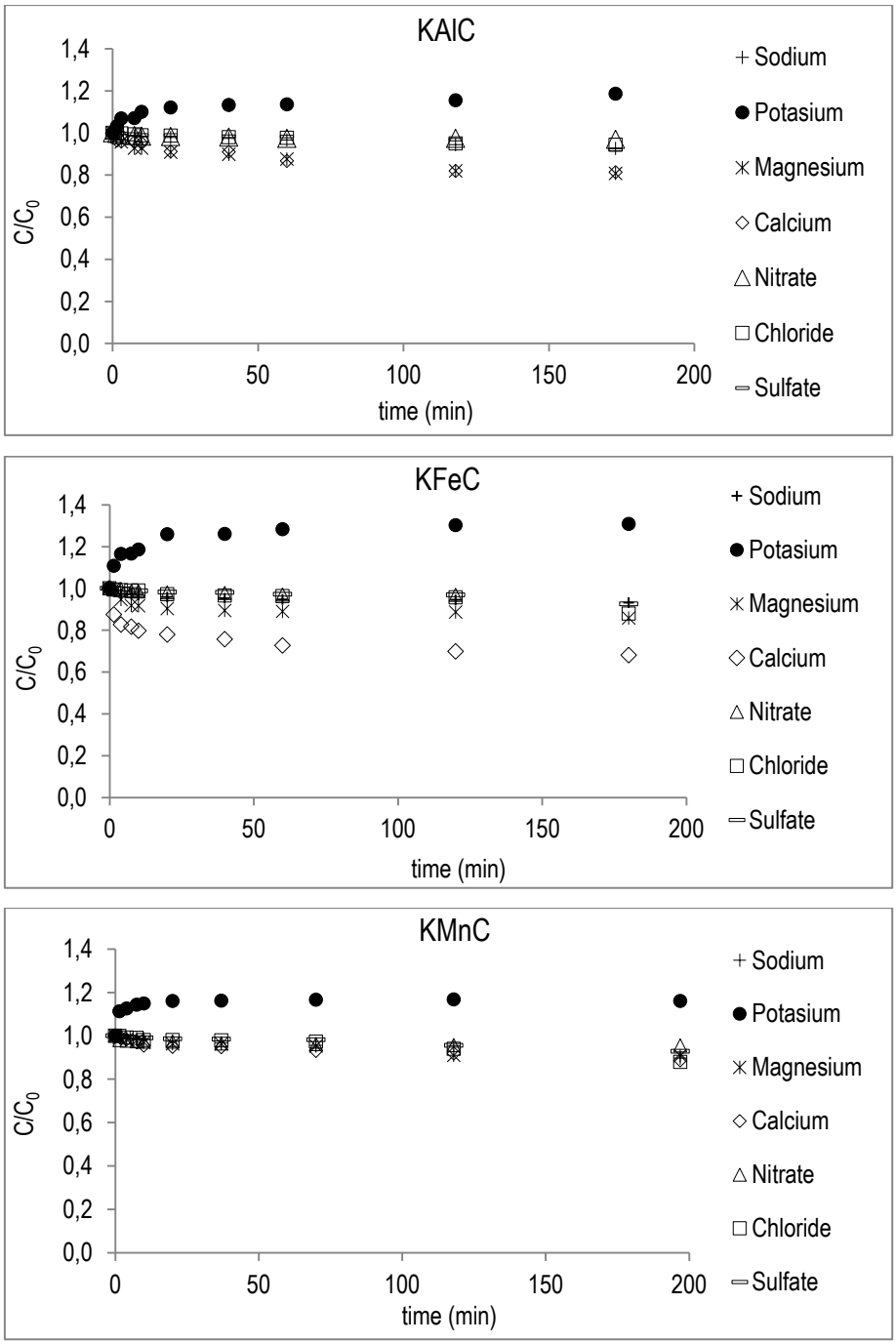

Figure 6.5. Sorption of cations and anions present in treated wastewater effluent for ammonium and phosphate sorption on modified zeolites KAlC, KFeC and KMnC.

The dissolved organic matter (DOM) sorption capacity of the zeolites, as a function of their major components, purgeable organic carbon (NPOC), total organic carbon (TOC), and total carbon (TC) is summarized in Table 6.4. Sorption values were below 0.3 mg/g indicating a limited sorption capacity of the zeolites for DOM under the working range evaluated (e.g., 20 mgTOC/L for the test solutions). Then a low influence of the DOM on ammonium and phosphate removal can be expected for the

three impregnated zeolites. This behaviour is in accordance with previous reports about inorganic sorbents used for nutrients removal which were not affected by low concentration of DOM [38]. However influence of the DOM was observed when high values are present in treated waters [6, 39].

Ion / Sample	Adsorption capacity ($mg \cdot g^{-1}$)											
	Na^+	K^+	Mg^{2+}	Ca^{2+}	NO_3^+	Cl^-	SO_4^{2-}	NPOC	NT	TOC	TC	IC
KAlC	1.6	-1.8*	0.9	1.4	0.1	2.5	1.8	0.1	1.6	0.3	0.1	0.2
KFeC	1.4	-3.0*	0.7	2.8	0.3	5.3	1.6	0.1	2.1	0.1	<l.d	0.1
KMnC	2.2	-1.3*	0.4	0.9	0.2	5.2	1.6	0.1	2.0	0.1	<l.d	<l.d

<l.d: values below the limit of detection

*Negative values means desorption of the ion from the zeolite to the solution

Table 6.4. Adsorption capacity of species present in treated wastewater samples.

6.3.4. Evaluation of phosphate bioavailability of loaded impregnated zeolites by sequential chemical phosphorus fractionation

Sequential chemical phosphorous fractionation data collected in Table 6.5 revealed that the major fraction of P after the leaching steps is associated with inorganic form (P_i). This in accordance with the fact that the treated wastewater effluent sample used contained mostly inorganic phosphorus forms.

The major P fraction was found to be the biological active HCO_3^- fraction that was around 35 – 39% of total P. The second P fraction was found to be the NaOH fraction which is associated with formation Fe-Al-Mn hydroxide minerals with 28 – 36% of total P. The third P fraction was found to be the HCl extractable fractions associated with Ca-P and Mg-P between 26 – 28% of total P. The minor P fraction was the H_2SO_4/H_2O_2 fraction accounting 2 – 3% of total P.

Treatment / Sample		HCO_3			NaOH			HCl			H_2SO_4/H_2O_2
	q	P_i	P_o	P_t	P_i	P_o	P_t	P_i	P_o	P_t	P_r
	$mg.g^{-1}$	$mg.g^{-1}$									
KAlC	6.3	1.7	0.3	2.0	1.6	0.3	1.9	1.3	0.3	1.5	0.2
KFeC	5.6	1.7	0.2	1.8	1.5	0.3	1.9	1.2	0.2	1.3	0.1
KMnC	9.6	2.0	0.3	2.3	1.4	0.3	1.7	1.5	0.20	1.7	0.2

Table 6.5. Sequential phosphorus fractionation of the loaded modified zeolite samples (P_i represents the inorganic fraction, P_o the organic fraction and P_r the residual fraction).

The sequential fractionation of the loaded modified zeolite revealed the existence of an important fraction of biological active phosphorus. Furthermore, the recovered phosphate can be suitable applied as fertilizer in P-deficient soils and finally it should be considered the abilities of the K-zeolites in soil improvement schemes. Cation exchange sites initially occupied by K^+ cations are selectively exchanged with NH_4^+ and in less extension with Na^+, Ca^{2+} and Mg^{2+}. Then, they can be used as a slow acting fertilizer, mainly for K^+ and NH_4^+.

6.4. Conclusions

The modification of a powder natural zeolite into the potassium aluminium, iron and manganese forms allowed the simultaneous removal of ammonium and phosphate sorption from a secondary wastewater effluent. The sorption mechanisms identified were ion exchange in the case of ammonium and the formation of inner sphere complexes with the functional groups ≅M-OH (M: Al^{3+}, Fe^{3+}, Mn^{2+}) in the case of phosphate. Moreover, it was also found that electrostatic interactions occurred in both ammonium and phosphate sorption on modified zeolite. Particularly, the chemical precipitation of ammonium manganese hydrogen phosphate ($NH_4MnPO_4 \cdot H_2O$) was identified on the loaded modified potassium manganese zeolite. The maximum phosphate sorption capacity for the three zeolites were 6.8 mg-P/g for KALC, 7.2 mg-P/g for KFeC and to 8.2 mg-P/g for KMnC. Contrary ammonium maximum sorption capacity was constant between pH 4 and 9 for the tree zeolites as the main sorption mechanism is the ion-exchange involves the K^+ ions of the zeolite. The maximum ammonium sorption capacity for the three zeolites was approximately 29±3 mg-N/g.

The existence of organic matter content in treated wastewater not represented interference on the ammonium and phosphate sorption capacities for the three modified zeolite. The sequential fractionation of the loaded modified zeolite revealed on one hand the existence of an important fraction of biological active phosphorus and on the other hand that recovered phosphate is suitable as fertilizer in P-deficient soils. However, due to the limited reusability of these materials, it could be an interesting option as additives for the soil quality enhancement.

6.5. References

1. Lin, L., et al., *Ammonium assists orthophosphate removal from high-strength wastewaters by natural zeolite.* Separation and Purification Technology, 2014. **133**: p. 351-356.

2. Escudero, A., et al., *Struvite precipitation for ammonium removal from anaerobically treated effluents.* Journal of Environmental Chemical Engineering, 2015. **3**(1): p. 413-419.
3. Lu, S.G., et al., *Removal mechanism of phosphate from aqueous solution by fly ash.* Journal of Hazardous Materials, 2009. **161**(1): p. 95-101.
4. Maaß, O., P. Grundmann, and C. von Bock und Polach, *Added-value from innovative value chains by establishing nutrient cycles via struvite.* Resources, Conservation and Recycling, 2014. **87**: p. 126-136.
5. Zelmanov, G. and R. Semiat, *The influence of competitive inorganic ions on phosphate removal from water by adsorption on iron (Fe+3) oxide/hydroxide nanoparticles-based agglomerates.* Journal of Water Process Engineering, 2015. **5**: p. 143-152.
6. Yin, H. and M. Kong, *Simultaneous removal of ammonium and phosphate from eutrophic waters using natural calcium-rich attapulgite-based versatile adsorbent.* Desalination, 2014. **351**: p. 128-137.
7. Xie, J., et al., *Chitosan modified zeolite as a versatile adsorbent for the removal of different pollutants from water.* Fuel, 2013. **103**: p. 480-485.
8. Xie, J., et al., *Removal of organic pollutants by surfactant modified zeolite: Comparison between ionizable phenolic compounds and non-ionizable organic compounds.* Journal of Hazardous Materials, 2012. **231–232**: p. 57-63.
9. Ji, X., et al., *Immobilization of ammonium and phosphate in aqueous solution by zeolites synthesized from fly ashes with different compositions.* Journal of Industrial and Engineering Chemistry, 2015. **22**: p. 1-7.
10. Margeta, K., et al., *Natural Zeolites in Water Treatment – How Effective is Their Use*. Water Treatment2013.
11. Figueiredo, H. and C. Quintelas, *Tailored zeolites for the removal of metal oxyanions: Overcoming intrinsic limitations of zeolites.* Journal of Hazardous Materials, 2014. **274**: p. 287-299.
12. Guaya, D., et al., *Simultaneous phosphate and ammonium removal from aqueous solution by a hydrated aluminum oxide modified natural zeolite.* Chemical Engineering Journal, 2015. **271**: p. 204-213.

13. Guaya, D., et al., *Modification of a natural zeolite with Fe(III) for simultaneous phosphate and ammonium removal from aqueous solutions.* Journal of Chemical Technology & Biotechnology, 2016. **91**(6): p. 1737-1746.
14. Villanueva, M.E., et al., *Point of zero charge as a factor to control biofilm formation of Pseudomonas aeruginosa in sol-gel derivatized aluminum alloy plates.* Surface and Coatings Technology, 2014(0).
15. APHA, A., WEF., *Standard methods for the examination of water and wastewater*, 2000, American Public Health Association, American Water Works Association, and Water Environment Federation.
16. Hedley, M.J., J.W.B. Stewart, and B.S. Chauhan, *Changes in Inorganic and Organic Soil Phosphorus Fractions Induced by Cultivation Practices and by Laboratory Incubations.* Soil Science Society of America Journal, 1982. **46**(5): p. 970-976.
17. Murphy, J. and J.P. Riley, *A modified single solution method for the determination of phosphate in natural waters.* Analytica Chimica Acta, 1962. **27**: p. 31-36.
18. Malik, M.A., P. Marschner, and K.S. Khan, *Addition of organic and inorganic P sources to soil – Effects on P pools and microorganisms.* Soil Biology and Biochemistry, 2012. **49**: p. 106-113.
19. Abdala, D.B., et al., *Long-term manure application effects on phosphorus speciation, kinetics and distribution in highly weathered agricultural soils.* Chemosphere, 2015. **119**: p. 504-514.
20. Valderrama, C., et al., *Kinetic evaluation of phenol/aniline mixtures adsorption from aqueous solutions onto activated carbon and hypercrosslinked polymeric resin (MN200).* Reactive and Functional Polymers, 2010. **70**(3): p. 142-150.
21. Moussavi, G., et al., *The investigation of mechanism, kinetic and isotherm of ammonia and humic acid co-adsorption onto natural zeolite.* Chemical Engineering Journal, 2011. **171**(3): p. 1159-1169.
22. Benaliouche, F., Y. Boucheffa, and F. Thibault-Starzyk, *In situ FTIR studies of propene adsorption over Ag- and Cu-exchanged Y zeolites.* Microporous and Mesoporous Materials, 2012. **147**(1): p. 10-16.
23. Nguyen, T.C., et al., *Simultaneous adsorption of Cd, Cr, Cu, Pb, and Zn by an iron-coated Australian zeolite in batch and fixed-bed column studies.* Chemical Engineering Journal, 2015. **270**: p. 393-404.

24. Zhang, W., et al., *Fabrication of TiO2/MoS2@zeolite photocatalyst and its photocatalytic activity for degradation of methyl orange under visible light.* Applied Surface Science, 2015. **358, Part A**: p. 468-478.
25. Chakarova, K., P. Nikolov, and K. Hadjiivanov, *Different Brønsted acidity of H-ZSM-5 and D-ZSM-5 zeolites revealed by the FTIR spectra of adsorbed CD3CN.* Catalysis Communications, 2013. **41**: p. 38-40.
26. Góra-Marek, K., et al., *IR studies of Fe modified ZSM-5 zeolites of diverse mesopore topologies in the terms of their catalytic performance in NH3-SCR and NH3-SCO processes.* Applied Catalysis B: Environmental, 2015. **179**: p. 589-598.
27. Ayodele, O.B., et al., *Hydrodeoxygenation of oleic acid into n- and iso-paraffin biofuel using zeolite supported fluoro-oxalate modified molybdenum catalyst: Kinetics study.* Journal of the Taiwan Institute of Chemical Engineers, 2015. **50**: p. 142-152.
28. Dhillon, A., et al., *Excellent fluoride decontamination and antibacterial efficacy of Fe–Ca–Zr hybrid metal oxide nanomaterial.* Journal of Colloid and Interface Science, 2015. **457**: p. 289-297.
29. Rida, K., S. Bouraoui, and S. Hadnine, *Adsorption of methylene blue from aqueous solution by kaolin and zeolite.* Applied Clay Science, 2013. **83–84**: p. 99-105.
30. Qi, F., et al., *Influence of aluminum oxides surface properties on catalyzed ozonation of 2,4,6-trichloroanisole.* Separation and Purification Technology, 2009. **66**(2): p. 405-410.
31. Simsek, E.B., E. Özdemir, and U. Beker, *Zeolite supported mono- and bimetallic oxides: Promising adsorbents for removal of As(V) in aqueous solutions.* Chemical Engineering Journal, 2013. **220**: p. 402-411.
32. Wang, L.-C., et al., *Gold nanoparticles supported on manganese oxides for low-temperature CO oxidation.* Applied Catalysis B: Environmental, 2009. **88**(1–2): p. 204-212.
33. Ortega-Gómez, E., et al., *Inactivation of natural enteric bacteria in real municipal wastewater by solar photo-Fenton at neutral pH.* Water Research, 2014. **63**: p. 316-324.

34. Murayama, N., et al., *Reaction, Mechanism and Application of Various Zeolite Syntheses from Coal Fly Ash.* MATERIALS TRANSACTIONS, 2003. **44**(12): p. 2475-2480.
35. Malovanyy, A., et al., *Concentration of ammonium from municipal wastewater using ion exchange process.* Desalination, 2013. **329**: p. 93-102.
36. Walker, G.M. and L.R. Weatherley, *Kinetics of acid dye adsorption on GAC.* Water Research, 1999. **33**(8): p. 1895-1899.
37. Onyango, M.S., et al., *Adsorptive Removal of Phosphate Ions from Aqueous Solution Using Synthetic Zeolite.* Industrial & Engineering Chemistry Research, 2007. **46**(3): p. 894-900.
38. Li, C., S. Wu, and R. Dong, *Dynamics of organic matter, nitrogen and phosphorus removal and their interactions in a tidal operated constructed wetland.* Journal of Environmental Management, 2015. **151**: p. 310-316.
39. Huang, H., et al., *Simultaneous removal of nutrients from simulated swine wastewater by adsorption of modified zeolite combined with struvite crystallization.* Chemical Engineering Journal, 2014. **256**: p. 431-438.

Chapter 7 Valorisation of N and P from waste water by k-zeolites impregnated with metal hydrated oxides as fertilizers: evaluation of nutrients release in amended soils by dynamic experiments

Abstract

A natural sodium zeolite (NaZ) was modified to its potassium form and impregnated by hydrated metal oxides (ZKAl, ZKFe and ZKMn) for the simultaneous ammonium and phosphate removal from domestic wastewater treatment plant (WWTP). Chemisorption was found the mechanism that controls the removal of ammonium (ion exchange) and phosphate (complexation) by zeolites. High selectivity was revealed towards common anions and cations, dissolved organic matter and micro-contaminants (e.g., metal transition) present in wastewater effluents. The phosphorus fractionation protocols revealed only a small portion of labile – P which may be bound to modified zeolites by physical sorption (e.g., weak complexes). The release of N, P and K from nutrient-poor soils amended with loaded zeolites was studied by column experiments. The columns were packed with a mixture of loaded NPK-zeolites and three different types of soils (e.g., one acidic and two basics). The columns were leached at different time intervals with water along 15 different leaching cycles and the resulting solutions were analysed. The three zeolites exhibited similar release behaivour for each soil sample used and the release of NPK elements was kept constant along the cycles. The release nutrient ratios, necessary for plants growth, were mainly controlled by the pH, organic matter content and main soil minerals.

Keywords: ammonium; phosphate; nutrients release; soil amendment; zeolite; resource recovery

7.1. Introduction

Soil fertility is a crucial aspect of agricultural development at worldwide in food production. The essential plant nutrients are nitrogen (N), phosphorus (P) and potassium (K) which are known as NPK elements [1]. The improvement of soils has become vital in order to make those nutrients available for plants. However it should be also limited their release to surface and groundwater that contributes to eutrophication [2]. Taking into account that nowadays NPK elements are extracted in excess from natural resources, particularly when there have been predicted in few years the depletion of phosphate rock deposits. Then, it is extremely necessary the development of new technologies to recover these nutrients from wastewater effluents which can be used as alternative resource. The natural zeolites due to their multiple properties as effective sorbents, safety and easy operation for ion exchange applications, seems to be the best inorganic material for this purpose. Zeolites are hydrated crystalline aluminium – silicate materials that include micro- and mesoporous with alkaline cations and water in their framework structure [3]. They have been widely used for ammonium removal applications and simultaneously the phosphate removal has been addressed due to a modification stage based on the impregnation of metal oxides species on their surface [4]. Additionally, zeolites have been applied as amendments materials for soils that could diminish the nutrient leaching providing slow release fertilizer application [5] and increase the crop water use efficiency [6]. Therefore, the purpose of this work is to evaluate the aluminium, iron and manganese forms of a natural potassium zeolite for nutrients recovery from wastewater effluents and their further application as slow release inorganic fertilizers for soils. The objectives of this study are: (i) modify a natural zeolite into the aluminium, iron and manganese forms of potassium zeolite, (ii) characterize the modified zeolites, (iii) remove phosphate and ammonium simultaneously from real wastewater effluent, (iv) perform the fractioning of phosphorus in loaded zeolite, (v) collect and characterize three nutrient-poor soil samples, (vi) amend the soil samples with the NPK loaded zeolites, and (vii) evaluate the nutrient release from amended soils through natural weathering simulation.

7.2. Materials and methods

7.2.1. Modification of natural zeolite

A natural zeolite (NaZ) was obtained from Zeocem Company (Slovak Republic). It was grounded until fine powder particles (<74 μm). Three samples of natural zeolite

were treated in separately solutions containing 0.1 M $AlCl_3$, 0.1 M $FeCl_3$ and 0.1 M $MnCl_2$, using a 1:5 relation powder – solution. At the beginning the pH of each solution was adjusted at pH 7±0.5 using KOH (10 M). After being treated two consecutive times during 3 hours under reflux conditions the aluminium (ZKAl), iron (ZKFe) and manganese (ZKMn) forms of zeolite were obtained. Finally, samples were washed until no chloride was detected by the $AgNO_3$ test and finally dried at 80 °C for 24 hours.

7.2.2. Soils sampling and characterization

Three different soils samples were collected from agricultural areas of NE Spain, Tordera and Sant Celoni (Barcelona) and Samitier (Huesca). They were coded based on their location S1, S2 and S3. The soil samples were air-dried at room temperature. The detectable vegetal and animal contaminants were apart from the soil samples before to sieve them < 2 mm. The main soil properties were determined: pH, humidity, bulk density, and organic matter. The soil pH was measured using a 1:5 (w/v) soil-water suspensions which were shaken for 1 h. The humidity was determined by drying soil during 24 h at 100 °C. Bulk density was determined using the soil core method described elsewhere [7]. Finally, organic matter was measured in 3 g of soil which was calcined at 600 °C during 8 hours. The organic matter content was determined by Eq 1.

$$\mathrm{OM}\ (\%) = \frac{(w_i - w_c)}{w_c} \times 100$$

where: w_i: is the soil weight before calcination and w_c: is the soil weight after calcination

7.2.3. Ammonium and phosphate sorption on modified zeolites

Weighted amounts of modified zeolite samples (6.5 g of ZKAl, ZKFe, ZKMn) were equilibrated in 500 mL of real wastewater at pH 7.5±0.5, 500 rpm and room temperature (21±1 °C). It was used an effluent stream from secondary treatment at the El Prat WWTP (Barcelona – Spain), which chemical composition is collected in Table 7.1. The adsorption capacity of modified zeolites was increased by increasing the ammonium (500 mg $N\text{-}NH_4^+$/L and 500 mg $P\text{-}PO_4^{3-}$/L) concentration in the wastewater effluent (addition of NH_4Cl and $NaH_2PO_4.2H_2O$, respectively). The suspension was settled in order to separate the solid content, which was dried at 60 °C for 24 h and further storage. Equilibrium test were performed several times until 250 g of each loaded modified zeolite were obtained. The ammonium and phosphate

concentrations were determined at the initial and remaining aqueous solution after being filtered by 45 μm of cellulose membrane filter.

ICP - MS elements											
	Na	Ca	S	K	Mg	Sr	Al	Si	Fe	Ba	
mg/L	246	127	81	36	35	1,3	0,2	0,03	0,03	0,02	
	Li	B	Ti	V	Cr	Mn	Co	Ni	Cu	Zn	As
μg/L	19	257	6	12	0,9	3,1	2	28	5	58	3
	Se	Rb	Sr	Mo	Sn	Sb	Ba	W	Pb	U	
μg/L	3	16	1091	15	0,3	3	19	3	0,2	1,7	
	Be, Sc, Ga, Ge, Y, Zr, Nb, Cd, Cs, La, Ce, Pr, Nd, Sm, Eu, Gd, Tb, Dy, Ho, Er, Tm, Yb, Lu, Hf, Ta, Tl, Bi, Th										
μg/L	<0,2										
TOC elements											
	NPOC		NT		TOC		TC		IC		
mg/L	12		590		10		50		42		
Ionic Elements											
	NH_4^+		PO_4^{3-}		NO_3^-		Cl^-				
mg/L	500		500		51		542				

Table 7.1. Chemical composition of the effluent stream from secondary treatment at the El Prat WWTP used for sorption experiments.

7.2.4. Sequential chemical fractionation and availability of phosphorous

The phosphorus of soil and zeolites were sequentially fractionated by a sequential chemical fractionation method using a modified procedure proposed by Hedley et al. (1982) [8] as described by Tiessen and Moir (1993) [9]. Two grams of sieved soil <2 mm or leaded modified zeolites samples <74 μm were weighed into centrifuge tubes containing 50 mL of extractant solutions at room temperature and 100 rpm during 16 h. The primary step of extraction for the labile phosphorus was performed in 0.5 M $NaHCO_3$ at pH 8.5. The Fe bounded phosphorus (slow) fraction was extracted in 1 M NaOH and the Ca bounded phosphorus (weathered mineral) in 1 M HCl solutions. The extracted organic matter was precipitate by acidification of an aliquot of the $NaHCO_3$ and NaOH extracts then the supernatant was analysed for inorganic phosphorus (P_i). In order to convert the organic into inorganic phosphorus another aliquot of the $NaHCO_3$ and NaOH extracts was digested with acidified ammonium persulfate at 121 °C during 90 min, then in the digest the total P (P_t) was analysed colorimetrically. The organic P (P_o) was determined by difference between P_t and P_i

in each $NaHCO_3$ and NaOH extract. The residual phosphorus was determined in samples after being digested with H_2SO_4/H_2O_2. The phosphorus concentration in extracts and digested solutions was determined by ascorbic acid method. The NaOH, HCl and residual phosphorus was considered as non-labile. The determination of the phosphorus availability was performed by the Olsen [10] and Nelson [11] methods to know the inorganic phosphorus that influences on plant nutrition. Before samples were analysed, the tubes were centrifuged at 5000 rpm for 10 min and the supernatant was filtered through a 0.45 μm of cellulose membrane filter. The assays were replied at least twice.

7.2.5. Ammonium and phosphate batch and column leaching assays

The ammonium and phosphate release assays were performed in batch and continuous mode. There were weighted 5 g of soil samples (S_1, S_2 and S_3) and loaded modified zeolite samples (ZKAl, ZKFe and ZKMn) in 50 mL tubes with ultrapure water for batch assays. The suspensions were shaken during 24 h, then the tubes were centrifuged at 5000 rpm for 10 min and the supernatant was filtered through a 0.45 μm of cellulose membrane filter. The test in continue mode were performed in polyethylene columns (100 mm length x 40 mm internal diameter) to simulate the natural soil arrangement shown in Figure 7.1. Twelve soil columns were used and distributed according to the disposition detailed Table 7.2.

Column	Code	Description
1	C-S_1	S_1 sample
2	C-S_1ZKAl	S_1 sample and P-N loaded Al modified zeolite
3	C-S_1ZKFe	S_1 sample and P-N loaded Fe modified zeolite
4	C-S_1ZKMn	S_1 sample and P-N loaded Mn modified zeolite
5	C-S_2	S_2 sample
6	C-S_2ZKAl	S_2 sample and P-N loaded Al modified zeolite
7	C-S_2ZKFe	S_2 sample and P-N loaded Fe modified zeolite
8	C-S_2ZKMn	S_2 sample and P-N loaded Mn modified zeolite
9	C-S_3	S_3 sample
10	C-S_3ZKAl	S_3 sample and P-N loaded Al modified zeolite
11	C-S_3ZKFe	S_3 sample and P-N loaded Fe modified zeolite
12	C-S_3ZKMn	S_3 sample and P-N loaded Mn modified zeolite

Table 7.2. Disposition of soil columns used for dynamic experiments.

An amendment of 100 kg $P.ha^{-1}$ of soil sample was established to dose the P-N loaded modified zeolites (ZKAl, ZKFe and ZKMn) in each soil column. Moreover, it was simulated the average rainfall of 0.8 mm in Central Europe using ultrapure water which was fed to the soil column continuously. A sample of 25 mL of liquid samples released from each column was collected every three days, therefore fifteen cycles were performed. Samples were filtered through a 0.45 μm of cellulose membrane filter and store at 5 °C until being analysed. Beside to the ammonium and phosphate release from soil columns also it was determined other anions, cations and heavy metals existent in the effluents.

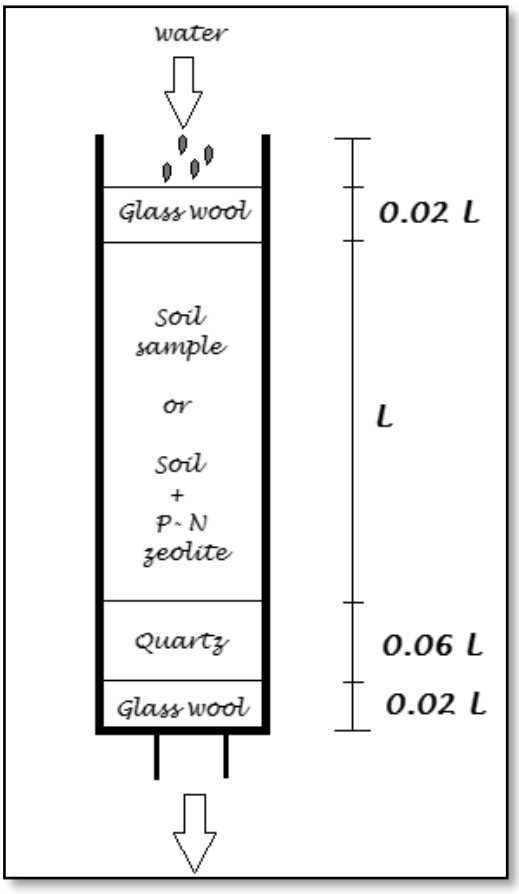

Figure 7.1. Columns arrangement for the release of ammonium and phosphate from loaded zeolites in continuous test.

7.2.6. Analytical methods

Standard methods were used for phosphate (PO_4^{3-}) and ammonium (NH_4^+) determination [12]. The vanadomolybdophosphoric acid colorimetric method (4500-P C) and the ascorbic acid method (4500-P E) allowed the phosphate quantification, while the ammonia-selective electrode method (4500-NH3 D) was employed for ammonium determination. The ions were determined using a Thermo Scientific Ionic Chromatograph (Dionex ICS-1100 and ICS-1000). An elemental analysis was performed by inductively coupled plasma atomic emission spectroscopy (ICP-AES, Thermo Scientific - ICAP 6500) and an inductively coupled plasma mass spectrometry or ICP-MS (ICP-MS, Thermo Scientific – X-series II). The non-purgeable organic carbon (NPOC), total carbon (TC), total organic carbon (TOC), inorganic carbon (IC) and total nitrogen (NT) were determined in a total organic carbon analyser (Shimadzu, TOC-V_{CPH}).

7.2.7. Characterization of zeolites and soils

The chemical composition and morphology of the natural and modified zeolites were determined by a Field Emission Scanning Electron Microscope (JEOL JSM-7001F) coupled to an Energy Dispersive Spectroscopy system (Oxford Instruments X-Max). Four individual EDX measurements were performed at different positions. The infrared absorption spectra of the natural and modified zeolites were recorded in a Fourier Transform FTIR 4100 (Jasco) spectrometer in the range of 4000 – 550 cm^{-1}. Also powder X-ray Diffractometer (D8 Advance A25 Bruker) was used for X-ray diffraction (XRD) characterization of modified zeolites and soil samples. The nitrogen gas adsorption method was used for the specific surface area determination of ZKAl, ZKFe and ZKMn samples on an automatic sorption analyser (Micrometrics). Also, the pH_{pzc} of the natural and modified zeolites was determined by the pH drift method described elsewhere [13]. The tests were replicated at least three times for each sample and the average values are reported.

7.3. Results and discussion

7.3.1. Zeolites and soils characterization

Mainly clinoptilolite and minor amounts of quartz and albite were found in natural zeolite. The slightly decrease of peaks intensity were identified in the XRD diffractograms of modified zeolites which is attributable to the distribution of aluminium, iron and manganese ions on zeolite framework; with absence of new mineralogical phases. The parent and modified zeolite chemical composition is listed in Table 7.3. The potassium, aluminium, iron and manganese content increase while the percentage of other ions decreases (e.g. sodium, magnesium and calcium) that suggest an ion exchanged as the mechanism responsible of this variability. Also, the parent zeolite morphology with a plate-like configuration of networks of crystal clusters with cavities and entries to the channels inside the framework revealed a variation with the small particles and crystals uniformly dispersed on the framework of modified zeolites. The FTIR spectra of the modified zeolite revealed variation in the range from 3700 cm^{-1} to 2951 cm^{-1} attributed to the hydroxyl region the zeolitic structure by changes occurred in the bridging groups: SiO–H, AlO–H, hydroxyls and H-bonded species; and at ~1630 cm^{-1} which corresponds to the deformation vibration of water. These changes were attributed to the new hydroxyl sites generation Al^{3+}–OH, Fe^{3+}–OH and Mn^{2+}–OH, which is confirmed by the peak at ~1012 cm^{-1} that occur due to transition metals incorporated in the zeolite structure. Additional information

was provided by the acid base characterization which revealed the change of pH_{pzc} from 5.2±0.4 NZ in comparison to 7.3±0.4 for ZKAl, 6.4±0.4 for ZKFe and 6.9±0.4 for ZKMn. In fact, those values are in agreement with the pH_{pzc} = 7.26 of the aluminium oxide γ-AlOOH (HAO) [14], 6.23 for iron oxide [15], and 6.7 for manganese oxide Mn_2O_3 [16].

Sample	*O*	*Na*	*Mg*	*Al*	*Si*	*K*	*Ca*	*Fe*	*Mn*
ZN	57.9±3	0.3±0	0.4±0	5.3±0	29.7±2	2.9±1	1.9±0	1.6±0	-
ZKAl	46.6±1	<loq*	<loq*	5.6±1	14.7±2	3.4±1	<loq*	<loq*	-
ZKFe	42.4±3	<loq*	<loq*	2.7±0	15.6±3	3.4±1	<loq*	8.9±1	-
ZKMn	47.8±3	<loq*	<loq*	3.8±1	21.9±5	3.4±1	<loq*	<loq*	1.6±0

*loq: limit of quantification

Table 7.3. Relative atomic percentages measured by EDX of parent and modified zeolites.

The main mineralogical phases as well as the physical properties for each soil sample are summarized in Table 7.4. The soil sample S3 was characterized as a slightly acidic soil with pH 6.8, so it is nominated as pure ferralitic soils due to the higher content of iron, aluminium and manganese. Otherwise, the sodic soils S1 and S2 with pH 8.5 and 9.2, respectively; can be described as mixed calcareous soils due to their high content of calcium with significant aluminium, iron and magnesium contents [17].

Properties	**S_1**	**S_2**	**S_3**
Mineralogical compounds	Quartz, Calcite, Illite, Clinochlore, Microcline, Albite	Quartz, Albite, Microcline, Calcite, Magnetite, Montmorillonite	Quartz, Albite, Microcline, Nontronite
pH	8.5±0.1	9.2±0.1	6.8±0.1
Humidity (%)	3.3±0.3	1.1±0.2	2.4±0.2
Bulk density (g/cm^3)	1.1±0.2	1.4±0.2	1.2±0.2
Organic matter (%)	8.8±0.5	2.4±0.4	5.4±0.4

Table 7.4.Chemical and physical characterization of soil samples (S_1, S_2, S_3).

7.3.2. Ammonium and phosphate sorption on modified zeolites

Ammonium and phosphate were selective sorbed by the modified zeolites in comparison to other ions. Sorption capacities measured were 7.1±1, 6.9±1 and 7.3±1 mg $N\text{-}NH_4^+$/g and 6.3±1, 5.6±1 and 9.6±1 mg $P\text{-}PO_4^{3-}$/g for ZKAl, ZKFe and ZKMn,

respectively. Taking into account the pH_{pzc} values (7.3 ZKAl, 6.4 ZKFe and 6.9 ZKMn) and the real wastewater pH of 7.5, it can be stated that removal of both ions is performed by ion exchange (e.g., NH_4^+) or by complexation (e.g., $H_2PO_4^-$) is favoured under these conditions. Analysis of the treated water before and after be in contact with zeolite shown that sodium and potassium were mainly released from modified zeolites due to the ion exchange with ammonium.

Particularly, in KZMn zeolite the higher values of phosphate and magnesium sorption capacities in comparison to the other two zeolite forms, could be associated with a precipitation reaction of phosphate and magnesium minerals on the zeolite surface as it was observed at the end of the tests. The chloride, sulphate and nitrate ions as well as NPOC, TOC, TC and IC were minimal sorbed in the three modified zeolites ZKAl, ZKFe and ZKMn (Figure 7.2). No other elements found in the treated wastewater were taking into account as they were negligible sorbed.

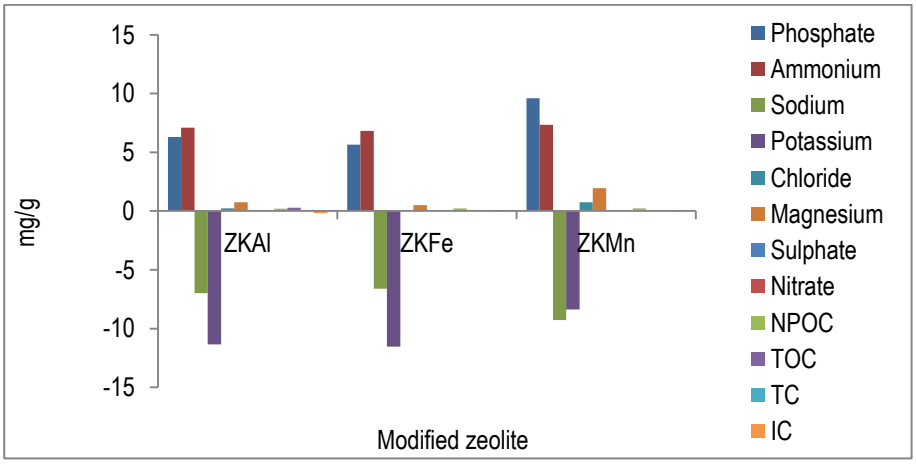

Figure 7.2. Sorption capacity of major components of treated wastewater (phosphate, ammonium, sodium, potassium, chloride, magnesium, sulfate, nitrate, NPOC, TOC, TC and IC) on modified zeolites (KZAl, KZFe, KZMn). Negative values indicates release from the zeolite forms (solid to aqueous phase ratio used was 6.5 g in 500 mL)

7.3.3. Availability of phosphorous from loaded zeolites and soils using sequential chemical fractionation of phosphorous

The chemical fractionation of sorbed phosphorus on the three modified zeolites and the three evaluated soils provides information about the solubility in soils of various fractions (Table 7.5). Phosphate is present in the extracted fractions as inorganic forms indicating that organic forms present on the treated wastewater at low extent were extracted. The soil samples revealed similar contents of organic and inorganic

phosphorus, and the HCl extractable fractions associated with Ca-P and Mg-P group fractions were found to be the major form of phosphorus. The biological active HCO_3 and the NaOH phosphorous fractions, associated to Fe-Al-Mn hydroxide minerals, were found to be almost the same for the soil samples.

In loaded zeolites the fractionation revealed that the phosphorus content in the HCO_3, NaOH and HCl fractions were proportionally the same. Therefore, only one third of phosphate is physical sorbed and easy labile while the rest is chemically bound to modified zeolites by means of complexation or precipitation reactions. An insignificant phosphorus fraction for soils and loaded zeolites was found to be the H_2SO_4/H_2O_2 residual fraction. The phosphorus availability by Olsen method is comparable with those values obtained by the HCO_3 fractioning stage for soils and zeolites. In this case the Nelson method allowed the extraction of higher contents of available phosphorus than Olsen, due to the strong effect of acid that promoted the partial destruction of soils and zeolites structure while the slight basic treatment is less aggressive.

Sample	HCO_3 fraction			NaOH fraction			HCl fraction			H_2SO_4/H_2O_2 fraction	Olsen availability	Nelson availability
	P_i	P_o	P_t	P_i	P_o	P_t	P_i	P_o	P_t	P_r		
	mg $P\text{-}PO_4^{3-}.g^{-1}$											
S_1	0.09	0.06	0.15	0.06	0.05	0.10	0.12	0.10	0.22	0.07	0.01	0.03
S_2	0.00	0.01	0.01	0.00	0.01	0.01	0.30	0.22	0.52	0.03	0.00	0.08
S_3	0.01	0.01	0.02	0.03	0.07	0.09	0.27	0.22	0.50	0.02	0.00	0.10
ZKAL	1.72	0.26	1.98	1.56	0.30	1.86	1.26	0.26	1.52	0.21	1.57	6.11
ZKFe	1.66	0.14	1.80	1.53	0.32	1.85	1.21	0.14	1.34	0.12	1.74	5.63
ZKMn	2.03	0.28	2.31	1.41	0.27	1.68	1.45	0.21	1.66	0.20	1.83	9.40

Table 7.5. Fractionation and availability of phosphorus ($P\text{-}PO_4^{3-}$) from soils and loaded modified zeolites, where P_i represents inorganic P, P_o represents organic P and P_t represents total P.

7.3.4. Ammonium, phosphate and potassium leaching from batch tests

Soil solutions reported low contents of ammonium, phosphate and potassium in comparison with three loaded zeolite solutions that revealed higher contents of these ions as shown Figure 7.3. In these solutions also were found significant contents of chloride, sulfate, NPOC, TOC, TC, IC and sodium, whereas Fe, Mn, Li, B, Zn, Cu were found as traces (µg/L) and negligible quantities of other elements. Modified K-zeolites revealed similar loading sorption capacities towards ammonium and

phosphate from treated wastewater and also their release were similar even including for K originally present on the zeolite. The amounts of ammonium, phosphate and potassium released during the leaching test are listed in Table 7.5. The small leached values of both ions could be attributed to the labile fraction that is sorbed to the modified zeolites due to physical sorption while the remaining part of phosphate and ammonium are still associated to zeolite by chemical forces. A significant amount of TOC, IC and TC is released in soil solution compared with zeolites samples. This could be explained in terms of organic matter content because modified zeolite revealed a negligible sorption of organic compounds from treated wastewater during the loading stage.

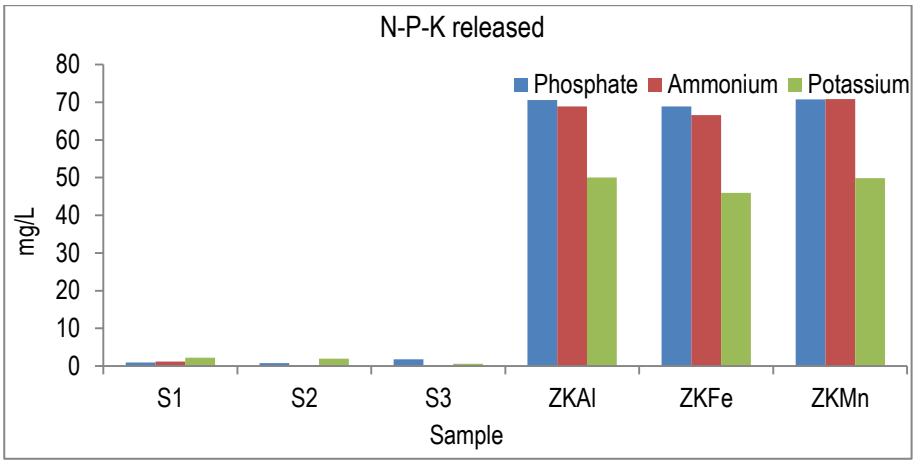

Figure 7.3. Ammonium, phosphorus and potassium release from soils and loaded zeolites samples using batch test (phase ratio 5 g of solid and 50 ml of solution).

7.3.5. Release of NPK and trace elements from zeolite amended soils by using column tests

Column studies were used to simulate the release of nutrients from zeolite amended soils at field scale. A sequence of 15 different cycles simulating raining events were developed and the composition of the effluent collected from each column are plotted in Figure 7.4 to 7.8. As it could be seen the chemical compositions of leaching solutions from columns through the leaching cycles had a minimal variation. Basic soils S1 and S2 with a high content of $CaCO_3$ exhibited values between 8.3 and 8.9 through the leaching cycles these pH values can controlling the dissolution of silicate base minerals present on the soils. Results on Figure 7.4, shown clearly the release of higher amounts of nutrients (N,P,K) from the amended columns compared with non-amended columns and is proportional in agreement with those reported in batch

tests. Even though the ammonium and phosphate sorption capacities are similar for ZKAl, ZKFe and ZKMn, there were exhibited different profiles of leaching of these compounds. Then, these differences can be effect of the soil mineral composition and their dissolution rates.

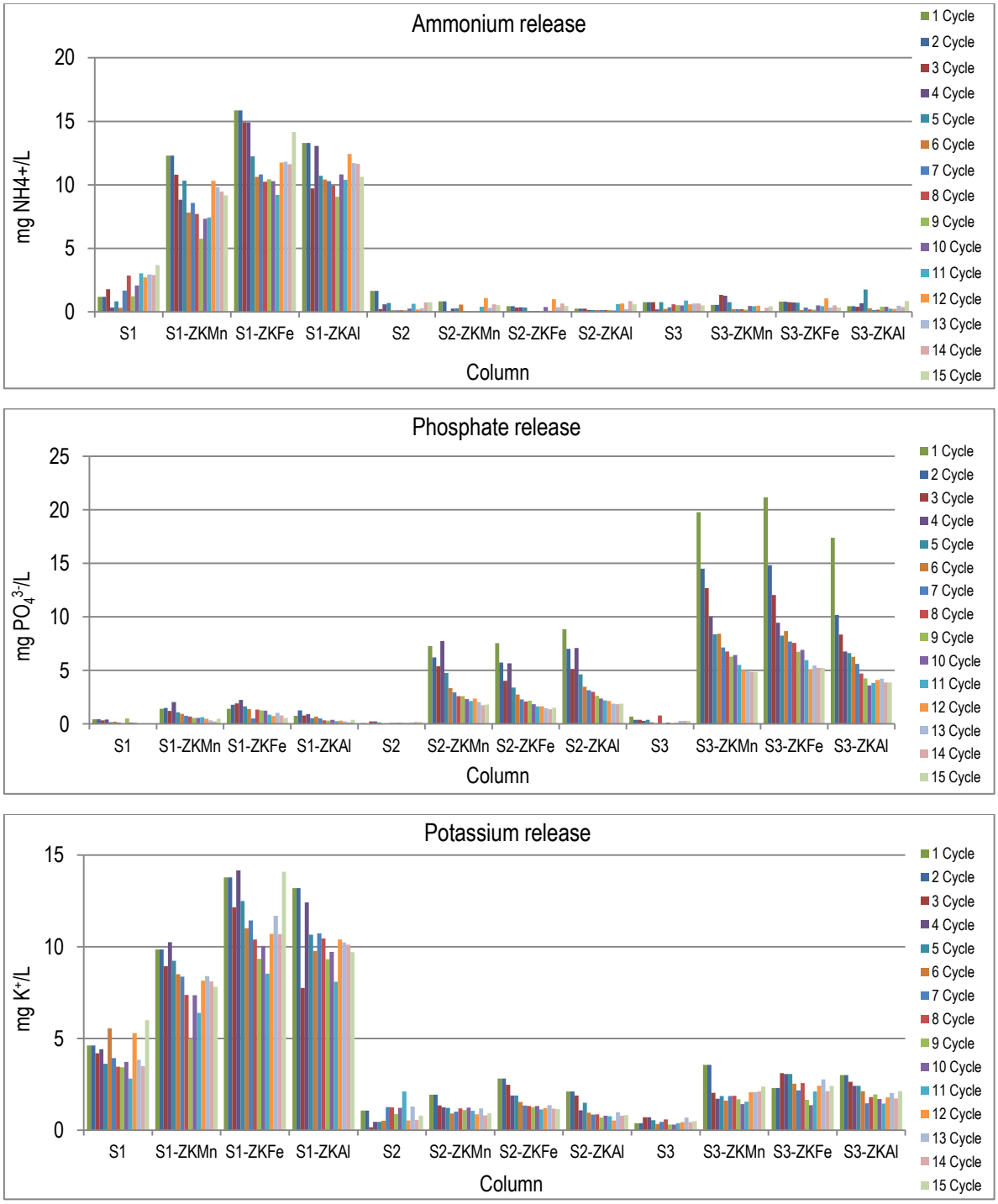

Figure 7.4. Amount of ammonium, phosphate and potassium released in solution from un-amended and amended soil columns through 15 continuous cycles.

The use of charged NPK zeolites as soil fertilizers effectively provided a gradual release of nutrients in solutions during the fifteen cycles. It was found that the release value for phosphate compound depends on soil nature as well as the modified zeolite used soil amendment which is shown in Table 7.6.

System	% Release	System	% Release	System	% Release
S1	3.5	S2	0.6	S3	4.0
S1-ZKMn	8.3	S2-ZKMn	31.5	S3-ZKMn	87.2
S1-ZKFe	8.9	S2-ZKFe	31.9	S3-ZKFe	93.4
S1-ZKAl	4.6	S2-ZKAl	37.7	S3-ZKAl	75.7

Table 7.6. Releases of phosphate in solutions from continue tests.

The soil S2 with the highest pH value around 9 the phosphate ions demonstrated a total release percentage of 32-38 after the 15 cycles, and similarly at pH value around 8 the soil S1 released 5-9%. Contrary for the case of acidic soils, were the sorption ions is less favoured as it can be seen up to 87-93% of the loaded P-PO_4^{3-} was desorbed. Only for the case of S3-ZKAl zeolite where only less than 5% was released, and at this moment not reasons to describe this behaviour were identified.
The phosphate content in solutions was low which is in accordance to previous reports about the low mobility of inorganic phosphorus in soils [18]. This is attributable to the chemical processes of inorganic phosphorus in soils such as complexation, solubilisation and sorption as well as the interaction with other ions which influence the phosphorous migration [19] or the formation of some metal complexes with iron and aluminium [20] and the chemical precipitation of some calcium, magnesium, iron and aluminium phosphates [21]. Soil samples S1 and S2 contain calcite in their mineralogical composition that affect even more the phosphate mobility as it was reported by Afif et al., 1993 [19]. In this study the highest availability in solutions of phosphate was associated with the pH of soil S3 at pH 6.8 in which occurs the solubility of inorganic forms of P, this result is in accordance to the report of Markus Anda et al., 2015. This fact could be attributable to the higher availability of some metals on the surface layers of basic soils that promote the phosphate fixation in comparison to acid soils [22]. Moreover, the oxidation condition for the existent oxyhydroxides metals forms can favoured the phosphate fixation while the reduced conditions promoted the phosphate release due to the dissolution of these (oxy)hydroxides forms, as it was studied for the arsenic behaviour in soils [23]. Then,

the redox potential has a strong influence on the phosphorus mobility in soils because also the development of reducing conditions produce P (V) reduction into P (III) which is less reactive with the (oxy)hydroxides forms [24].

The highest ammonium release was found in soil solutions S1 and it was almost negligible for S2 and S3. The soil solution S1 demonstrated the highest release of ammonium and a similar behaviour was observed for the other multivalent cations (K, Na, Ca, Mg) existent in loaded zeolites. The increase of cations content in solutions could be an effect of the occurrence of their aqueous complexation to dissolved organic matter avoiding their fixation to soil [25]. Soil sample S1 revealed the highest organic matter content and basic pH 8.2 that favoured the release of organic matter in soil solution [26] due to the deprotonation of organic molecules that becomes more negatively charged and hydrophilic. The low content of ammonium in solutions S2 and S3 could be explained in terms of ammonium attachment to colloid particles of soil samples which is in accordance with the reports of Moradzadeh et. al, 2014 [27]. The ammonium retention was demonstrated taking place on the ion exchange sites of soils while exchangeable cations (Na^{+}, Mg^{2+}) are released [2].

It is worth to be mentioned that other mechanism described in soils environments should be discarded (e.g. volatilization, nitrification) as well interlayer fixation of ammonium ions should be discarded due to the short test duration (e.g., weeks)

As it was mentioned before potassium revealed a similar behaviour to ammonium, so the highest potassium release was found for solution S1. The processes that described the ammonium release influenced by organic matter content and ion exchange in soils are also pertinent for potassium; additionally the existence of illite as mineral clay of soil S1 may contribute to the potassium release in solution [28].

In this study the nitrate concentration in solutions is lower than ammonium because in the loaded stage the modified zeolite sorbed selectively ammonium as is plotted in Figure 7.5. In general low values of nitrate were measured as the sorption capacity was very limited due to low selectivity of HMO for nitrate which is an important inorganic form of N which is commonly uptake by plants due to its good mobility [23]. The highest release of nitrate anion was observed in soil solution S2 at pH 9.2 followed by S1 at pH 8.2 and almost negligible by S3 at pH 6.3. This result is in accordance with previous reports about the increase of nitrate release in soils solutions as the soil pH increases [24].

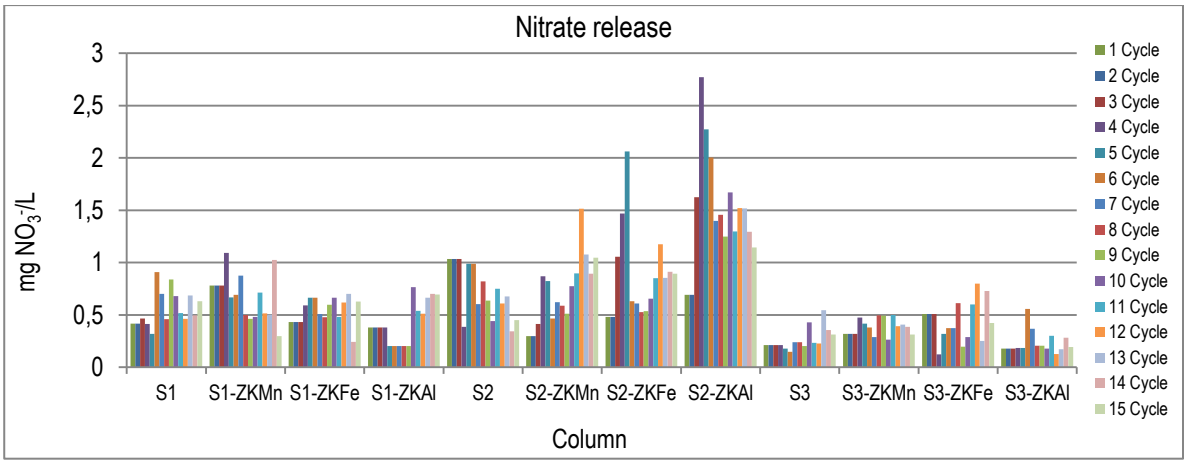

Figure 7.5. Amount of nitrate released in solution from un-amended and amended soil columns through 15 continuous cycles.

Anions with lower fertilizing properties as sulfate and chloride exhibited a minor leaching in solutions as Figure 7.6 shown because their sorption by HFO is not favoured . The highest chloride content was found in the first cycle of study suggesting that it is released almost completely after first cycle. The sulfate revealed the highest release in soil S1 cycle 1 in comparison with soils solutions S2 and S3 that released gradually. The sulfate retention in soils S2 and S3 could be explained in terms of the electrostatic factors and inner sphere complexes however the release in S1 may be occurred due to the dissolved organic matter effect that reduce the sulfate retention [29].

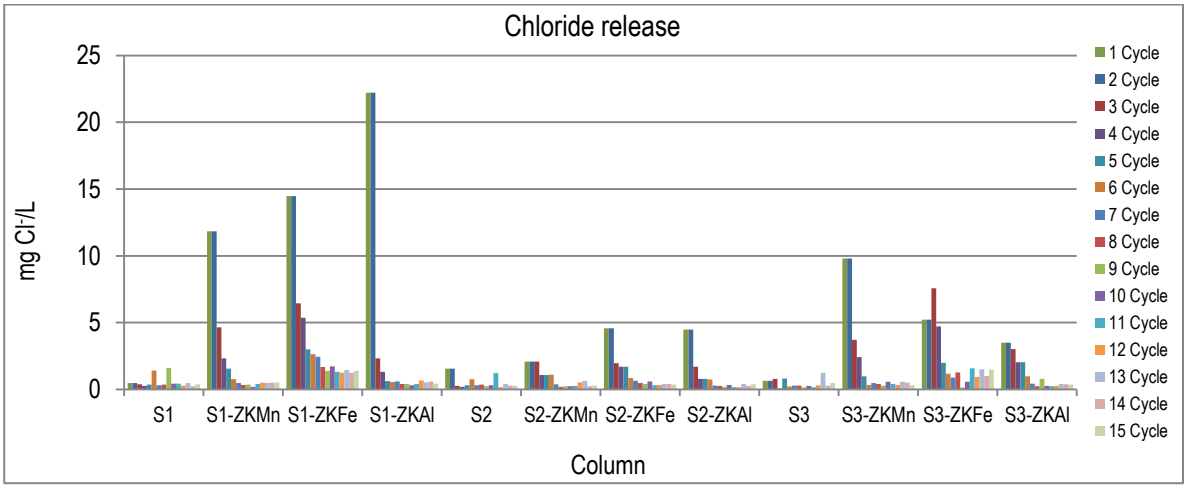

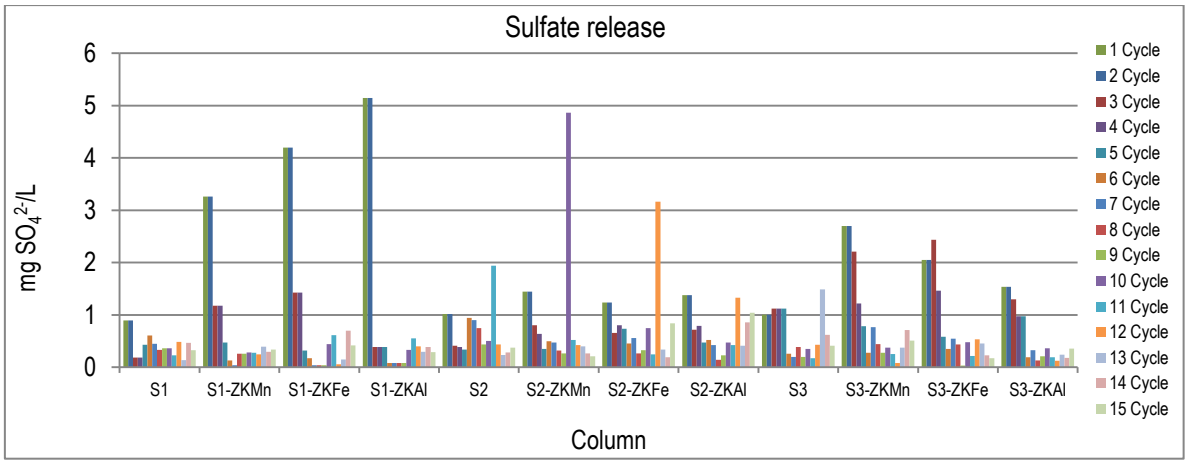

Figure 7.6. Amount of nitrate released in solution from un-amended and amended soil columns through 15 continuous cycles.

Regarding to the presence of metal transition ions including from the use on the impregnation of the zeolites, very low contents of iron, aluminium and manganese were determined in all solutions as shown in Figure 7.7. HFO forms expected on the zeolites have very low solubility values under the expected pH conditions of the leaching solution typically between 6.5 and 9. Results of the variation of the concentrations for the different columns are plotted on Figure 7.7.

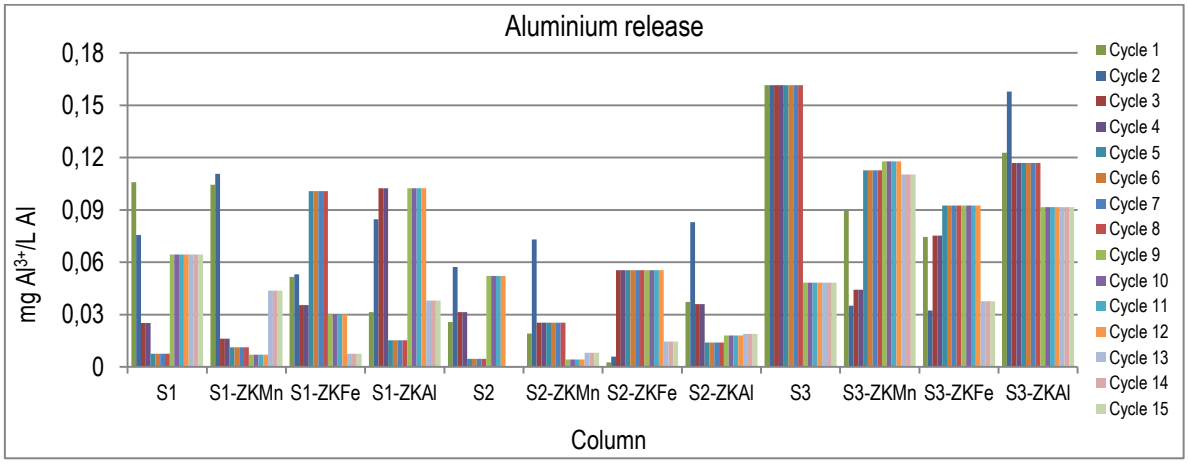

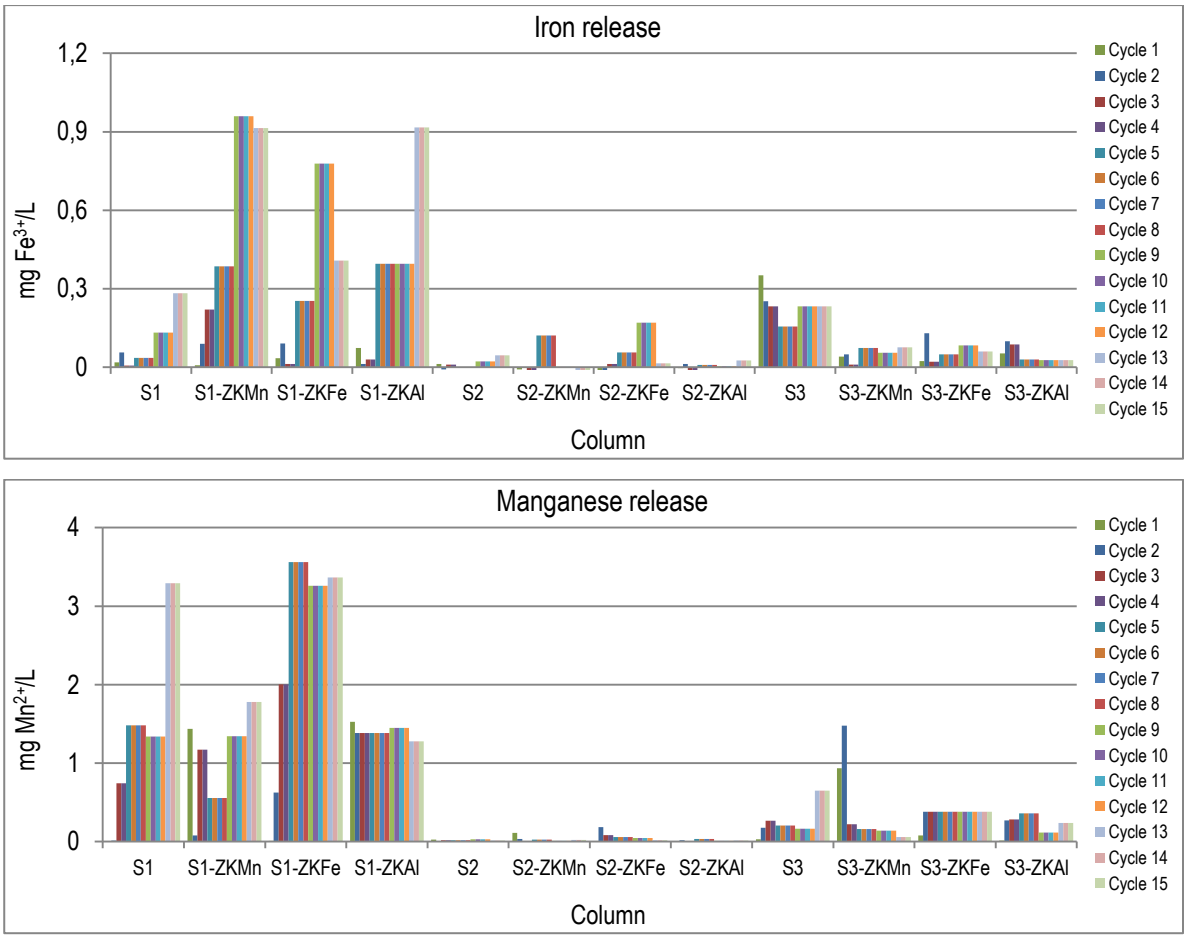

Figure 7.7. Amount of aluminium, iron and manganese released in solution from un-amended and amended soil columns through 15 continuous cycles.

A significant release of silicon was found in all columns as it is shown in Figure 7.8, consequence of using a natural mineral as fertilizers which has become strategic for increasing the NPK fertilizers effectiveness [30].

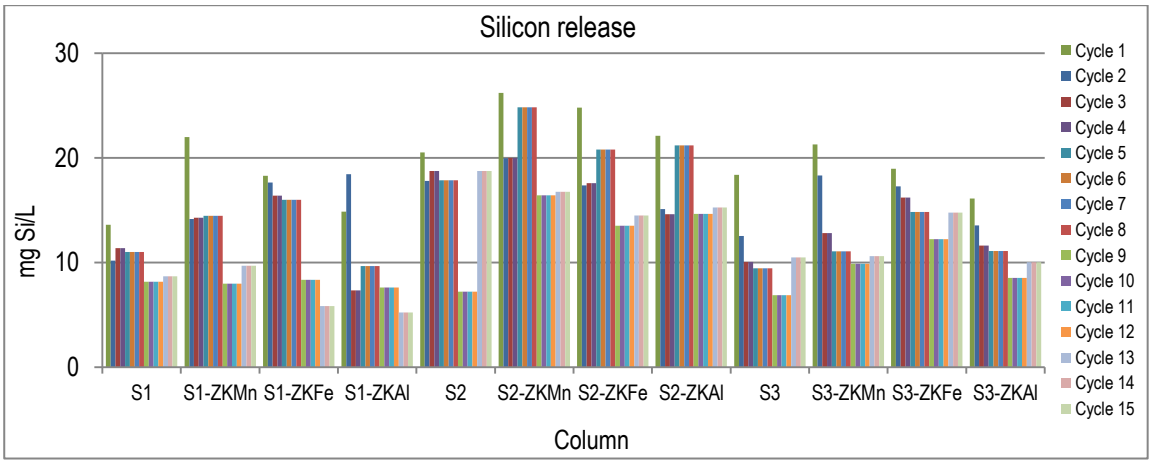

Figure 7.8. Amount of silicon released in solution from un-amended and amended soil columns through 15 continuous cycles.

In solution there were found important amounts of Na, Mg, Ca, these elements that are fundamental for soil environment. Also, there were found in solution traces of some elements such as: Sr, Li, B, Ti, V, Cr, Co, Ni, Cu, Zn, As, Rb, Mo, Sb, Ba, The low amount released of these last compounds represents an advantage for fertilizing applications due to the low toxicity for plants growth. There were found in solutions negligible contents of other elements as Be, Se, Cd or Pb, with potential toxicological concerns at plant and human level as it was observed in batch studies.

7.4. Conclusions

The three modified zeolites forms, ZKAl, ZKFe and ZKMn were used for simultaneous removal of ammonium and phosphate from treated wastewater effluent. The chemical sorption of ammonium by ion exchange occurred as it was corroborated by the ion chromatography analysis. Also, phosphate complexation and chemical precipitation were corroborated by the fractioning assay, with a small portion of labile – P that could be used for plant growth. The negligible sorption of other pollutant elements by the three modified forms of zeolite was observed confirming the high selectivity towards ammonium and phosphate. The batch release assays demonstrated that a small fraction of the ammonium, phosphate and potassium sorbed on zeolites was released at the equilibrium. Moreover, the loaded zeolites released negligible contents of aluminium, iron, manganese and other pollutants like heavy metal that in high concentration are considered dangerous for agricultural application purposes. The NPK loaded zeolites were used for the amendment of three nutrient-poor soil samples and the release of nutrients was evaluated in continuous cycles of natural watering simulation conditions. The availability of nutrients and other elements depend on the soil properties such as, pH, mineralogical composition and organic matter content. Finally, in this study it was confirmed the potential application of the three loaded modified zeolites as slow release of inorganic NPK fertilizers for soils.

7.5. References

1. de Castro, R.C., et al., *Phosphorus migration analysis using synchrotron radiation in soil treated with Brazilian granular fertilizers.* Applied Radiation and Isotopes, 2015. **105**: p. 233-237.
2. Colombani, N., et al., *Batch and column experiments on nutrient leaching in soils amended with Italian natural zeolitites.* CATENA, 2015. **127**: p. 64-71.

3. Król, M., et al., *Application of IR spectra in the studies of zeolites from D4R and D6R structural groups.* Microporous and Mesoporous Materials, 2012. **156**: p. 181-188.
4. Guaya, D., et al., *Simultaneous phosphate and ammonium removal from aqueous solution by a hydrated aluminum oxide modified natural zeolite.* Chemical Engineering Journal, 2015. **271**: p. 204-213.
5. Ming, D.W. and E.R. Allen, *Use of Natural Zeolites in Agronomy, Horticulture and Environmental Soil Remediation.* Reviews in Mineralogy and Geochemistry, 2001. **45**(1): p. 619-654.
6. Gholamhoseini, M., et al., *Zeolite-amended cattle manure effects on sunflower yield, seed quality, water use efficiency and nutrient leaching.* Soil and Tillage Research, 2013. **126**: p. 193-202.
7. Hossain, M.F., W. Chen, and Y. Zhang, *Bulk density of mineral and organic soils in the Canada's arctic and sub-arctic.* Information Processing in Agriculture, 2015. **2**(3–4): p. 183-190.
8. Hedley, M.J., J.W.B. Stewart, and B.S. Chauhan, *Changes in Inorganic and Organic Soil Phosphorus Fractions Induced by Cultivation Practices and by Laboratory Incubations1.* Soil Science Society of America Journal, 1982. **46**(5).
9. Tiessen, H. and J.O. Moir, *Characterization of available P by sequential fractionation*, in *Soil Sampling and Methods of Analysis*, M.R.E. Carter, Editor 1993, Lewis Publishers: Boca Raton. p. 75-86.
10. Olsen, S.R., et al., *Estimation of available phosphorus in soils by extraction with sodium bicarbonate*, in *USDA Circula Nr 939*1954, US GOv. Print. Office: Washington, D.C.
11. Nelson, W.L., A. Mehlich, and E. Winters, eds. *The development, evaluation, and use of soil tests for phosphorus availability*. Soil and Fertiliser Phosphorus in Crop Nutrition, ed. W.H.N. Pierre, A.G. (eds.) 1953, Academic Press Inc. Publishers: New York. p. 153–188.
12. APHA., AWA., and WEF., *Standard methods for the examination of water and wastewater*, 2000, American Public Health Association, American Water Works Association, Water Environment Federation.

13. Villanueva, M.E., et al., *Point of zero charge as a factor to control biofilm formation of Pseudomonas aeruginosa in sol-gel derivatized aluminum alloy plates.* Surface and Coatings Technology, 2014. **254**: p. 145-150.
14. Qi, F., et al., *Influence of aluminum oxides surface properties on catalyzed ozonation of 2,4,6-trichloroanisole.* Separation and Purification Technology, 2009. **66**(2): p. 405-410.
15. Simsek, E.B., E. Özdemir, and U. Beker, *Zeolite supported mono- and bimetallic oxides: Promising adsorbents for removal of As(V) in aqueous solutions.* Chemical Engineering Journal, 2013. **220**: p. 402-411.
16. Wang, L.-C., et al., *Gold nanoparticles supported on manganese oxides for low-temperature CO oxidation.* Applied Catalysis B: Environmental, 2009. **88**(1–2): p. 204-212.
17. Gunkel-Grillon, P., et al., *Effects of long term raw pig slurry inputs on nutrient and metal contamination of tropical volcanogenic soils, Uvéa Island (South Pacific).* Science of The Total Environment, 2015. **533**: p. 339-346.
18. Marofi, S., et al., *Effect of wastewater and compost on leaching nutrients of soil column under basil cultivation.* Agricultural Water Management, 2015. **158**: p. 266-276.
19. Han, F., L. Ren, and X.-C. Zhang, *Effect of biochar on the soil nutrients about different grasslands in the Loess Plateau.* CATENA, 2016. **137**: p. 554-562.
20. Rashid, M.I., et al., *Bacteria and fungi can contribute to nutrients bioavailability and aggregate formation in degraded soils.* Microbiological Research, 2016. **183**: p. 26-41.
21. Lombi, E., et al., *Mobility and Lability of Phosphorus from Granular and Fluid Monoammonium Phosphate Differs in a Calcareous Soil.* Soil Science Society of America Journal, 2004. **68**(2).
22. Anda, M., et al., *Strategy to reduce fertilizer application in volcanic paddy soils: Nutrient reserves approach from parent materials.* Soil and Tillage Research, 2015. **150**: p. 10-20.
23. Rinklebe, J., S.M. Shaheen, and K. Yu, *Release of As, Ba, Cd, Cu, Pb, and Sr under pre-definite redox conditions in different rice paddy soils originating from the U.S.A. and Asia.* Geoderma.

24. Song, Y., et al., *Effects of nutrient and sulfate additions on As mobility in contaminated soils: A laboratory column study.* Chemosphere, 2015. **119**: p. 902-909.
25. Fisher-Power, L.M., T. Cheng, and Z.S. Rastghalam, *Cu and Zn adsorption to a heterogeneous natural sediment: Influence of leached cations and natural organic matter.* Chemosphere, 2016. **144**: p. 1973-1979.
26. Dijkstra, J.J., J.C.L. Meeussen, and R.N.J. Comans, *Leaching of Heavy Metals from Contaminated Soils: An Experimental and Modeling Study.* Environmental Science & Technology, 2004. **38**(16): p. 4390-4395.
27. Moradzadeh, M., et al., *Transport of nitrate and ammonium ions in a sandy loam soil treated with potassium zeolite – Evaluating equilibrium and non-equilibrium equations.* Acta Ecologica Sinica, 2014. **34**(6): p. 342-350.
28. Wang, R., Y. Kang, and S. Wan, *Effects of different drip irrigation regimes on saline–sodic soil nutrients and cotton yield in an arid region of Northwest China.* Agricultural Water Management, 2015. **153**: p. 1-8.
29. Escudey, M., et al., *Effect of ash from forest fires on leaching in volcanic soils.* CATENA, 2015. **135**: p. 383-392.
30. Klotzbücher, T., et al., *Plant-available silicon in paddy soils as a key factor for sustainable rice production in Southeast Asia.* Basic and Applied Ecology, 2015. **16**(8): p. 665-673.

Chapter 8 Conclusions

The nutrients overloading of urban waste water effluents from WWTP and the close need to recover them motivate this experimental work with the interest to contribute with knowledge a) to the reduction of surface water pollution , b) to provide new routes of synthesis of materials with selective sorption properties to recover ammonium and phosphate, and c) to identify potential implementation solutions (e.g granular forms for conventional sorption and desorption cycles or powder materials for hybrid sorption and filtration systems. This thesis is focused in the removal and valorization of phosphate and ammonium from urban waste water by ion exchangers. Particularly, hydrated metal hydroxides have been supported on natural zeolites to remove simultaneously both ions from a waste water effluent to obtain a by-product with agricultural use for soil amendment. So, the natural cycle of phosphorus and nitrogen could be closed and an economic opportunity could be identified in the waste water use and recycle. The most important research conclusions that have been achieved are described below.

a. The synthesis of supported hydrated metal hydroxides on natural zeolites outcomes in an important increase of these compounds in the chemical composition of each modified zeolite. Similarly results were obtained in zeolites modification when sodium was used as intermediate stage as well as when potassium was incorporated directly on the treatment This phenomena is attributed to the occurrence of ion exchange reactions of Al^{3+}, Fe^{2+} and Mn^{2+} between Mg^{2+}, K^{+} and Ca^{2+} ions. Besides, the characterization of natural and modified zeolites demonstrates that structure and morphology of the parent material did not change. The incorporation of aluminium and manganese on zeolite surface resulted in the formation of amorphous mineral phases. Particularly, the iron form of zeolite obtained from its sodium form revealed the existence of Fe-Cl complexes as well as it was found the appearance of akaganeite (β-FeOOH) phase.
b. The phosphate and ammonium removal capacity of the Al^{3+}, Fe^{2+} and Mn^{2+} modified zeolites was found to be extremely dependent on the pH of the solutions. Also, the point of cero charge of modified zeolites demonstrates to be determinant on favored or not the adsorption. It revealed that one mechanism for phosphate and ammonium ions adsorption on modified zeolites occurred by means of columbic forces due to the attraction or repulsion of charges. So, phosphate was adsorbed favorably below pH_{PZC} in comparison to ammonium that

show the same behaviour above pH_{PZC}. Also, the behaivour of ammonium sorption at the basic zone was associated with the decrease of the NH_4^+ concentration as it was converted to the NH_3. However, a particular performance was found by manganese zeolite that revealed the formation of a precipitate which was identified as ammonium manganese phosphate hydrate oxide ($NH_4MnPO_4 \cdot H_2O$).

c. Phosphate and ammonium were chemisorbed on the Al^{3+}, Fe^{2+} and Mn^{2+} modified zeolites. Phosphate was specifically adsorbed on the hydroxyl surface groups of the hydrated metal hydroxides layer impregnated on the zeolite structure. The chemical reaction occurred is characterized by the formation of inner sphere species by means of monodentate and bidentate mononuclear and binuclear complexation. Ammonium cations were adsorbed on zeolites by ion exchange reaction with sodium ions that involves valence forces through the sharing or exchange of electrons between zeolite sites with negative charge.

d. Phosphate was not efficiently desorbed in comparison to ammonium using NaOH, $NaHCO_3$, Na_2CO_3, and mixtures of $NaHCO_3/Na_2CO_3$ in the first sorption – desorption cycle. This phenomenon is attributed to the chemical adsorption that inhibits the easy release of sorbed phosphate on modified zeolites. In the subsequent sorption cycles, the regenerated modified zeolites samples revealed a substantial decrease of phosphate sorption while ammonium removal capacity was practically maintained.

e. The modified zeolites revealed a similar behaviour. Ammonium sorption rates are greater than phosphate ones to reach the equilibrium. So, it suggested that ion exchange reaction between NH_4^+/Na^+ or NH_4^+/K^+ occurred faster than complexation reactions of phosphate ions. This phenomenon was explained in terms of better access of ammonium ions to the correspondent exchange sites in comparison to the hydroxide groups available on the zeolite particles surface. Also, it should be considered that another sorption mechanism involved in phosphate uptake for manganese zeolite was the precipitation reactions. However, it should be pointed out a distinctive characteristic of modified zeolites obtained from sodium form of zeolite that reached the phosphate and ammonium equilibrium sorption capacity in 200 minutes. This performance is not comparable with the three potassium modified zeolites which reached in 15 minutes the ammonium sorption equilibrium; whereas the phosphate sorption rates were lower

and more than 60 minutes were needed. It was concluded that sorption rate mechanism that governed the ammonium and phosphate ions is particle diffusion. So, it implies that in a first stage of NH_4^+ and $HPO_4^{2-}/H_2PO_4^-$ diffusion from the solution to the external surface of zeolite is followed by a sorption stage along the zeolite internal surface.

f. The Al^{3+}, Fe^{2+} and Mn^{2+} modified zeolites demonstrated to be high selectively for the phosphate and ammonium adsorption. A slight improvement of phosphate removal was promoted by the cations Mg^{2+}, K^+, Na^+, and Ca^{2+}. An important reduction of ammonium adsorption was obtained due to the presence of cationic species K^+, Ca^{2+}, Na^+, and Mg^{2+}. The phosphate and ammonium ions were not affected by the presence of anions such as NO_3^-, SO_4^{2-}, Cl^-. It is noteworthy to mention the important increase of phosphate sorption on Mn^{2+} zeolite due to the presence of HCO_3^- and all anions by the effect of raising the pH of the solution (~7) which enhances the phosphate removal. Contrary, the phosphate adsorption on Al^{3+} and Fe^{2+} zeolites was slightly affected in presence of HCO_3^- anion. However, when anions and cations were present at solutions simultaneously a slight reduction in the phosphate and ammonium adsorption was developed.

g. In dynamic conditions a limited capability was developed by granular modified zeolites due to the low bed volumes of influent treated until obtaining phosphate and ammonium column saturation. The competing ions saturated faster the columns packed with Al^{3+}, Fe^{2+} and Mn^{2+} modified zeolites than in absence of these interferences. Also, the phosphate and ammonium removal capacity was significantly reduced due to the dynamic variables that conditioned the sorption process on zeolites in comparison to batch assays. Higher rate and enrichment factor of sorbed ammonium was obtained in comparison to phosphate. Therefore, the deficient performance in the regeneration indicates that reusing the modified zeolites will require re-impregnation after cycling.

h. The powder natural zeolite was modified into the potassium aluminium, iron and manganese forms for the simultaneous removal of ammonium and phosphate sorption from a secondary waste water effluent. Comparable sorption mechanisms were developed by these modified forms and the ones obtained from the sodium form of zeolite. However, the main mechanism for ammonium sorption by the tree zeolites involves ion-exchange with the K^+ ions of the zeolite. Sorption selectivity patterns were developed by modified zeolites for ammonium and

phosphate in front of sodium, calcium, magnesium, chloride, sulphate and nitrate, which were the major ions present in the treated waste water. Also, the organic matter content of treated waste water did not affect the sorption capacities of the three modified zeolites. Besides, no other pollutants like heavy metals and similarly were sorbed on modified zeolties. The loaded zeolites could be used for soil quality improvement as powder fertilizer composed by NPK elements.

i. The characterization of the phosphorus fractions available on loaded zeolites demonstrated that a significant portion of phosphorus was immobilized through ligand exchange complexation reactions with each Al^{3+}, Fe^{2+} and Mn^{2+} hydroxides. Also there were found important contents of phosphorus bounded to calcium and magnesium elements of zeolite. Particularly, manganese modified zeolites revealed an increase of this phosphorus fraction, which support the previous statement of phosphate removal by means of chemical precipitation with these cationic species even though these mineral phases were not identified by XRD analysis. Also, the sequential fractionation of the loaded modified zeolite revealed the existence of an important fraction of biological active phosphorus. This portion was attributed to the phosphorus physisorbed by means of coulombic forces. This fact sets the possibility of recovering this phosphate to be applied as fertilizer in P-deficient soils.

j. The loaded potassium modified zeolites were evaluated in soil quality improvement applications. The ammonium, phosphate and potassium sorbed on modified zeolites were partially released at the equilibrium through batch assays. Also, these loaded zeolites demonstrated to be safe for agricultural applications due to the concentrations of the elements leached. There were found negligible contents of aluminium, iron, manganese and other pollutants like heavy metal that, released in high concentration, could be considered dangerous for agricultural application purposes. In continuous conditions the NPK loaded zeolites were used for the amendment of three nutrient-poor soil samples simulating continuous cycles of natural raining conditions for the release of these elements. The pH, mineralogical composition and organic matter content of soils demonstrated to be the determinant variables for the nutrients and other elements availability. Also, the continuous released of elements from the NPK loaded zeolites in each cycle demonstrated their capability for being used as inorganic soils fertilizers.

k. Analysis of trace toxic metals and non-metals on the leached samples were always on the µg/L to ng/L levels indicating that although present at low levels on the treated waste water, their accumulation of the zeolites is not providing values of concerns for potential transfer from soils-to plants.